A stochastic volatility model with realized measures for option pricing

Giacomo Bormetti[*] Roberto Casarin[†] Fulvio Corsi[‡]
Giulia Livieri [§]

This version: March 21, 2019

Abstract

Based on the fact that realized measures of volatility are affected by measurement errors, we introduce a new family of discrete-time stochastic volatility models having two measurement equations relating both observed returns and realized measures to the latent conditional variance. A semi-analytical option pricing framework is developed for this class of models. In addition, we provide analytical filtering and smoothing recursions for the basic specification of the model, and an effective MCMC algorithm for its richer variants. The empirical analysis shows the effectiveness of filtering and smoothing realized measures in inflating the latent volatility persistence – the crucial parameter in pricing Standard and Poor's 500 Index options.

1 Introduction

Thanks to the availability of high-frequency data, a number of realized measures of daily volatility (henceforth RVs) has been introduced so far (see Andersen and Bollerslev, 1998;

[*]Department of Mathematics, University of Bologna, IT.
[†]Department of Economics, Ca' Foscari University of Venice, IT.
[‡]Department of Economics and Management, University of Pisa, IT and City University London.
[§]Scuola Normale Superiore, Piazza dei Cavalieri, Pisa, IT.

Andersen et al., 2001; Barndorff-Nielsen, 2002; Barndorff-Nielsen and Shephard, 2004; Andersen et al., 2008; Hansen and Horel, 2009, to cite only a few). These measures are considerably more informative than the squared returns about the (true) conditional variance (henceforth CV). RVs present two crucial, although antithetic, features. On one hand, these measures lead to large economic and statistical gains when incorporated in volatility models (see, for instance, Dobrev and Szerszen, 2010; Maheu and McCurdy, 2011; Hansen et al., 2012; Christoffersen et al., 2014, 2015). On the other hand, on empirical data, they are affected by measurement errors and overnight biases. For these reasons, it is common practice in the recent literature to use RVs in the dynamic model for the latent CV (see Shephard and Sheppard (2010); Hansen et al. (2012) in a GARCH framework, Engle and Gallo (2006); Gallo and Otranto (2015) in a MEM framework, and Takahashi et al. (2009); Dobrev and Szerszen (2010); Koopman and Scharth (2013) in a stochastic volatility one). However, little work has been devoted to *semi-analytical* option pricing with stochastic volatility (henceforth SV) models incorporating RVs. We mention Khrapov and Renault (2016) who propose an affine discrete-time option pricing SV model exploiting RV which preserves the structure of the dynamics when changing measure. However, while in the theoretical part returns are assumed to be driven by a latent volatility process linked to the RV through a model-dependent relation, the empirical application focuses on the volatility factor as *observed* and proxied by RV.

In the present paper, we introduce a new family of flexible and tractable discrete-time SV models which allows for filtering the latent conditional variance process from *both* observed returns and RV-measures. Combining in an SV framework the two sources of information reduces measurement errors and permits to recover the high persistence of the CV. The proposed SV models accurately reproduce well-established stylized facts observed in financial time series, while preserving closed-form formulas for option pricing and for filtering and smoothing the latent SV process.

The first contribution of the paper is on modeling. Inspired by the above mentioned strands of literature, we employ the RV-measure in a measurement equation for the latent CV. Thus, our proposed model has two measurement densities: a Gaussian density for the daily log-returns and a gamma density for the RV-measure. In turn, the dynamics of the latent CV is modeled by borrowing from the flexible class of Heterogeneous Autoregressive Gamma process (HARG) of order p with Leverage (L) RV-LHARG(p) introduced by Majewski et al. (2015). Therefore, we label the general version of the proposed SV model as SV-LHARG(p).

As a second theoretical contribution, we show that SV-LHARG(p) belongs to the class of affine models. This allows for analytical tractability of the option pricing. Remarkably, although the option pricing literature in discrete-time traces back to Heston and Nandi (2000), analytical tractability is guaranteed only for rather specific types of models. These include: GARCH (Christoffersen et al., 2008, 2013; Bormetti et al., 2015; Huang et al., 2017) and realized volatility approaches (Stentoft, 2008; Corsi et al., 2013; Christoffersen et al., 2014; Majewski et al., 2015), later extended to separately deal with the continuous and discontinuous components of RV (Christoffersen et al., 2015; Alitab et al., 2019). Moreover, in accordance with the recent option pricing literature (see, for instance Christoffersen et al., 2013), we use a flexible pricing kernel incorporating a variance-dependent risk premium in addition to the common equity risk premium.

SV models offer increased flexibility over GARCH-type specifications since they assume separate innovation processes for the conditional mean and variance of the observables (Taylor, 1994). However, the presence of variance-specific disturbances makes inference on latent volatility more challenging and requires the adoption of suitable inference tools such as stochastic filtering and smoothing, and simulation-based inference. Filtering and smoothing recursions can be used to define a pseudo maximum likelihood estimator of the parameters (see Christoffersen et al. (2012)). Nevertheless, as argued in Durham et al. (2015), a valid statistical analysis should account for the state uncertainty. Thus, we follow a Bayesian approach where the posterior distribution of the parameters is derived jointly with the distribution of the latent states.

The third contribution relates to the state-space models and stochastic filtering literature. Takahashi et al. (2009), Shirota et al. (2014) and Bekierman and Gribisch (2016) propose to augment the state-space SV model with a RV equation and come up with flexible models for forecasting return and volatility dynamics. However, in these works neither exact filtering nor analytical pricing formulas are provided. For the SV-LHARG(p) with one lag (i.e. $p = 1$) and no leverage components (SV-ARG henceforth) we provide exact analytical filtering and smoothing of the latent variables. In this direction, we contribute to the filtering literature by extending the results of Creal (2017) for non-linear and non-Gaussian models with one measurement equation to the case of two measurement equations. Indeed, for these type of models filtering and smoothing are usually obtained through analytical or numerical approximation techniques (Tanizaki, 1996; Doucet et al., 2001). Exceptions are Smith and Miller (1986); Shephard (1994); Ferrante and Vidoni (1998); Vidoni (1999); Deschamps (2011); de Pinho et al. (2016). The analytical recursions for SV-ARG allow to evaluate its likelihood function exactly and to develop an efficient inference procedure.

The fourth contribution of the paper is the development of an effective Bayesian inference procedure for both parameters and latent CV in the general SV-LHARG(p), and an efficient Markov Chain Monte Carlo (henceforth MCMC) procedure for posterior approximation. Specifically, we use SV-ARG as an auxiliary model in combination with the block sampling strategy introduced by Shephard and Pitt (1997) for state-space models and then successfully combined with Metropolis-Hastings (henceforth MH) for latent variable estimation (e.g., see So (2006), Casarin et al. (2011) and Billio et al. (2016)). A simulation study assesses the efficiency of the proposed MCMC algorithm.

Finally, we apply SV-LHARG on a large sample of S&P500 index options and we benchmark its performance to competitor models. In particular, we consider RV-LHARG(p) and the two-component GARCH model (henceforth CGARCH) introduced in Christoffersen et al. (2008). The comparison with RV-LHARG confirms the importance of a proper management of the RV measurement error. The effective filtering of the latent volatility in SV-LHARG translates in a better conditioning of the return process and ensures an higher persistence of the CV. Both effects improve the pricing performances across all moneyness and maturities, both in-sample and out-of-sample. Concerning CGARCH, in-sample SV-LHARG takes advantage of the RV measure economic content and fares better then the benchmark at short maturities. On the contrary, CGARCH outperforms SV-LHARG for long maturities, where the very high level of persistence of GARCH models becomes crucial. Out-of-sample, the picture is much less clear. The superior behavior of CGARCH in the long run is less striking, whereas it may happen that – in the short run and especially for out-of-the-money calls – it over-performs SV-LHARG. However, the overall performance of SV-LHARG remains superior. Additionally, results are very much dependent on the out-of-sample period under scrutiny. For instance, SV-LHARG fares much better during the high volatility January 1, 2008–December 31, 2008 episode. In the comparison, we consider as benchmark also the (so-dubbed) RVM model by Christoffersen et al. (2015, 2016). The model exploits RV measures, filters the latent volatility, and provides a GARCH-type level of persistence. However, in the option-pricing exercise SV-LHARG fares better than RVM both in-sample and out-of-sample. In particular, the RVM performance severely deteriorate at longer horizon. The empirical analysis, along with the discussion of some mis-specification issues of RVM, is not reported in the main text, but it is extensively documented in the on-line Appendix.

The remainder of the paper proceeds as follows. Section 2 introduces the SV-LHARG(p) and presents new results on analytical filtering and smoothing for SV-ARG. Section 3 describes the Bayesian inference procedure for the general model. Section 4 benchmarks SV-LHARG against competitor models in an option pricing exercise. Section 5 concludes.

2 The model

2.1 Dynamics under physical probability $\mathbb{P}$

Consider a risky asset with closing price S_t and geometric log-return $r_t = \log(S_{t+1}/S_t)$. We indicate with h_t a continuous latent volatility process and with z_t a latent volatility state. Let $\mathcal{F}_t \doteq \sigma\left(\{r_u, \mathrm{RV}_u\}_{u \le t}\right)$ be the filtration containing the information about observable quantities, i.e. log-return r_u and RV_u, available up to time t, $\widetilde{\mathcal{F}}_t \doteq \sigma\left(\mathcal{F}_t \vee \{h_u, z_u\}_{u \le t}\right)$ the filtration $\mathcal{F}_t$ enlarged with latent processes up to time t, and $\widetilde{\mathcal{F}}_t^H \doteq \sigma\left(\widetilde{\mathcal{F}}_t \vee \{h_{t+1}\}\right)$ and $\widetilde{\mathcal{F}}_t^Z \doteq \sigma\left(\widetilde{\mathcal{F}}_t \vee \{z_{t+1}\}\right)$ the filtration $\widetilde{\mathcal{F}}_t$ enlarged with the latent processes in $(t+1)$. We assume the following dynamic model for the log-returns:

$$r_t = \mu + \gamma h_t + \sqrt{h_t}\varepsilon_t, \quad \varepsilon_t \overset{i.i.d.}{\sim} \mathcal{N}(0,1), \tag{2.1}$$

$t = 1, \ldots, T$, where μ is the risk-free rate, $(\gamma + 1/2)$ is the market price of risk, and $\mathcal{N}(m, \sigma^2)$ indicates the univariate normal distribution with mean m and variance σ^2. We refer to Eq. (2.1) as *return equation*. The dynamics in Eq. (2.1) differ from that proposed in Corsi et al. (2013); Majewski et al. (2015) for daily log-returns since the authors consider RV as driving process for returns. Specifically, they employ the continuous part of the realized variance (see Andersen et al. (2001); Barndorff-Nielsen (2002) for the definition), hereafter RV_t. Since RV contains information on the latent volatility process, we follow Hansen and Lunde (2006); Engle and Gallo (2006); Shephard and Sheppard (2010); Takahashi et al. (2009) and introduce another measurement equation termed *realized variance equation* which relates RV to the latent volatility process. Specifically, we assume that RV_t is sampled from a gamma distribution:

$$\mathrm{RV}_t|\widetilde{\mathcal{F}}^H_{t-1} \overset{ind}{\sim} \mathcal{G}\left(\varphi\, e^{-\kappa_2}, h_t\, e^{\kappa_2}\right),$$

where $\varphi \in \mathbb{R}_+$ and $\kappa_2 \in \mathbb{R}$ are two constants, and $\mathcal{G}(k, \vartheta)$ denotes a (central) gamma distribution with positive shape, k, and scale parameter, ϑ, respectively. In this way, we ensures a non-negative definite RV-measure and, in contrast to a log-normal specification, it preserves the analytical tractability of filtering and smoothing recursions and of derivative pricing. Under above assumptions, the first two conditional moments of return and realized variance are readily derived:

$$\mathbb{E}^{\mathbb{P}}\left[r_t|\widetilde{\mathcal{F}}^H_{t-1}\right] = \mu + \gamma h_t,\ \mathbb{V}^{\mathbb{P}}\left[r_t|\widetilde{\mathcal{F}}^H_{t-1}\right] = h_t,\ \mathbb{E}^{\mathbb{P}}\left[\mathrm{RV}_t|\widetilde{\mathcal{F}}^H_{t-1}\right] = \varphi h_t,\ \mathbb{V}^{\mathbb{P}}\left[\mathrm{RV}_t|\widetilde{\mathcal{F}}^H_{t-1}\right] = \varphi e^{\kappa_2} h_t^2.$$

The expression of the conditional variance of r_t suggests that h_t can be interpreted as the latent conditional variance of the daily log-return. The computation of $\mathbb{E}^{\mathbb{P}}\left[e^{r_t}|\widetilde{\mathcal{F}}^H_{t-1}\right] = e^{\mu+(\gamma+1/2)h_t}$ confirms the interpretation of $(\gamma + 1/2)$ as the market price of risk. Concerning the RV conditional moments, we recall that the RV estimator has two potential drawbacks.

First, it is biased by the market micro-structure noise (induced by infrequent trading, bid-ask spread, and rounding effects). Various methods are available in the literature to mitigate this bias (Hansen and Lunde, 2005; Zhang et al., 2005; Bandi and Russell, 2006, 2008; Barndorff-Nielsen et al., 2008). Here, we adopt the Two-Scale estimator of Zhang et al. (2005). Second, the absence of trading during the overnight periods prevents us to compute the whole day RV. Therefore, the computation of the RV only from available intra-day returns results in the downward bias named overnight bias. The RV conditional mean indicates that the parameter φ is intended to adjust the overnight bias in the RV estimator. In our financial application we use data for the S&P500 index which is quoted from 9:30 AM to 4:00 PM Eastern time, thus we should expect $\varphi < 1$. A similar approach to bias correction has been proposed by Takahashi et al. (2009), Dobrev and Szerszen (2010), Koopman and Scharth (2013) and Hansen et al. (2012).

Regarding the dynamics of the volatility process, we assume that h_t depends on the past realizations $\mathbf{h}_{t-1} = (h_{t-1}, \cdots, h_{t-p})^{'}$ and on the past leverage components $\mathbf{l}_{t-1} = (l_{t-1}, \cdots, l_{t-p})^{'}$, with $l_{t-i} = \left(\varepsilon_{t-i} - \lambda\sqrt{h_{t-i}}\right)^2$ and $\lambda \in \mathbb{R}_+$. It follows an autoregressive gamma process with transition distribution (see Gouriéroux and Jasiak, 2006):

$$h_t|\widetilde{\mathcal{F}}_{t-1} \overset{d}{\sim} \bar{\mathcal{G}}(\delta, \Theta(\mathbf{h}_{t-1}, \mathbf{l}_{t-1}), c), \tag{2.2}$$

where $\bar{\mathcal{G}}(\delta, \Theta, c)$ denotes the non-central gamma distribution with shape $\delta \in \mathbb{R}_+$, scale $c \in \mathbb{R}_+$, and non-centrality parameter $\Theta \in \mathbb{R}_+$ (more details are provided in the on-line Appendix). The non-centrality parameter is given by:

$$\Theta(\mathbf{h}_{t-1}, \mathbf{l}_{t-1}) = \sum_{i=1}^{p} \beta_i h_{t-i} + \sum_{i=1}^{p} \alpha_i l_{t-i},$$

where $(\beta_1, \cdots, \beta_p)$ and $(\alpha_1, \cdots, \alpha_p)$ are the autoregressive and leverage coefficients, respectively. Note that the non-central gamma distribution arises as a Poisson mixture of a (central) gamma distributions (see Gouriéroux and Jasiak, 2006, for more details). Precisely, we can rewrite Eq. (2.2) as:

$$
\begin{aligned}
h_t|\widetilde{\mathcal{F}}_{t-1}^{Z} &\overset{ind}{\sim} \mathcal{G}\left(\delta + z_t, c\right), \\
z_t|\widetilde{\mathcal{F}}_{t-1} &\overset{ind}{\sim} \mathcal{P}o\left(\Theta(\mathbf{h}_{t-1}, \mathbf{l}_{t-1})\right),
\end{aligned}
\tag{2.3}
$$

where $\mathcal{P}o(v)$ indicates the Poisson distribution with intensity parameter $v > 0$. The latter representation will be used later on in this paper for the characterization of h_t and in the inference procedure. The conditional mean and variance of the process h_t, i.e.

$$
\begin{aligned}
\mathbb{E}^{\mathbb{P}}\left[h_t|\widetilde{\mathcal{F}}_{t-1}\right] &= c\delta + c\left(\sum_{i=1}^{p}\beta_i h_{t-i} + \sum_{i=1}^{p}\alpha_i l_{t-i}\right) \\
\mathbb{V}^{\mathbb{P}}\left[h_t|\widetilde{\mathcal{F}}_{t-1}\right] &= c^2\delta + 2c^2\left(\sum_{i=1}^{p}\beta_i h_{t-i} + \sum_{i=1}^{p}\alpha_i l_{t-i}\right),
\end{aligned}
$$

are affine functions of the lagged values of the volatility and leverage processes. Summarising, SV-LHARG(p) has the following distributional state-space representation:

$$
\begin{aligned}
r_t|\widetilde{\mathcal{F}}_{t-1}^{H} &\overset{d}{\sim} \mathcal{N}(\mu + \gamma h_t, h_t), \\
\mathrm{RV}_t|\widetilde{\mathcal{F}}_{t-1}^{H} &\overset{d}{\sim} \mathcal{G}\left(\varphi e^{-\kappa_2}, h_t e^{\kappa_2}\right), \\
h_t|\widetilde{\mathcal{F}}_{t-1}^{Z} &\overset{d}{\sim} \mathcal{G}\left(\delta + z_t, c\right), \\
z_t|\widetilde{\mathcal{F}}_{t-1} &\overset{d}{\sim} \mathcal{P}o\left(\Theta(\mathbf{h}_{t-1}, \mathbf{l}_{t-1})\right).
\end{aligned}
\tag{2.4}
$$

It is worth mentioning that our framework allows for the inclusion of exogenous variables in the log-return and RV dynamics, such overnight corrections, jump components, and possible structural changes of some model parameters.

We conclude this section by presenting some properties of SV-LHARG(p). First, in the following proposition we give the stationary condition for our model.

Proposition 1. *The* SV-LHARG(p) *in Eq.* (2.4) *is stationary if the following condition*

$$
c\left(\sum_{i=1}^{p}\beta_i + \lambda^2\sum_{i=1}^{p}\alpha_i\right) < 1 \tag{2.5}
$$

is satisfied.

Proof. See on-line Appendix. □

Additionally, from Eq.(2.4), it is possible to compute analytically the invariant unconditional mean and variance of both the latent and the observable variables:

$$\mathbb{E}^{\mathbb{P}}[h_1] = \frac{c\left(\delta + \alpha^{(1)}\right)}{1 - c\left(\beta^{(1)} + \lambda^2\alpha^{(1)}\right)},$$
$$\mathbb{V}^{\mathbb{P}}[h_1] = \frac{c^2\left(\delta + 2\alpha^{(1)} + 2\alpha^{(2)}\right) + 2c^2\mathbb{E}^{\mathbb{P}}[h_1]\left(\beta^{(1)} + \lambda^2\alpha^{(1)} + 4\lambda^2\alpha^{(2)}\right)}{1 - c^2\left(\beta^{(2)} + \lambda^4\alpha^{(2)}\right)},$$
$$\mathbb{E}^{\mathbb{P}}[r_1] = \mu + \gamma\mathbb{E}^{\mathbb{P}}[h_1], \qquad \mathbb{V}^{\mathbb{P}}[r_1] = \mathbb{E}^{\mathbb{P}}[h_1] + \gamma^2\mathbb{V}^{\mathbb{P}}[h_1],$$
$$\mathbb{E}^{\mathbb{P}}[\mathrm{RV}_1] = \varphi\mathbb{E}^{\mathbb{P}}[h_1], \qquad \mathbb{V}^{\mathbb{P}}[\mathrm{RV}_1] = \left(\varphi e^{\kappa_2} + \varphi^2\right)\mathbb{V}^{\mathbb{P}}[h_1] + \varphi e^{\kappa_2}\left(\mathbb{E}^{\mathbb{P}}[h_1]\right)^2.$$

where $\alpha^{(1)} = \sum_{i=1}^{p}\alpha_i$, $\alpha^{(2)} = \sum_{i=1}^{p}\alpha_i^2$, $\beta^{(1)} = \sum_{i=1}^{p}\beta_i$, $\beta^{(2)} = \sum_{i=1}^{p}\beta_i^2$. Finally, SV-LHARG($p$) satisfies the affine property, whose importance has been acknowledged in many studies (see, for instance Duffie et al., 2000; Darolles et al., 2006; Majewski et al., 2015). It enables us to provide an exhaustive probabilistic description of the log-return and conditional variance dynamics, and to obtain a closed-form expression for the conditional moment generating function of the SV-LHARG(p) under the physical and risk-neutral measures. Also, it allows us to derive an explicit one-to-one mapping between the parameters of SV-LHARG(p) under the measures $\mathbb{P}$ and $\mathbb{Q}$. Results linked to the affine property largely follow from Majewski et al. (2015). Therefore, hereafter, we present only the essential materials needed to understand the rest of the paper and refer to the on-line Appendix for further details.

2.2 Dynamics under the risk-neutral probability $\mathbb{Q}$

We risk-neutralize the model by employing a Stochastic Discount Factor (SDF) within the exponential affine family. Such SDF has been extensively used in the literature (see Bertholon et al., 2008; Gagliardini et al., 2011; Corsi et al., 2013; Majewski et al., 2015;

Alitab et al., 2019, among others). We assume the following form:

$$M_{t,t+1} = \frac{e^{-\nu_1 h_{t+1} - \nu_2 r_{t+1}}}{\mathbb{E}^{\mathbb{P}}\left[e^{-\nu_1 h_{t+1} - \nu_2 r_{t+1}} | \widetilde{\mathcal{F}}_t\right]}, \tag{2.6}$$

which represents the Esscher transform from the physical log-return density to the risk-neutral one (see, for instance Gerber et al., 1994; Bühlmann et al., 1996). The main advantage in using the SDF in (2.6) is the clear identification of the sources of risk and their explicit compensation by means of specific risk premia. This functional form allows for both a conditional variance premium, ν_1, and the usual equity premium, ν_2. The parameter ν_2 is fixed by no-arbitrage conditions (see the on-line Appendix), whereas ν_1 is a free parameter which is calibrated from option prices (see the on-line Appendix for a precise description of the calibration procedure). Besides, it is possible to show that under the risk-neutral measure $\mathbb{Q}$ the conditional variance follows an SV-LHARG(p) process, i.e. SV-LHARG(p) admits a structure-preserving change of measure.

2.3 Special cases

Here, we shall introduce some notations and present four instances of SV-LHARG(p) which will be used in our financial applications. We define with $\mathbf{r}_{s:t} = (r_s, \cdots, r_t)' \in \mathbb{R}^{t-s+1}$, $\text{RV}_{s:t} = (\text{RV}_s, \cdots, \text{RV}_t)' \in \mathbb{R}_+^{t-s+1}$, $\mathbf{h}_{s:t} = (h_s, \cdots, h_t)' \in \mathbb{R}_+^{t-s+1}$, $\mathbf{z}_{s:t} = (z_s, \cdots, z_t)' \in \mathbb{R}_+^{t-s+1}$ the collections, from time s to time t, of daily log-returns, realized variances, conditional variances and state variables, respectively.

The first model considered is an SV-LHARG model with an heterogeneous autoregressive dynamics for the CV and the leverage term. It is an SV-LHARG(22) with the following restrictions: $\beta_1 = \beta^{(d)}$, $\beta_2 = \ldots = \beta_5 = 4\beta^{(w)}$, $\beta_6 = \ldots = \beta_{22} = 17\beta^{(m)}$, $\alpha_1 = \alpha^{(d)}$, $\alpha_2 = \ldots = \alpha_5 = 4\alpha^{(w)}$, $\alpha_6 = \ldots = \alpha_{22} = 17\alpha^{(m)}$. This type of parametrization was introduced in Majewski et al. (2015) to describe the dynamics of the RV, and allows us to re-write the non centrality parameter of the non-central gamma random variable in Eq.

(2.4), $\Theta\left(\mathbf{h}_{t-1},\mathbf{l}_{t-1}\right) \doteq \Theta^{(h)}\left(\mathbf{h}_{t-1},\mathbf{l}_{t-1}\right)$, as:

$$\Theta^{h}\left(\mathbf{h}_{t-1},\mathbf{l}_{t-1}\right) = \beta^{(d)}h_{t-1}^{(d)} + \beta^{(w)}h_{t-1}^{(w)} + \beta^{(m)}h_{t-1}^{(m)} + \alpha^{(d)}l_{t-1}^{(d)} + \alpha^{(w)}l_{t-1}^{(w)} + \alpha^{(m)}l_{t-1}^{(m)}$$

where the quantities $h_{t-1}^{(d)}$, $h_{t-1}^{(w)}$ and $h_{t-1}^{(m)}$ are defined as:

$$h_{t-1}^{(d)} = h_{t-1}, \quad h_{t-1}^{(w)} = \frac{1}{4}\sum_{i=2}^{5} h_{t-i}, \quad h_{t-1}^{(m)} = \frac{1}{17}\sum_{i=6}^{22} h_{t-i}. \tag{2.7}$$

Analogous expressions are used to define $l_{t-1}^{(d)}$, $l_{t-1}^{(w)}$ and $l_{t-1}^{(m)}$. The previous quantities represent the heterogeneous components corresponding to the short-term or daily (d), medium-term or weekly (w) and long-term or monthly (m) conditional variance and leverage terms. This specification captures the persistence observed in financial data as well as the multi-component structure of volatility and leverage, while it preserves parameter parsimony (see Majewski et al., 2015, and reference therein). The second model derives from the SV-LHARG by setting $\beta^{(w)} = \beta^{(m)} = 0$ and $\alpha^{(w)} = \alpha^{(m)} = 0$. The third model is the SV-HARG model, which is an heterogeneous autoregressive model for the CV without leverage term, i.e. $\alpha^{(d)} = \alpha^{(w)} = \alpha^{(m)} = 0$. Finally, the last model is an SV-LHARG(p) without leverage and heterogeneous structure, thus labelled SV-ARG. This model extends the class of non-Gaussian state-space models introduced in Creal (2017) by allowing for two observation equations, while preserving analytical tractability. The distribution of the observable log-returns and the RV are normal and (central) gamma, respectively. Specifically, SV-ARG is described by Eq.(2.4) with $\Theta\left(\mathbf{h}_{t-1},\mathbf{l}_{t-1}\right) = \beta^{(d)}c$.

A crucial feature of SV-ARG is that the likelihood function is tractable and can be used to develop efficient inference procedures for richer versions. In the following propositions, by applying similar arguments as in Creal (2017), we are able to provide analytical expressions for the conditional likelihood, the Markov transition, and the initial distribution of z_t. Also, we obtain analytical filtering and smoothing recursions for the latent processes.

Proposition 2. *For the* SV-ARG *model, the conditional likelihood,* $p(r_t, \mathrm{RV}_t|\widetilde{\mathcal{F}}_{t-1}^{Z})$*, the*

Markov transition, $p(z_t|\widetilde{\mathcal{F}}_{t-1})$, and the initial distribution of z_t, $p(z_1)$, are given by:

$$
\begin{aligned}
p(r_t, \mathrm{RV}_t|\widetilde{\mathcal{F}}^Z_{t-1}) &= 2\eta(z_t) K_{\lambda(z_t)}\left(\sqrt{\psi\chi^{(t)}}\right)\left(\sqrt{\frac{\chi^{(t)}}{\psi}}\right)^{\lambda(z_t)}, \\
p(z_t|\widetilde{\mathcal{F}}_{t-1}) &\propto \mathcal{S}\left(\lambda(z_{t-1}), \chi^{(t-1)}\beta^{(d)}, \psi\frac{1}{\beta^{(d)}}\right), \\
p(z_1) &\propto \mathcal{NB}\left(\delta, c\beta^{(d)}\right),
\end{aligned}
$$

with

$$
\begin{aligned}
\eta(z_t) &= \frac{\exp\left(\gamma\mu_{1t}\right)}{\sqrt{2\pi}}\frac{\mathrm{RV}_t^{\varphi_t-1}}{\Gamma(\varphi_t)\left(\exp\left(\kappa_2\right)\right)^{\varphi_t}}\frac{1}{\Gamma(\delta+z_t)c^{\delta+z_t}}, \quad \mu_{1t} = r_t - \mu, \quad \varphi_t = \varphi\exp\left(-\kappa_2\right) \\
\lambda(z_t) &= \delta + z_t - \varphi_t - 1/2, \quad \chi^{(t)} = \mu_{1t}^2 + 2\mu_{2t}, \quad \mu_{2t} = \frac{\mathrm{RV}_t}{\exp\left(\kappa_2\right)}, \quad \psi = \gamma^2 + \frac{2}{c},
\end{aligned}
$$

where $K_\lambda(x)$ is the modified Bessel function of the second kind, $\mathcal{S}(\lambda, \chi, \psi)$ the Sichel distribution with parameters $\lambda \in \mathbb{R}$, $\chi \in \mathbb{R}_+$, $\psi \in \mathbb{R}_+$ and $\mathcal{NB}(\omega, p)$ the Negative Binomial distribution with parameters $\omega \in \mathbb{R}_+$ and $p \in (0,1)$.

Proof. See on-line Appendix, where definitions of the Sichel and the Negative Binomial distribution are also provided. □

Proposition 3. *Let $p\left(r_t, \mathrm{RV}_t|z_t = k\right)$, $k \geq 0$, be the joint observables density $p(r_t, \mathrm{RV}_t|\widetilde{\mathcal{F}}^Z_{t-1})$ of Proposition 2, conditional to $\{z_t = k\}$ and let $p\left(z_t = k|z_{t-1} = l, r_{t-1}, \mathrm{RV}_{t-1}\right)$, $k, l \geq 0$ be the transition probabilities given by $p(z_t|\widetilde{\mathcal{F}}_{t-1})$ of Proposition 2 evaluated at $\{z_t = k\}$ and conditional to $\{z_{t-1} = l\}$. The predictive $p(z_t|\mathcal{F}_{t-1})$, filtered $p(z_t|\mathcal{F}_t)$ and smoothed $p(z_t|\mathcal{F}_T)$ distributions are defined by the recursions:*

$$
\begin{aligned}
p(z_t = k|\mathcal{F}_{t-1}) &= \sum_{l=0}^{\infty} p(z_{t-1} = l|\mathcal{F}_{t-1}) p\left(z_t = k|z_{t-1} = l, r_{t-1}, \mathrm{RV}_{t-1}\right), \ t = 1, \ldots, T \\
p(z_t = k|\mathcal{F}_t) &\propto \sum_{l=0}^{\infty} p(z_{t-1} = l|\mathcal{F}_{t-1}) p\left(z_t = k|z_{t-1} = l, r_{t-1}, \mathrm{RV}_{t-1}\right) p\left(r_t, \mathrm{RV}_t|z_t = k\right), \ t = 1, \ldots, T \\
p(z_t = k|\mathcal{F}_T) &\propto p(z_t = k|\mathcal{F}_t) \sum_{l=0}^{\infty} p\left(z_{t+1} = l|z_t = k, r_t, \mathrm{RV}_t\right) \frac{p(z_{t+1} = l|\mathcal{F}_T)}{p(z_{t+1} = l|\mathcal{F}_t)}, \ t = T-1, \ldots, 1
\end{aligned}
$$

Proposition 4. *Let $\mathcal{F}^Z_t \doteq \sigma\left(\mathcal{F}_t \vee \{z_u\}_{u \leq t}\right)$ be the filtration $\mathcal{F}_t$ enlarged with the hidden states z_u up to time t, and $\lambda(z_t)$, $\chi^{(t)}$ and ψ the quantities defined in Proposition 2. The* *marginal filtered,* $p(h_t|\mathcal{F}_t^Z)$*, and smoothed,* $p(h_t|\mathcal{F}_T^Z)$ *distributions are*

$$p(h_t|\mathcal{F}_t^Z) \propto \mathcal{G}ig\left(\lambda(z_t), \chi^{(t)}, \psi\right), \quad t = 1, \dots, T$$
$$p(h_t|\mathcal{F}_T^Z) \propto \mathcal{G}ig\left(\lambda(z_t) + z_{t+1}, \chi^{(t)}, \psi + 2\beta^{(d)}\right), \quad t = T-1, \dots, 1,$$

with $\mathcal{G}ig\,(\lambda, \chi, \psi)$ *the Generalized Inverse Gaussian distribution with parameters* $\lambda \in \mathbb{R}$*,* $\chi \in \mathbb{R}_+$*,* $\psi \in \mathbb{R}_+$*.*

Proof. See on-line Appendix, where a definition of the Generalized Inverse Gaussian distribution is also provided. □

3 Bayesian Inference

In this section, we discuss the estimation procedure for SV-LHARG(p), emphasizing the role of Proposition 2 and 4. We consider heterogeneous dynamics and $p = 22$ – which corresponds to a monthly horizon – following a common specification in the recent financial econometrics literature (Corsi, 2009). However, the methodology can be easily adapted to the SV-LHARG(p) specification without restrictions.

As it commonly happens in latent variable modeling, the likelihood function of SV-LHARG is a high-dimensional integral with no closed-form solution. Hence, we apply a data-augmentation principle (see Tanner and Wong, 1987) and include the latent variables in the set of observations, thus obtaining a complete-data likelihood function. As regards the initial 22 values of SV-LHARG , we follow Vermaak et al. (2004) and Casarin et al. (2012) and consider a pseudo-likelihood approach by assuming that the observations start at $t = p + 1$. Denoting with $\boldsymbol{\xi}$ and $\mathbf{w}_t$ the two 2-dimensional vectors $\boldsymbol{\xi} = (\mu, \gamma)'$ and

$\mathbf{w}_t = (1, h_t)^{'}$, the complete-data pseudo-likelihood function is given by:

$$\begin{aligned}
&\mathcal{L}\left(r_{p+1:T}, \mathrm{RV}_{p+1:T}, \mathrm{h}_{p+1:T}, z_{p+1:T}|\boldsymbol{\theta}\right)\\
&= \prod_{t=p+1}^{T} \frac{1}{\sqrt{2\pi h_t}} \exp\left(-\frac{1}{2}\frac{(r_t - \boldsymbol{\xi}'\mathbf{w}_t)^2}{h_t}\right) \frac{\mathrm{RV}_t^{\varphi_t - 1}}{\Gamma(\varphi_t)(h_t \exp(\kappa_2)^{\varphi_t})} \exp\left(-\frac{\mathrm{RV}_t}{h_t \exp(\kappa_2)}\right) \\
&\cdot \prod_{t=p+1}^{T} \frac{h_t^{\delta + z_t - 1}}{\Gamma(\delta + z_t)c^{\delta + z_t}} \exp\left(-\frac{h_t}{c}\right) \frac{1}{z_t!} \left(\Theta(\mathbf{h}_{t-1}, \mathbf{l}_{t-1})\right)^{z_t} \exp\left(-\Theta(\mathbf{h}_{t-1}, \mathbf{l}_{t-1})\right).
\end{aligned} \tag{3.1}$$

The description of our Bayesian analysis is completed by the specification of the prior distribution $\pi\left(\boldsymbol{\theta}\right)$ on the parameters $\boldsymbol{\theta}$. Let $\boldsymbol{\beta} = \left(\beta^{(d)}, \beta^{(w)}, \beta^{(m)}\right)$ and $\boldsymbol{\alpha} = \left(\alpha^{(d)}, \alpha^{(w)}, \alpha^{(m)}\right)$, we assume $\pi\left(\boldsymbol{\theta}\right) \propto \mathbb{I}_{\mathbb{R}^2}(\boldsymbol{\xi})\mathbb{I}(\varphi)_{\mathbb{R}_+}\mathbb{I}_{\mathbb{R}}(\kappa_{\mathbf{2}})\mathbb{I}_{\mathbb{R}_+}(\delta)\mathbb{I}_{\mathbb{R}^3_+}(\boldsymbol{\beta})\mathbb{I}_{\mathbb{R}_+}(\boldsymbol{\alpha})\mathbb{I}_{\mathbb{R}^3_+}(\lambda)\mathbb{I}_{\mathcal{A}_{\boldsymbol{\theta}}}(\boldsymbol{\theta})$, where $\mathbb{I}_{\boldsymbol{\Theta}}\left(\boldsymbol{\theta}\right)$ is the indicator function which takes value 1 if $\boldsymbol{\theta} \in \boldsymbol{\Theta}$ and 0 otherwise, and $\mathcal{A}_{\boldsymbol{\theta}}$ is the set of parameter values which satisfy the stationarity condition in Proposition 1. The parameters and latent variables *joint* posterior distribution is

$$\pi\left(\boldsymbol{\theta}, \mathbf{h}_{p+1:T}, \mathbf{z}_{p+1:T}|\mathbf{r}_{p+1:T}, \mathrm{RV}_{p+1:T}\right) \propto \pi\left(\boldsymbol{\theta}\right)\mathcal{L}\left(\mathbf{r}_{p+1:T}, \mathrm{RV}_{p+1:T}, \mathbf{h}_{p+1:T}, \mathbf{z}_{p+1:T}|\boldsymbol{\theta}\right).$$

This distribution is not tractable, thus we follow an MCMC approach and develop a Gibbs sampling algorithm to generate random draws from the posterior distribution and to approximate all posterior quantities of interest (see Casella and Robert, 2004). Note that, in a data-augmentation framework, the estimation of the parameters under the physical measure $\mathbb{P}$ involves an extra computational cost due to the estimation of the latent variables. Despite this difficulty, it is possible to use the analytical filtering and smoothing recursions derived for SV-ARG in order to design an effective MCMC algorithm for posterior approximation.

In particular, the proposed Gibbs sampler for SV-LHARG iterates over the following steps: i) Initialize $\boldsymbol{\theta}$, $\mathbf{z}_{p+1:T}$ and $\mathbf{h}_{p+1:T}$. ii) Sample $\boldsymbol{\theta}$ given $(\mathbf{r}_{p+1:T}, \mathrm{RV}_{p+1:T}, \mathbf{h}_{p+1:T}, \mathbf{z}_{p+1:T})$. iii) Sample $(\mathbf{z}_{p+1:T}, \mathbf{h}_{p+1:T})$ given $(\mathbf{r}_{p+1:T}, \mathrm{RV}_{p+1:T}, \boldsymbol{\theta})$. iv) Go to the second step.

In sampling $\boldsymbol{\theta}$, we consider the following blocks of parameters $\{\boldsymbol{\xi}, \varphi, \kappa_2, \delta, c, \boldsymbol{\beta}, \boldsymbol{\alpha}, \lambda\}$ where $\boldsymbol{\xi} = (\mu, \gamma)$, $\boldsymbol{\beta} = \left(\beta^{(d)}, \beta^{(w)}, \beta^{(m)}\right)$, $\boldsymbol{\alpha} = \left(\alpha^{(d)}, \alpha^{(w)}, \alpha^{(m)}\right)$ are sampled jointly. As emphasized in Chib et al. (2002), sampling parameters by groups is important for reducing the serial dependence in the MCMC output. In the on-line Appendix, we provide some details on the full conditional distributions of the parameters and their sampling methods.

In the third step of the Gibbs sampler we design a multi-move proposal distribution by assuming an auxiliary SV-ARG: we use the analytical relationships in Proposition 2 and 4. Indeed, to sample $(\mathbf{h}_{p+1:T}, \mathbf{z}_{p+1:T})$, we first develop an effective Forward Filtering Backward Sampling (FFBS) for the SV-ARG (see Frühwirth-Schnatter, 2006), then we use this sampler as proposal distribution for $\mathbf{h}_{p+1:T}$ and $\mathbf{z}_{p+1:T}$ in a MH step, in order to sample from $\pi\left(\mathbf{z}_{p+1:T}|\mathbf{r}_{p+1:T}, \mathrm{RV}_{p+1:T}, \mathbf{h}_{p+1:T}, \boldsymbol{\theta}\right)$ and $\pi\left(\mathbf{h}_{p+1:T}|\mathbf{r}_{p+1:T}, \mathrm{RV}_{p+1:T}, \mathbf{z}_{p+1:T}, \boldsymbol{\theta}\right)$. Specifically, we follow the strategy used in Creal (2017) by reformulating the original SV-ARG model as a Markov-switching model with state variable z_t. The regime $z_t \in \{0, \dots, N-1\}$ is the outcome of an N-state inhomogeneous Markov chain with $N < \infty$. Truncating the transition distribution of Proposition 2 and the filtered and smoothed distributions of Proposition 3 on the support set $\{0, \dots, N-1\}$, we obtain a FFBS procedure for the SV-ARG. We apply the Hamilton's filter forward in time, t from $p+1$ to T, to find $p\left(z_t = l|\mathcal{F}_t, \boldsymbol{\theta}\right)$, then the Kim's algorithm backward in time, t from T to $p+1$, to find $p\left(z_t = l|\mathcal{F}_T, \boldsymbol{\theta}\right)$, and draw z_t by multinomial sampling with probabilities $p\left(z_t = l|\mathcal{F}_T, \boldsymbol{\theta}\right)$. Finally, given $\mathbf{z}_{p+1:T}$ a realization of $\mathbf{h}_{p+1:T}$ is obtained by sampling h_t from $p\left(h_t|\mathcal{F}_T\right)$ as in Proposition 4. We investigate the efficiency of the FFBS procedure through a simulation study.

In the MH step for the SV-LHARG latent variables, we improve the MH acceptance rate by applying a random block strategy (see Takahashi et al., 2009; Fiorentini et al., 2014; Billio et al., 2016). At the $j-th$ iteration of the Gibbs sampler we generate the proposals $\mathbf{z}^{(*)}_{\tau:\tau+\delta}$ and $\mathbf{h}^{(*)}_{\tau:\tau+\delta}$, by the FFBS procedure described here above with $\tau \in \{1, \dots, T\}$ and $\delta \in \mathbb{N}_+$ selected randomly such that $\tau + \delta \leq T$. The proposals are either accepted or rejected with probability $\rho\left((\mathbf{z}^{(j-1)}_{\tau:\tau+\delta}, \mathbf{h}^{(j-1)}_{\tau:\tau+\delta}), (\mathbf{z}^{(*)}_{\tau:\tau+\delta}, \mathbf{h}^{(*)}_{\tau:\tau+\delta})\right)$ given by the minimum between 1 and the exponential transform of:

$$
\begin{aligned}
&\log\left(\mathcal{L}\left(r_{\tau+1:\tau+\delta}, \mathrm{RV}_{\tau+1:\tau+\delta}, h^{(*)}_{\tau+1:\tau+\delta}, z^{(*)}_{\tau+1:\tau+\delta}|\boldsymbol{\theta}\right)\right) - \log\left(\mathcal{L}\left(r_{\tau+1:\tau+\delta}, \mathrm{RV}_{\tau+1:\tau+\delta}, h^{(j-1)}_{\tau+1:\tau+\delta}, z^{(j-1)}_{\tau+1:\tau+\delta}|\boldsymbol{\theta}\right)\right) \\
&+ \sum_{t=\tau+1}^{\tau+\delta-1} \log\left(p\left(z^{(j-1)}_t|z^{(j-1)}_{t-1}, r_{t-1}, \mathrm{RV}_{t-1}, \boldsymbol{\theta}\right)\right) + \log\left(p\left(h^{(j-1)}_t|r_{p+1:T}, \mathrm{RV}_{p+1:T}, z^{(j-1)}_{p+1:T}\right)\right) \\
&- \log\left(p\left(z^{(*)}_t|z^{(*)}_{t-1}, r_{t-1}, \mathrm{RV}_{t-1}\right)\right) - \log\left(p\left(h^{(*)}_t|r_{p+1:T}, \mathrm{RV}_{p+1:T}, z^{(*)}_{p+1:T}\right)\right),
\end{aligned}
$$

where $\mathcal{L}$ is the conditional likelihood function in Eq.(3.1). The multi-move proposal allows for a rapid mixing of the MCMC chain. We show the efficiency of the MCMC through some simulation exercises. See on-line Appendices for further details.

4 Financial applications

The goal of the present section is to show that the approach we have proposed so far is of substantial interest in financial applications, especially from an option pricing perspective. A comparison with two benchmark models is also presented. The first one is the RV-LHARG model introduced in Majewski et al. (2015). The second model belongs to the class of GARCH-type option pricing models, the CGARCH by Christoffersen et al. (2008). The RV-LHARG is described by the following equations:

$$\begin{aligned} r_t &= \mu + \gamma \mathrm{RV}_t + \sqrt{\mathrm{RV}_t}\varepsilon_t \\ \mathrm{RV}_t | \mathcal{F}_{t-1} &\overset{d}{\sim} \bar{\mathcal{G}}\left(\delta, \Theta\left(\mathbf{RV}_{t-1}, \mathbf{l}_{t-1}\right), c\right), \end{aligned}$$

where $\varepsilon_t \overset{i.i.d.}{\sim} \mathcal{N}(0,1)$ and $\mathcal{F}_t = \sigma\left(\{r_u, \mathrm{RV}_u\}_{u \leq t}\right)$ is the filtration containing the information about observable quantities available up to time t. The conditional distribution of RV_t is taken as that of h_t in SV-LHARG . Differently, the CGARCH is specified as follows:

$$\begin{aligned} r_t &= \mu + \gamma h_t + \sqrt{h_t}\varepsilon_t \\ h_t &= q_t + b_s\left(h_{t-1} - q_{t-1}\right) + a_s\left(\left(\varepsilon_{t-1} - c_s\sqrt{h_{t-1}}\right)^2 - \left(1 + c_s^2 q_{t-1}\right)\right) \\ q_t &= \omega + \rho q_{t-1} + \varphi\left(\left(\varepsilon_{t-1}^2 - 1\right) - 2c_l\sqrt{h_{t-1}}\varepsilon_{t-1}\right), \end{aligned}$$

where $(h_{t-1} - q_{t-1})$ and q_t represent the short- and long-run persistent volatility components, respectively. Both benchmark models are estimated by means of maximum likelihood (ML henceforth). In the RV-LHARG model all quantities are observable, so that ML estimation is straightforward. Estimation of the CGARCH proceeds as customary for GARCH models combining filtering of the latent short- and long-run conditional volatility components with ML.

4.1 Model comparison

We present our empirical results on daily log-returns and realized variances for the S&P500 Futures. Our sample spans the period from January 1, 1997 to December 31, 2009. Realized variances are computed from tick-by-tick data over the same time interval. To remove the jump component from the RV, we employ the same methodology as in Corsi et al. (2013) and Majewski et al. (2015). Specifically: i) the total variation of the log-price process is estimated using the Two-Scale estimator by Zhang et al. (2005); ii) the fraction of total variation due to jumps is identified and eliminated by means of the Threshold Bi-power variation method of Corsi et al. (2010); iii) finally, most extreme observations (seemingly due to volatility jumps) are discarded from the volatility series. Neglecting the jump component and extreme observations may introduce possible misspecification, especially in pricing options. A similar remark applies for the overnight component, for which no realized measures are available. As explained in the on-line Appendix, we account for these effects by means of the parameter φ. It is sampled MCMC, but the initial value is fixed as in Hansen and Lunde (2005). In this respect, SV-LHARG is well-designed, since the two measurement equations properly account for both trading hour and daily scale effects.

We estimate SV-ARG, SV-LARG, and SV-HARG by using the Bayesian inference procedure – more details can be found in the on-line Appendix – on the sample from January 1, 1997 to December 31, 2006. We estimate SV-LHARG on the three periods: from January 1, 1997 to December 31, 2006, from January 1, 1998 to December 31, 2007 and from January 1, 1999 to December 31 2008. RV-LHARG and CGARCH are estimated over the three time periods, too. In this way we can discuss the option pricing performance, both in-sample and out-of-sample, of the different models, in particular over the global 2007-2008 financial crisis. For sake of space, the main text reports parameter estimates for the periods January 1, 1997 – December 31, 2006 (Table 1) and January 1, 1998 – December 31, 2007 (Table 2). Further estimation results are collected in the on-line Appendix. Parameters δ for SV-LHARG and RV-LHARG, and ω for CGARCH are computed by targeting the sample mean of RV and the variance of returns, respectively (see also Christoffersen et al., 2015). Tables report the risk premium ν_1, too. Details about the option sample used to calibrate the premium are postponed to Section 4.2.

Table 1: From left to right: ML estimates with robust standard errors for the RV-LHARG, MCMC estimates with standard errors for the SV-LHARG, SV-ARG, SV-LARG, SV-HARG, ML estimates with standard errors for the CGARCH. Period: January 1, 1997 to December 31, 2006.

	RV-LHARG	SV-LHARG	SV-ARG	SV-LARG	SV-HARG		CGARCH
Parameters						Parameters	
γ	0.9	-0.03	-0.13	-0.08	-0.13	γ	1.0
	(1.7)	(0.03)	(0.03)	(0.03)	(0.03)		(0.8)
φ	–	0.60	0.62	0.62	62	b_s	0.73
		(0.01)	(0.01)	(0.01)	(0.01)		(0.05)
κ_2	–	-2.72	-2.61	-2.36	-2.65	a_s	3e-06
		(0.05)	(0.04)	(0.03)	(0.04)		(1e-06)
c	1.29e-05	4.75e-06	2.23e-06	3.19e-06	2.30e-06	c_s	4e+02
	(1e-07)	(8e-08)	(5e-08)	(5e-08)	(8e-09)		(2e+02)
δ	1.22	1.15	3.02	2.66	1.15	ω	1.30e-06
β_d	1.8e+04	2.9e+04	4.29e+05	2.79e+05	3.61e+05	c_l	1.4e+02
	(1e+03)	(5e+03)	(8e+03)	(5e+03)	(4e+03)		(2e+01)
β_w	1.5e+04	2.3e+04	—	—	3.8e+04	φ	2.4e-06
	(1e+03)	(3e+03)			(4e+03)		(4e-07)
β_m	1.0e+04	1.8e+04	—	—	2.7e+04	ρ	0.991
	(4e+03)	(4e+03)			(3e+03)		(2e-03)
α_d	0.263	0.56	—	1	—		
	(1e-03)	(0.05)		(0.1)			
α_w	0.195	0.45	—	—	—		
	(4e-03)	(0.08)					
α_m	0.03	4e-04	—	—	—		
	(0.03)	(1e-04)					
λ	214	350		92			
	(4)	(10)		(8)			
ν_1	-1424	-2439	-2537	-2938	-2327	ν_1	-12242
Persistence	0.84	0.93	0.95	0.92	0.98		0.997

Let us start by commenting on the parameter estimates within the SV-LHARG framework over the period January 1, 1997, to December 31, 2006. In the present work, we adopt the same convention used in Creal (2017) by writing the drift term of the log-return dynamics as $\mu + \gamma h_t$. In Creal (2017), the estimated γ is negative and significant, implying that the distribution of returns is negatively skewed (see the discussion in the cited paper). In our case, γ is negative and significant for SV-ARG, SV-LARG, and SV-HARG , whereas it is not significant in SV-LHARG . For all models, the estimated overnight factor φ is

Table 2: From left to right: ML estimates with robust standard errors for the RV-LHARG, MCMC estimates with standard errors for the SV-LHARG , ML estimates with standard errors for the CGARCH. Period: January 1, 1998 to December 31, 2007.

	RV-LHARG	SV-LHARG		CGARCH
Parameters			Parameters	
γ	0.1	-0.02	γ	0.9
	(1.8)	(0.03)		(0.7)
φ	–	0.60	b_s	0.75
		(0.02)		(0.04)
κ_2	–	-2.79	a_s	2e-06
		(0.06)		(1e-06)
c	1.24e-05	4.7e-06	c_s	6e+02
	(1e-07)	(1e-07)		(3e+02)
δ	1.30	1.22	c_l	1.6e+02
				(3e+01)
β_d	1.34e+04	3.2e+04	ω	1.37e-06
	(1e+02)	(5e+03)		
β_w	6.1e+03	8e+03	φ	2.2e-06
	(3e+02)	(3e+03)		(4e-07)
β_m	3.9e+03	2.2e+04	ρ	0.990
	(4e+02)	(5e+03)		(2e-03)
α_d	0.169	0.44		
	(8e-03)	(0.05)		
α_w	0.168	0.32		
	(1e-03)	(0.07)		
α_m	0.069	2.4e-04		
	(2e-03)	(9e-04)		
λ	333	411		
	(3)	(30)		
ν_1	-1584	-2308		-17339
Persistence	0.84	0.93		0.998

smaller than one – as expected – and indicates that the volatility during the trading hours ranges between 60% to 62% of the total daily variation. Concerning the persistence – computed by means of the first term inequality (2.5) – its value decreases from 0.95 (SV-ARG) to 0.92 (SV-LARG), and from 0.98 (SV-HARG) to 0.93 (SV-LHARG) when the leverage effect is included into the model. This fact is in accordance with findings in Corsi et al. (2013) and Majewski et al. (2015). Within SV-LHARG , the impact of past lags on the current value of the conditional variance is determined by the partial auto-correlation coefficients. According to our estimates, the sensitivity of the conditional mean h_t on h_{t-1}, $h_{t-1}^{(w)}$

and $h_{t-1}^{(m)}$ is $c\left(\beta^{(d)}+\lambda^2\alpha^{(d)}\right)=0.46$, $c\left(\beta^{(w)}+\lambda^2\alpha^{(w)}\right)=0.38$ and $c\left(\beta^{(m)}+\lambda^2\alpha^{(m)}\right)=0.09$, respectively. We find evidence of a decreasing impact of past lags on the current value of the conditional variance (see also the estimates of the SV-HARG model). This fact has already been documented for the RV-LHARG class of models (see Corsi et al., 2013; Majewski et al., 2015). Concerning the comparison of SV-LHARG to competitors, its persistence is 0.93, while the persistence of RV-LHARG and CGARCH are equal to 0.84 and 0.997, respectively. With respect to RV-LHARG, it is evident that the introduction of the latent process mitigates the impact of the RV measurement errors and favours a more persistent conditional variance. For CGARCH, the persistence is very high, leading to a nearly integrated variance process. The level of persistence has important consequences on the term structure of skewness and kurtosis. Both are crucial ingredients in reproducing the correct shape of the implied volatility surface (Das and Sundaram, 1999). Figure 1 plots the skewness (left panel) and excess kurtosis (right panel) associated to the six models RV-LHARG, SV-LHARG, SV-ARG, SV-LARG, SV-HARG, and CGARCH under the risk-neutral measure $\mathbb{Q}$. It confirms that SV-ARG and SV-HARG are not designed to replicate the negative skewness. For RV-LHARG and for all SV models with no heterogeneous volatility structure, the level of both skewness and kurtosis is moderate and rapidly declines toward zero. The picture is significantly different for SV-LHARG and CGARCH. Among the SV class of models, SV-LHARG reaches the highest (lowest) levels of excess kurtosis (skewness). On the other hand, CGARCH is the model with the maxima level of excess kurtosis. This fact will have important consequences on the pricing performances. We expect the best performance of the CGARCH for long-term options in in-sample tests. However, the very high level of persistence can lead to systematic over-pricing of long-term options, whenever the model miss-fits the short-term level of volatility – as it may happen out-of-sample.

Figure 2 shows the daily realized variance annualized and in percentage terms scaled by the estimated overnight factor (*black line*) and the filtered realized variance (*gray-line*) in SV-LHARG from 1999 to 2009. The filtering procedure reduces significantly the fluctuations of the conditional latent volatility. Finally, to check for possible model miss-

Figure 1: Skewness and excess kurtosis of RV-LHARG , SV-LHARG , SV-ARG , SV-LARG , SV-HARG ,and CGARCH processes under the risk-neutral measure $\mathbb{Q}$. The parameter estimates are taken from Table 1.

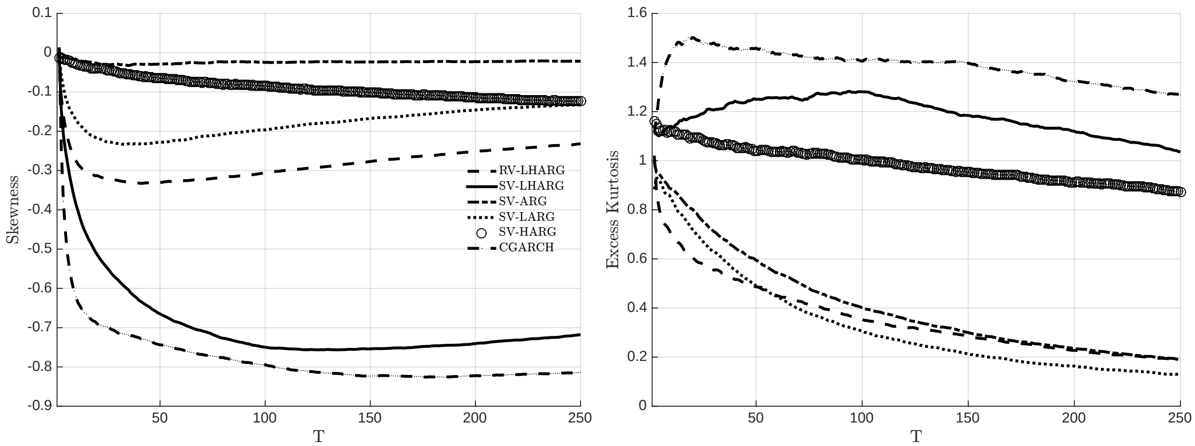

specifications, we consider demeaned log-returns standardized either by the square root of the RV and by the filtered CV (Andersen et al., 2010, see). Table 3 summarizes the results for the period 1999-2009, but similar conclusions hold true for the other time frames. At the 5% significance level, the Jarque-Bera test does not reject normality for SV-LHARG and rejects it for RV-LHARG. Then, SV-LHARG provides a better description of the empirical data.

Figure 2: Daily realized variance scaled by the estimated overnight factor (black line) and filtered realized variance (gray line) from 1999 to 2009.

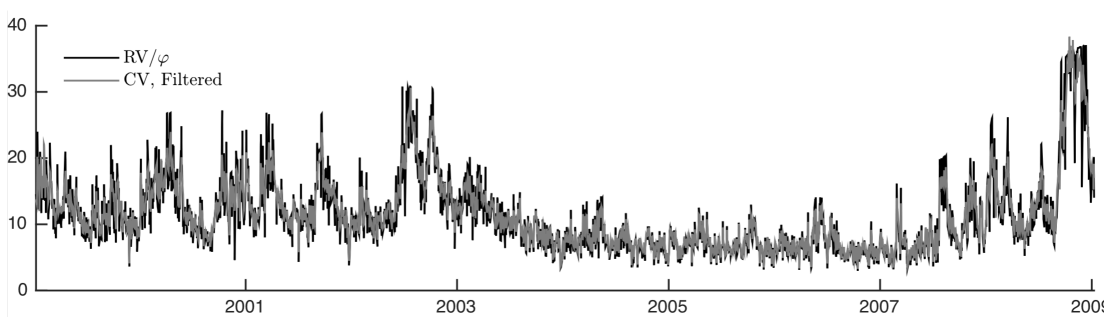

4.2 Option pricing: Performance assessment

As for option pricing, we perform our analysis on European options, written on the S&P500 index. The option price data sample is provided by Optionmetrics for the period from January 1, 1997 to January 6, 2010 – which is the last date included in this specific dataset.

Table 3: Model misspecification tests for log-returns standardized by $\sqrt{RV_t}$ and $\sqrt{h_t}$. Lines one to four: Mean, variance, skewness, and kurtosis of standardized log-returns. Last line: Statistics and p-values (between parenthesis) for the Jarque-Bera test.

Statistics	RV-LHARG		SV-LHARG	
	1999-2009		1999-2009	
Mean	0.063		0.001	
Variance	0.928		0.917	
Skewness	0.264		-0.076	
Kurtosis	3.599		3.057	
Jarque-Bera	64.22	(6.9e-15)	2.75	(0.25)

As it is customary in the literature, a filter removes options with maturity less that 10 days and more that 365 days, and prices less than 5 cents (see Barone-Adesi et al., 2008; Corsi et al., 2013; Majewski et al., 2015). Following Corsi et al. (2013), we consider only Out-of-The-Money (OTM) put and call options for each Wednesday. Using K/S_t as definition of moneyness, we filter out Deep-Out-The-Money (DOTM) options with moneyness larger than 1.2 for call options and less than 0.8 for put options. Wider range of moneyness could be considered. However, for DOTM options all models should require a correction to include the impact of jumps. We investigated what happens for moneyness ranging from 0.5 to 1.5. The comparative performances among models do not change. Moreover, when moneyness varies within the interval $(0.8, 1.2)$, the fraction of neglected volume is 4% for the shortest time-to-maturities, 4.9% for the short, 6% for the medium, and 18% for the longest ones. We refer to put as DOTM options if their moneyness is between 0.8 and 0.9 and as Out-The-Money (OTM) if $0.9 < m \leq 0.98$. On the other hand, call options are termed DOTM if $1.1 < m \leq 1.2$ and OTM if $1.02 < m \leq 1.1$; options are at-the-money (ATM) if $0.98 < m \leq 1.02$. As far as the time to maturity τ is concerned, we classify options as short maturity ($\tau \leq 50$ days), short-medium maturity ($50 < \tau \leq 90$ days), long-medium maturity ($90 < \tau \leq 160$ days), and long maturity ($\tau > 160$ days).

We now analyse the option pricing performance. In our in-sample analysis, we consider the problem faced by a trader who knows the true model, but does not have the ability to see the future level of variance. We fix the parameters for each models at their full sample estimates and in the pricing kernel (i.e. the SDF) of both SV and CGARCH models we replace the latent volatility by its filtered value. In the out-of-sample exercises, we fix the parameters at the values estimated in-sample and use the filtered volatility in the pricing kernel. In order to derive the risk-neutral dynamics, the value for risk premium parameters (ν_1, ν_2) has to be specified. The value of ν_2 is reported in Tables 1 and 2 and is computed from option prices spanning the in-sample time period used for estimation. For models in the SV-LHARG family risk-neutralization is achieved by means of the SDF in Eq. (2.6) replacing $\{h_u\}_{u\leq t}$ in $\widetilde{\mathcal{F}}_t$ by their filtered values. In the recent option pricing practice, the pricing kernel employed for the risk-neutralization of CGARCH does depend on volatility (Christoffersen et al., 2013). Thus, to ensure a fair comparison among the models, we assume the following SDF for the CGARCH

$$M_{t,t+1} = \frac{e^{-\nu_1 h_{t+2} - \nu_2 r_{t+1}}}{\mathbb{E}^{\mathbb{P}}\left[e^{-\nu_1 h_{t+2} - \nu_2 r_{t+1}} | \widetilde{\mathcal{F}}_t\right]},$$

where the variance risk premium ν_1 multiplies the latent conditional variance. Since h_{t+1} is predictable, following Christoffersen et al. (2013), the pricing kernel depends on h_{t+2}. In the applications, we replace the latent conditional variance by its filtered value. In particular, the conditioning set of volatilities – $h_t, \ldots, h_{t-21}$ for SV-LHARG, h_t for CGARCH, and $\mathrm{RV}_t, \ldots, \mathrm{RV}_{t-21}$ for RV-LHARG – is fixed equal to the unconditional volatility level of each model. In order to compute option prices and the associated implied volatilities, we adopt the COS method (Fang and Oosterlee, 2008), which has been proven to be numerically efficient. The method is based on Fourier-cosine expansion and it is feasible as long as the log-return characteristic function is available in closed-form. To sum up, we proceed pricing options following four steps: i) Estimation of the model under the physical measure $\mathbb{P}$; ii) unconditional calibration of the parameter ν_1; iii) mapping of the estimated parameters into the parameters under $\mathbb{Q}$, and iv) computation of option prices via COS method using the MGF formula (see on-line Appendix 1) with risk-neutral parameters.

4.2.1 Discussion of the results

We assess both static and dynamic performances. Following previous works (Renault, 1997; Corsi et al., 2013; Majewski et al., 2015), as static performance measure we employ the

Root Mean Square Error on the percentage IV (henceforth RMSE_{IV}):

$$\text{RMSE}_{\text{IV}} = \sqrt{\sum_{i=1}^{\text{N}} \frac{\left(\text{IV}_i^{\text{MOD}} - \text{IV}_i^{\text{MKT}}\right)^2}{\text{N}}},$$

where N is the number of options, and IV^{MOD} and IV^{MKT} are the model and the market implied volatility, respectively. Instead, as a dynamic properties we investigate the ability of the different models to describe the time evolution of the implied volatility surface, focusing our attention on the ATM short-end of the IV surface. Importantly, we assess the option pricing performance both in-sample and out-of-sample.

The comparison between models in the SV class are reported in the on-line Appendix. SV-LHARG consistently shows the best option pricing performance among the models and, for this reason, hereafter, only SV-LHARG will be used in the comparison with the RV-LHARG and CGARCH models. Let us focus on the estimation period January 1, 1998 – December 31, 2007. The analogous analyses for the other two periods are available in the on-line Appendix. We proceed as follows: i) estimate the three models over the selected time interval and calibrate the variance risk-premium ν_1; ii) price options over the estimation intervals (*in-sample* pricing); iii) keep the parameter values and risk premium fixed as at point i) and price options over the following year, from January 1, 2008 to December 31, 2008 (*out-of-sample* pricing). The overnight correction factor φ, the shape parameter δ for RV models, and the CGARCH parameter ω are fixed via targeting on the estimation period and kept unchanged out-of-sample.

Table 4 reports the in-sample option pricing performance. The significance of the relative performances is assessed by means of a t-test using HAC standard errors to take into account the dependence structure of RMSE that are likely to be a function of time, moneyness, time-to-maturity, and level of the market and its volatility (see also Christoffersen et al., 2016). Overall (Panel D), SV-LHARG outperforms both RV-LHARG and CGARCHin all the ranges of moneyness. Nonetheless, CGARCH fares better than RV-LHARG . This latter result deserves a more detailed discussion. Indeed, Corsi et al. (2013), Table 4 second row, reported a comparison between the HARGL model and CGARCH assessing the (global) superiority of the former over the period January 1, 1997 – December 31, 2004.

Table 4: Option pricing performance on S&P500 OTM options from January 1, 1998 to December 31, 2007. Parameters values are from Table 2. Panel A: Percentage implied volatility root mean squared error ($\mathrm{RMSE_{IV}}$) of the SV-LHARG model sorted by moneyness and maturity. Panels B and C: Relative $\mathrm{RMSE_{IV}}$ with statistical significance from a t-test ($^{*}: p$-value < 0.05, $^{**}: p$-value < 0.01, $^{***}: p$-value < 0.001) . Panel D: global option pricing performance. $\mathrm{RMSE_{IV}}$ of the SV-LHARG model for different moneyness range (first row). Second and last rows: Relative $\mathrm{RMSE_{IV}}$.

Moneyness	Maturity			
	$\tau \leq 50$	$50 < \tau \leq 90$	$90 < \tau \leq 160$	$160 < \tau$
Panel A	SV-LHARG Implied Volatility RMSE			
$0.8 \leq m \leq 0.9$	13.01	7.45	6.32	4.80
$0.9 < m \leq 0.98$	5.74	3.88	4.15	3.97
$0.98 < m \leq 1.02$	3.08	2.93	3.39	3.80
$1.02 < m \leq 1.1$	3.33	3.66	3.94	6.29
$1.1 < m \leq 1.2$	7.41	2.97	2.79	5.67
Panel B	SV-LHARG/RV-LHARG Implied Volatility RMSE			
$0.8 \leq m \leq 0.9$	0.98***	0.91***	0.88***	0.84***
$0.9 < m \leq 0.98$	0.99***	0.89***	0.88***	0.88***
$0.98 < m \leq 1.02$	0.91***	0.80***	0.83**	0.89***
$1.02 < m \leq 1.1$	0.90***	0.74***	0.77***	0.89***
$1.1 < m \leq 1.2$	1.12***	0.95***	0.79***	0.92***
Panel C	SV-LHARG/CGARCH Implied Volatility RMSE			
$0.8 \leq m \leq 0.9$	1.06***	1.03***	1.03***	1.07***
$0.9 < m \leq 0.98$	0.99	0.94	0.99***	1.05***
$0.98 < m \leq 1.02$	0.80***	0.90	0.96**	0.99***
$1.02 < m \leq 1.1$	0.79***	1.17***	1.15***	1.03
$1.1 < m \leq 1.2$	0.70***	0.85**	1.12***	1.06***
Panel D				
Model	Moneyness			
	$0.9 < m < 1.1$		$0.8 < m < 1.2$	
SV-LHARG	4.48		5.65	
SV-LHARG/RV-LHARG	0.91***		0.93***	
SV-LHARG/CGARCH	0.94***		0.97*	

To dig into this result, we repeated the estimation and calibration of SV-LHARG , RV-LHARG , and CGARCH over the same period. Consistently with Corsi et al. (2013), the global pricing performance favours SV-LHARG , while RV-LHARG and CGARCH rank second and third, respectively. When including periods following 2004, the results advocate for those models with the largest persistence (CGARCH and SV-LHARG). To provide an explanation of why this happens, let us look (again) at Figure 2. When compared with the previous ten years, the years 2005–2006 are characterized by a low level of unconditional volatility. RV models struggle to capture the downward swing in volatility. To track the 2005-2006 regime, the conditional volatility should decrease. In order to do so, the conditional mean of gamma models has to decrease, without compromising the unconditional target level. This effect can be achieved by inflating the model persistence and by decreasing the level of the shape parameter δ. The latter is bounded from below by one, the so-called Feller condition. Beside, being the conditional variance of the latent volatility proportional to the shape parameter, a decrease in δ lowers the dispersion of the conditional volatility. These constraints tighten the relation between persistence, unconditional targeting, conditional mean and variance of the volatility process in RV models. The same constraints do not hold for CGARCH. Consistently, CGARCH provides the best description of the market ATM volatility during 2005-2006, when it is sizeably low. During the same period, SV-LHARG partially catches up CGARCH, while RV-LHARG is not adequately flexible. The SV dynamics describes a conditional volatility process which is less disperse than the RV time series. Then, the shape parameter can take a smaller value, thus decreasing the conditional mean and preserving the long-term level by inflating the volatility persistence. This picture is confirmed by the value of the estimated parameters, and also by looking at the dynamic side of the pricing performance. More precisely, Figure 3 reports the evolution of the IV level (i.e., the average IV of short-term, ATM options) implied by SV-LHARG, RV-LHARG, and CGARCH for the period January 1, 1999 – December 31, 2008. The degree of accuracy in tracking the short-end of the IV surface before and after 2004 varies across different models. Before 2004 and after 2006, both SV-LHARG and RV-LHARG have more reactive dynamics than CGARCH, which tends to reproduce the empirical level dynamics with some delay. Within the intermediate time window – which corresponds to the low volatility period – contrary to both SV-LHARG and CGARCH, RV-LHARG is not able to adequately track the IV level. It systematically over-estimates the volatility unconditional level. Consistently with explanation above, the persistence of RV-LHARG is moderate and never exceeds 0.85. Finally, the choice of the 1999–2008 time period allows to assess graphically the relative performance of the three models in the final part of 2008, after the rise of volatility ignited by the Lehman Brothers default. It is clear that – at variance with the CGARCH– the RV measure provides the SV-LHARG with the ability to promptly react to sudden changes of market volatility.

To gain a deeper understanding of the pricing performances, Panel B and C of Table 4 reports the results in terms of RMSEs disaggregated for different maturities and moneyness. SV-LHARG always outperforms the RV-LHARG model (Panel B). When compared to CGARCH, the performance is more balanced (Panel C). For short time-to-maturities, SV-LHARG takes advantage of the economic content of the realized measures and fares much better. On the contrary, in the long-run, the strongest persistence of the CGARCH guarantees to this model the best in-sample performance.

As far as the out-of-sample analysis is concerned, Tables 5 ans 6 confirm that, globally, SV-LHARG model outperforms RV-LHARG. When considering CGARCH, the same is approximately true only for the period January 1, 2008 – December 31, 2008. In the other two periods – from January 1, 2007 to December 31, 2007 and from January 1, 2009 to December 31, 2009 – reported for completeness, the picture is much less clear and the RMSE_{IV} ratio is not always statistical significant. For 2007, this fact is consistent with the observation that during the preceding two years the ability of SV-LHARG to track the short term ATM IV volatility is slightly worse than that of CGARCH.

This section concludes reporting two examples of implied volatility smiles reproduced by the three classes of models explored in this paper. For the in-sample smiles, we consider time-to-maturities ranging from 50 to 90 days. For the out-of-sample exercise, we move to time-to-maturities ranging from 10 to 50 days. In both cases, the smile of empirical data is quite pronounced. The left panel in Figure 4 shows the in-sample smiles from the market together with those of SV-LHARG, RV-LHARG, and CGARCH averaged over the period January 1, 1999 – December 31, 2008. The right panel reports the smiles obtained averaging the data on the out-of-sample period January 1, 2008 – December 31, 2008. The plots confirm the ability of the SV model to adequately track the ATM level of the IV at short time-to-maturities, and to reproduce the qualitative features of the smile in a comparatively better way than competitor models.

Figure 3: *Level* dynamic from January 1, 1999 to December 31, 2008. *Level* is defined as the average implied volatility of ATM options (precisely, options with moneyness $0.95 < m < 1.05$) at the shortest available maturity on a given day. In each panel, the black line represents the data, the gray line, the model. The parameter estimates are taken from Table 10 in the on-line Appendix.

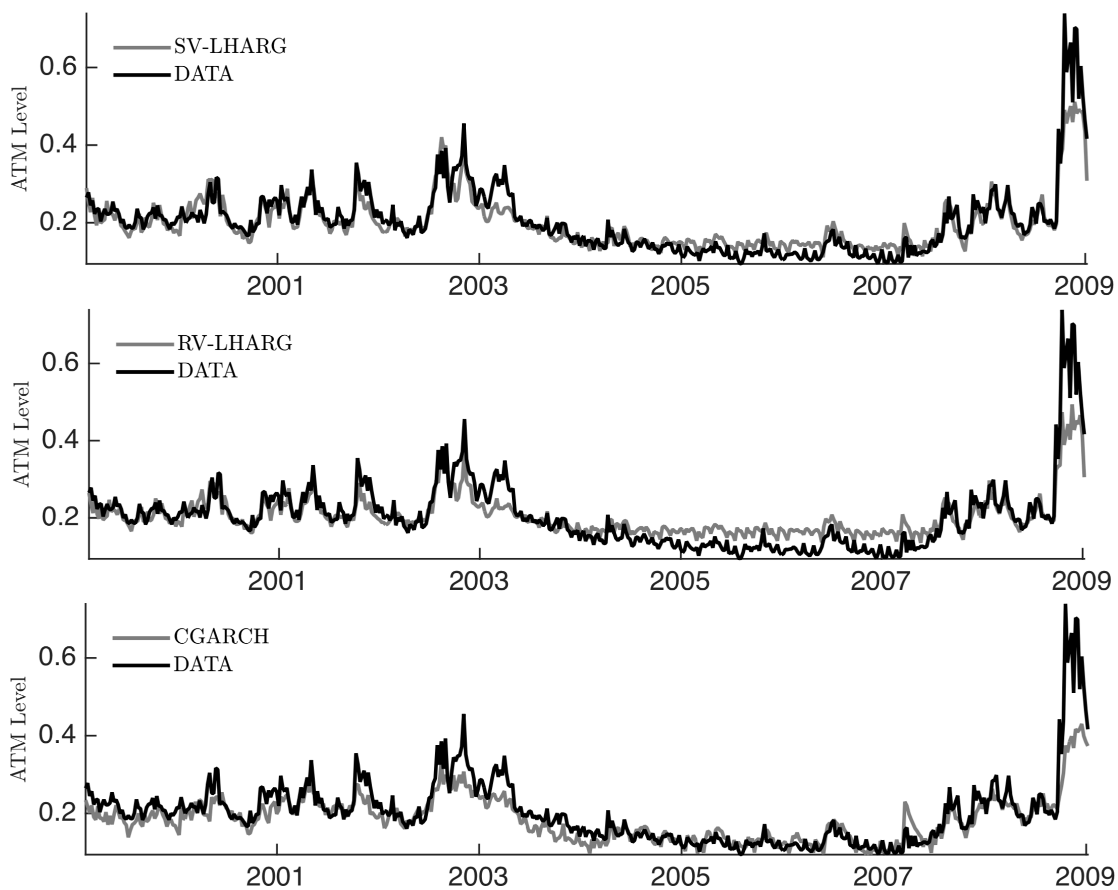

Table 5: Out-of-sample option pricing performance on S&P500 OTM options. In each panel the relative RMSE_{IV} with significance levels, sorted by moneyness (rows) and maturity (columns).

Moneyness	Maturity $\tau \leq 50$	$50 < \tau \leq 90$	$90 < \tau \leq 160$	$160 < \tau$
Out of sample period: January 1, 2007 – December 31, 2007				
Panel A1	SV-LHARG/RV-LHARG Implied Volatility RMSE			
$0.8 \leq m \leq 0.9$	0.85***	0.69***	0.70***	0.72*
$0.9 < m \leq 0.98$	0.78***	0.68***	0.43**	0.93
$0.98 < m \leq 1.02$	1.00	0.93*	0.90	1.00
$1.02 < m \leq 1.1$	1.18**	1.06	0.94	1.04***
$1.1 < m \leq 1.2$	1.14***	1.39	1.08	1.02
Panel A2	SV-LHARG/CGARCH Implied Volatility RMSE			
$0.8 \leq m \leq 0.9$	0.99**	0.81***	0.88***	0.85*
$0.9 < m \leq 0.98$	0.83***	0.67***	0.82	0.97
$0.98 < m \leq 1.02$	0.86	0.79	1.02	1.07
$1.02 < m \leq 1.1$	1.46***	1.46***	1.20***	1.10***
$1.1 < m \leq 1.2$	0.86	2.97***	1.73***	1.14***
Out of sample period: January 1, 2008 – December 31, 2008				
Panel B1	SV-LHARG/RV-LHARG Implied Volatility RMSE			
$0.8 \leq m \leq 0.9$	0.59***	0.45***	0.43***	0.49***
$0.9 < m \leq 0.98$	0.47***	0.34***	0.38***	0.44***
$0.98 < m \leq 1.02$	0.52***	0.38***	0.38***	0.41***
$1.02 < m \leq 1.1$	0.98	1.01	1.09	0.90
$1.1 < m \leq 1.2$	1.05	1.49**	1.46	1.05
Panel B2	SV-LHARG/CGARCH Implied Volatility RMSE			
$0.8 \leq m \leq 0.9$	0.55***	0.45***	0.49***	0.61***
$0.9 < m \leq 0.98$	0.39***	0.32***	0.43***	0.54***
$0.98 < m \leq 1.02$	0.39***	0.30***	0.38***	0.49***
$1.02 < m \leq 1.1$	0.64	0.78	0.99	1.03
$1.1 < m \leq 1.2$	0.57***	1.02**	1.35	1.21

5 Conclusions

Motivated by the presence of measurement errors in the empirical RV measures, we introduce a new family of discrete-time SV option pricing models, named SV-LHARG(p). The SV-LHARG(p) model is characterized by two *measurement equations* (one extracting information from the daily returns and the other from the RV measure) and a transition equation for the latent CV states described by a Heterogeneous Autoregressive Gamma process with leverage effects. SV-LHARG(p) represents the first semi-analytical option pricing framework for discrete-time SV models incorporating RV. Indeed, it is completely characterized in several respects: (i) the recursive formula of the conditional MGF un-

Table 6: (Continued from Table 5) Panel D: Global option pricing performance over the three out-of-sample periods.

Moneyness	Maturity $\tau \leq 50$	$50 < \tau \leq 90$	$90 < \tau \leq 160$	$160 < \tau$
Out of sample period: January 1, 2009 – December 31, 2009				
Panel C1	SV-LHARG/RV-LHARG Implied Volatility RMSE			
$0.8 \leq m \leq 0.9$	0.98	0.93	0.92	0.90
$0.9 < m \leq 0.98$	0.95**	0.91	0.94***	0.92***
$0.98 < m \leq 1.02$	0.95***	0.95***	0.96**	0.92***
$1.02 < m \leq 1.1$	1.04*	0.95***	0.95***	0.85***
$1.1 < m \leq 1.2$	1.07***	0.97**	0.91***	0.85***
Panel C2	SV-LHARG/CGARCH Implied Volatility RMSE			
$0.8 \leq m \leq 0.9$	1.05	1.06	1.05	0.99
$0.9 < m \leq 0.98$	1.04	1.05	1.04	0.97
$0.98 < m \leq 1.02$	0.99	1.03*	1.00	0.93
$1.02 < m \leq 1.1$	0.85*	0.92	0.91	0.85
$1.1 < m \leq 1.2$	0.80	0.77	0.80	0.75

Panel D Model	Moneyness $0.9 < m < 1.1$	$0.8 < m < 1.2$
Out of sample period: January 1, 2007 – December 31, 2007		
SV-LHARG/RV-LHARG	0.93	0.97***
SV-LHARG/CGARCH	1.01	1.03
Out of sample period: January 1, 2008 – December 31, 2008		
SV-LHARG/RV-LHARG	0.62***	0.59***
SV-LHARG/CGARCH	0.52***	0.49***
Out of sample period: January 1, 2009 – December 31, 2009		
SV-LHARG/RV-LHARG	0.92***	0.94***
SV-LHARG/CGARCH	0.98*	0.98*

der $\mathbb{P}$, (ii) the explicit change of measure for a general and flexible exponentially affine SDF, (iii) the no-arbitrage condition in terms of risk premia, (iv) the explicit one-to-one mapping between the parameters of the latent processes under $\mathbb{P}$ and $\mathbb{Q}$, (v) the recursive formula for the conditional MGF under $\mathbb{Q}$. In addition, building on Creal (2017), we derive the analytical filtering and smoothing for the basic specification of the SV-LHARG(p) with $p = 1$ and no leverage effect, dubbed SV-ARG. We employ these results to design an effective Bayesian inference procedure for both the parameters and the latent factor of the general model SV-LHARG(p). The estimation methodology is extensively tested on simulated data and applied to real data on the S&P 500 Future index. The financial application in the context of option pricing consent to benchmark SV-LHARG with competitor

Figure 4: IV smiles from the market (triangles), from the CGARCH (circles), from the SV-LHARG (diamonds), and from the RV-LHARG (squares). Left panel: in-sample period, January 1, 1999 to December 31, 2008. Right panel: out-of-sample smiles from January 1, 2008 to December 31, 2008.

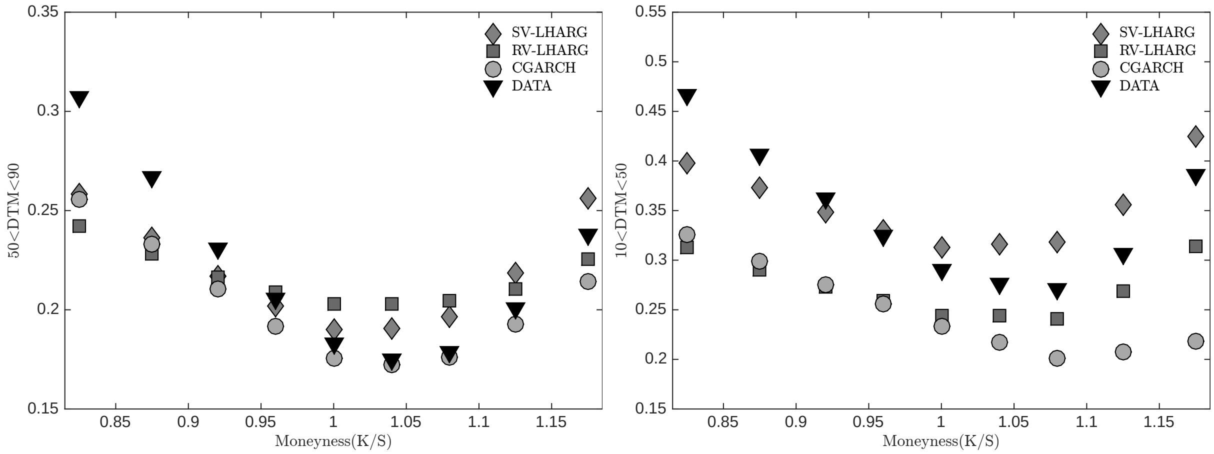

models. Our findings shows that the SV-LHARG model tracks the dynamics of the short time-to-maturity ATM implied volatility surface with remarkable realism. Consistently with what has been documented in Corsi et al. (2013), the CGARCH tends to reproduce the empirical level with some delay (especially during periods of high volatility), whereas the SV model reacts more dynamically to changes in the volatility level. The high level of persistence of volatility in the SV-LHARG model guarantees a better pricing performance than that of the RV-LHARG model. This holds true both in-sample and out-of-sample. Concerning the CGARCH, the SV-LHARG performs better in the short-run and although its behaviour worsen comparatively for longer horizons, the overall performance remain superior. Additionally, SV-LHARG fares better than CGARCH in periods of market turmoil, in particular during the (out-of-sample) high volatility January 1, 2008–December 31, 2008 episode.

6 Acknowledgements

All authors warmly thank Drew D. Creal for helpful comments on the implementation of the algorithm for computing the Bessel function of the second kind and Dario Alitab for support during the development of the pricing code. All authors thank Mark Jensen, Christian P. Robert, Francesco Ravazzolo, Herman K. van Dijk for helpful comments and fruitful discussion. We also thank all the participants of the European Seminar on Bayesian Econometrics 2016 in Venice, of the 1st DEM Workshop in Financial Econometrics 2016 in Verona. The research activity of RC is supported by funding from the European Union, Seventh Framework Programme `FP7/2007-2013` under Grant agreement `FP7/2007-2013`, and by the Italian Ministry of Education, University and Research (`MIUR`) `PRIN 2010-11` Grant `MISURA`. GL acknowledges research support from the Scuola Normale Superiore Grant `SNS_14_BORMETTI` and `CI14_UNICREDIT_MARMI`. This research used the SCSCF multiprocessor cluster system at University Ca' Foscari of Venice.

References

Alitab, D., G. Bormetti, F. Corsi, and A. A. Majewski (2019). A jump and smile ride: Jump and variance risk premia in option pricing. *Journal of Financial Econometrics*, doi: 10.1093/jjfinec/nbz001.

Andersen, T. G. and T. Bollerslev (1998). Answering the skeptics: Yes, standard volatility models do provide accurate forecasts. *International Economic Review 39*(4), 885–905.

Andersen, T. G., T. Bollerslev, F. X. Diebold, and P. Labys (2001). The distribution of realized exchange rate volatility. *Journal of the American Statistical Association 96*(453), 42–55.

Andersen, T. G., T. Bollerslev, P. Frederiksen, and M. Ørregaard Nielsen (2010). Continuous-time models, realized volatilities, and testable distributional implications for daily stock returns. *Journal of Applied Econometrics 25*(2), 233–261.

Andersen, T. G., D. Dobrev, and E. Schaumburg (2008). Duration based volatility estimation. *Working Paper*.

Bandi, F. M. and J. R. Russell (2006). Separating microstructure noise from volatility. *Journal of Financial Economics 79*(3), 655–692.

Bandi, F. M. and J. R. Russell (2008). Microstructure noise, realized variance, and optimal sampling. *The Review of Economic Studies 75*(2), 339–369.

Barndorff-Nielsen, O. E. (2002). Econometric analysis of realized volatility and its use in estimating stochastic volatility models. *Journal of the Royal Statistical Society: Series B (Statistical Methodology) 64*(2), 253–280.

Barndorff-Nielsen, O. E., P. R. Hansen, A. Lunde, and N. Shephard (2008). Designing realized kernels to measure the ex post variation of equity prices in the presence of noise. *Econometrica*, 1481–1536.

Barndorff-Nielsen, O. E. and N. Shephard (2004). Power and bipower variation with stochastic volatility and jumps. *Journal of Financial Econometrics 2*(1), 1–37.

Barone-Adesi, G., R. F. Engle, and L. Mancini (2008). A GARCH option pricing model with filtered historical simulation. *Review of Financial Studies 21*(3), 1223–1258.

Bekierman, J. and B. Gribisch (2016). Estimating stochastic volatility models using realized measures. *Studies in Nonlinear Dynamics & Econometrics 20*(3), 279–300.

Bertholon, H., A. Monfort, and F. Pegoraro (2008). Econometric asset pricing modelling. *Journal of Financial Econometrics 6*(4), 407–458.

Billio, M., R. Casarin, and A. Osuntuyi (2016). Efficient Gibbs sampling for markov switching garch models. *Computational Statistics & Data Analysis 100*(C), 37–57.

Bormetti, G., F. Corsi, and A. A. Majewski (2015). Term structure of variance risk premium and returns' predictability. *Available at SSRN 2619278*.

Bühlmann, H., F. Delbaen, P. Embrechts, and A. N. Shiryaev (1996). No-arbitrage, change of measure and conditional Esscher transforms. *CWI quarterly 9*(4), 291–317.

Casarin, R., R. V. Craiu, and F. Leisen (2011). Interacting multiple try algorithms with different proposal distributions. *Statistics and Computing 23*(2), 185–200.

Casarin, R., L. Dalla Valle, F. Leisen, et al. (2012). Bayesian model selection for beta autoregressive processes. *Bayesian Analysis 7*(2), 385–410.

Casella, G. and C. P. Robert (2004). *Monte Carlo Statistical Methods*. New York: Springer Verlag.

Chib, S., F. Nardari, and N. Shephard (2002). Markov chain Monte Carlo methods for stochastic volatility models. *Journal of Econometrics 108*(2), 281–316.

Christoffersen, P., B. Feunou, K. Jacobs, and N. Meddahi (2014). The economic value of realized volatility: Using high-frequency returns for option valuation. *Journal of Financial and Quantitative Analysis 49*(03), 663–697.

Christoffersen, P., B. Feunou, and Y. Jeon (2015). Option valuation with observable volatility and jump dynamics. *Journal of Banking & Finance 61*, S101–S120.

Christoffersen, P., B. Feunou, and Y. Jeon (May 13, 2016). Option valuation with observable volatility and jump dynamics. *Available at SSRN 2494379.*.

Christoffersen, P., S. Heston, and K. Jacobs (2013). Capturing option anomalies with a variance-dependent pricing kernel. *The Review of Financial Studies 26*(8), 1963–2006.

Christoffersen, P., K. Jacobs, and C. Ornthanalai (2012). Dynamic jump intensities and risk premiums: Evidence from S&P500 returns and options. *Journal of Financial Economics 106*(3), 447–472.

Christoffersen, P., K. Jacobs, C. Ornthanalai, and Y. Wang (2008). Option valuation with long-run and short-run volatility components. *Journal of Financial Economics 90*(3), 272–297.

Corsi, F. (2009). A simple approximate long-memory model of realized volatility. *Journal of Financial Econometrics 7*(2), 174–196.

Corsi, F., N. Fusari, and D. La Vecchia (2013). Realizing smiles: Options pricing with realized volatility. *Journal of Financial Economics 107*(2), 284–304.

Corsi, F., D. Pirino, and R. Reno (2010). Threshold bipower variation and the impact of jumps on volatility forecasting. *Journal of Econometrics 159*(2), 276–288.

Creal, D. D. (2017). A class of non-Gaussian state space models with exact likelihood inference. *Journal of Business & Economic Statistics 35*(4), 585–597.

Darolles, S., C. Gourieroux, and J. Jasiak (2006). Structural Laplace transform and compound autoregressive models. *Journal of Time Series Analysis 27*(4), 477–503.

Das, S. R. and R. K. Sundaram (1999). Of smiles and smirks: A term structure perspective. *Journal of financial and quantitative analysis 34*(2), 211–239.

de Pinho, F. M., G. C. Franco, and R. S. Silva (2016). Modeling volatility using state space models with heavy tailed distributions. *Mathematics and Computers in Simulation 119*, 108 – 127.

Deschamps, P. (2011). Bayesian estimation of an extended local scale stochastic volatility model. *Journal of Applied Econometrics 162*, 369–382.

Dobrev, D. and P. Szerszen (2010). The information content of high-frequency data for estimating equity return models and forecasting risk. FEDS Working Paper, International Finance Discussion Papers, Number 1005.

Doucet, A., N. de Freitas, and N. Gordon (2001). *Sequential Monte Carlo Methods in Practice*. Springer-Verlag.

Duffie, D., J. Pan, and K. Singleton (2000). Transform analysis and asset pricing for affine jump-diffusions. *Econometrica*, 1343–1376.

Durham, G., J. Geweke, and P. Ghosh (2015). A comment on Christoffersen, Jacobs, and Ornthanalai (2012), Dynamic jump intensities and risk premiums: Evidence from S&P500 returns and options. *Journal of Financial Economics 115*(1), 210–214.

Engle, R. F. and G. M. Gallo (2006). A multiple indicators model for volatility using intra-daily data. *Journal of Econometrics 131*(1), 3–27.

Fang, F. and C. W. Oosterlee (2008). A novel pricing method for European options based on Fourier-cosine series expansions. *SIAM Journal on Scientific Computing 31*(2), 826–848.

Ferrante, M. and P. Vidoni (1998). Finite dimensional filters for nonlinear stochastic difference equations with multiplicative noises. *Stochastic processes and their applications 77*(1), 69–81.

Fiorentini, G., C. Planas, and A. Rossi (2014). Efficient MCMC sampling in dynamic mixture models. *Statistics and Computing 24*(1), 77–89.

Frühwirth-Schnatter, S. (2006). *Finite mixture and Markov switching models*. Springer Science & Business Media.

Gagliardini, P., C. Gourieroux, and E. Renault (2011). Efficient derivative pricing by the extended method of moments. *Econometrica*, 1181–1232.

Gallo, G. M. and E. Otranto (2015). Forecasting realized volatility with changing average levels. *International Journal of Forecasting 31*(3), 620–634.

Gerber, H. U., E. S. Shiu, et al. (1994). Option pricing by Esscher transforms. *Transactions of the Society of Actuaries 46*(99), 140.

Gouriéroux, C. and J. Jasiak (2006). Autoregressive gamma processes. *Journal of Forecasting 25*(2), 129–152.

Hansen, P. R. and G. Horel (2009). Quadratic variation by Markov chains. (2009-13). Univ. of Aarhus Dept. of Economics Research Paper.

Hansen, P. R., Z. Huang, and H. H. Shek (2012). Realized GARCH: a joint model for returns and realized measures of volatility. *Journal of Applied Econometrics 27*(6), 877–906.

Hansen, P. R. and A. Lunde (2005). A forecast comparison of volatility models: Does anything beat a GARCH (1, 1)? *Journal of Applied Econometrics 20*(7), 873–889.

Hansen, P. R. and A. Lunde (2006). Realized variance and market microstructure noise. *Journal of Business & Economic Statistics 24*(2), 127–161.

Heston, S. L. and S. Nandi (2000). A closed-form GARCH option valuation model. *Review of Financial Studies 13*(3), 585–625.

Huang, Z., T. Wang, and P. Hansen (2017). Option pricing with the realized GARCH model: An analytical approximation approach. *Journal of Futures Markets 37*(4), 328–358.

Khrapov, S. and E. Renault (2016). Affine option pricing model in discrete time. Technical report, Working paper.

Koopman, S. J. and M. Scharth (2013). The analysis of stochastic volatility in the presence of daily realized measures. *Journal of Financial Econometrics 11*(1), 76–115.

Maheu, J. M. and T. H. McCurdy (2011). Do high-frequency measures of volatility improve forecasts of return distributions? *Journal of Econometrics 160*(1), 69–76.

Majewski, A. A., G. Bormetti, and F. Corsi (2015). Smile from the past: A general option pricing framework with multiple volatility and leverage components. *Journal of Econometrics 187*(2), 521–531.

Renault, E. (1997). Econometric models of option pricing errors. *Econometric Society Monographs 28*, 223–278.

Shephard, N. (1994). Local scale model: state space alternative to integrated garch processes. *Journal of Applied Econometrics 60*, 181–202.

Shephard, N. and M. Pitt (1997). Likeklihood analysis of non-Gaussian measurement time series. *Biometrika 84*, 653–667.

Shephard, N. and K. Sheppard (2010). Realising the future: Forecasting with high-frequency-based volatility (HEAVY) models. *Journal of Applied Econometrics 25*(2), 197–231.

Shirota, S., T. Hizu, and Y. Omori (2014). Realized stochastic volatility with leverage and long memory. *Computational Statistics & Data Analysis 76*, 618–641.

Smith, R. L. and J. E. Miller (1986). A non-gaussian state space model and application to the prediction of records. *Journal of the Royal Statistical Society. Series B 48*, 79–88.

So, M. K. (2006). Bayesian analysis of nonlinear and non-Gaussian state space models via multiple-try sampling methods. *Statistics and Computing 16*(2), 125–141.

Stentoft, L. (2008). Option pricing using realized volatility. Working Paper at CREATES, University of Copenhagen.

Takahashi, M., Y. Omori, and T. Watanabe (2009). Estimating stochastic volatility models using daily returns and realized volatility simultaneously. *Computational Statistics & Data Analysis 53*(6), 2404–2426.

Tanizaki, H. (1996). *Nonlinear Filters*. Spring.

Tanner, M. A. and W. H. Wong (1987). The calculation of posterior distributions by data augmentation. *Journal of the American Statistical Association 82*(398), 528–540.

Taylor, S. J. (1994). Modeling stochastic volatility: A review and comparative study. *Mathematical Finance 4*(2), 183–204.

Vermaak, J., C. Andrieu, A. Doucet, and S. Godsill (2004). Reversible jump Markov Chain Monte Carlo strategies for Bayesian model selection in autoregressive processes. *Journal of Time Series Analysis 25*(6), 785–809.

Vidoni, P. (1999). Exponential family state space models based on a conjugate latent process. *Journal of the Royal Statistical Society. Series B 61*(1), 213–221.

Zhang, L., P. A. Mykland, and Y. Aït-Sahalia (2005). A tale of two time scales: Determining integrated volatility with noisy high-frequency data. *Journal of the American Statistical Association 100*(472), 1394–1411.

Appendix: A stochastic volatility model with realized measures for option pricing

Giacomo Bormetti* Roberto Casarin† Fulvio Corsi‡
Giulia Livieri §

This version: March 21, 2019

Abstract

This on-line Appendix contains: i) Definitions of the distributions used throughout the paper. ii) The derivation of the *conditional likelihood*, the *Markov transition*, and the *initial distribution* of the SV-ARG. iii) Details on the sampling strategies for the parameters' full conditional distributions. iv) A simulation study to test the efficiency of the proposed MCMC algorithm with a general setting and a setting that resembles the main features of the financial data. v) Properties of the SV-LHARG. vi) Details about the Section "Financial Applications". vii) Additional comments on the option valuation.

*Department of Mathematics, University of Bologna, IT.
†Department of Economics, Ca' Foscari University of Venice, IT.
‡Department of Economics and Management, University of Pisa, IT and City University London.
§Scuola Normale Superiore, Piazza dei Cavalieri, Pisa, IT.

A Definition of the distributions

A.1 Generalized Inverse Gaussian and Gamma distribution

A Generalized Inverse Gaussian (GIG) random variable $X \overset{d}{\sim} \mathcal{G}ig(\lambda,\chi,\psi)$ has probability density function given by:

$$p(x|\lambda,\chi,\psi) = \left(\sqrt{\frac{\psi}{\chi}}\right)^{\lambda} \frac{1}{2K_{\lambda}(\sqrt{\chi\psi})} x^{\lambda-1} \exp\left(-\frac{1}{2}\left(\chi\frac{1}{x}+\psi x\right)\right).$$

The GIG distribution has the Gamma distribution as special case. More specifically, the Gamma distribution $\mathcal{G}\left(k,\vartheta\right)$ with shape $k>0$ and scale $\vartheta>0$ can be obtained setting $\lambda=k$, $\psi=2/\vartheta$ ad $\chi=0$ in a $\mathcal{G}ig(\lambda,\chi,\psi)$.

The non-central moments of order δ of a GIG distribution are defined as

$$\mathbb{E}\left(X^{\delta}\right) = \left(\sqrt{\frac{\chi}{\psi}}\right)^{\delta} \frac{K_{\lambda+\delta}(\sqrt{\chi\psi})}{K_{\lambda}(\sqrt{\chi\psi})}.$$

Figure 1 shows the probability density function of a $\mathcal{G}ig$ random variable for three different parameters settings.

Figure 1: Probability density function (p.d.f) of a $\mathcal{G}ig$ random variable for three different parameter setting (λ,χ,ψ).

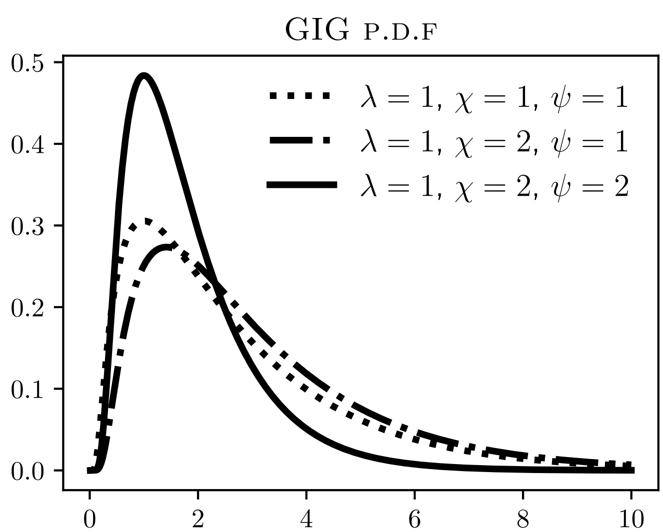

A.2 Sichel and Negative Binomial distribution

A Sichel ($\mathcal{S}$) random variable $Z \overset{d}{\sim} \mathcal{S}(\lambda, \chi, \psi)$ is obtained by assuming the mean X of a Poisson ($\mathcal{P}o$) random variable $Z \overset{d}{\sim} \mathcal{P}o(X)$ follows a GIG distribution (see Subsection **??** above), $X \overset{d}{\sim} \mathcal{G}ig(\lambda, \chi, \psi)$. A Sichel random variable has probability mass function:

$$p(z|\lambda, \chi, \psi) = \left(\sqrt{\frac{\psi}{\psi + 2}}\right)^{\lambda} \left(\frac{\chi}{\psi + 2}\right)^{z} \frac{1}{z!} \frac{K_{\lambda+z}\left(\sqrt{\chi(\psi+2)}\right)}{K_{\lambda}(\sqrt{\chi\psi})},\ z \geq 0.$$

The first two moments of a Sichel random variable are :

$$\begin{aligned}
\mathbb{E}\left(Z\right) &= \left(\sqrt{\frac{\chi}{\psi}}\right) \frac{K_{\lambda+1}(\sqrt{\chi\psi})}{K_{\lambda}(\sqrt{\chi\psi})}, \\
\mathbb{E}\left(Z^2\right) &= \left(\sqrt{\frac{\chi}{\psi}}\right) \frac{K_{\lambda+1}(\sqrt{\chi\psi})}{K_{\lambda}(\sqrt{\chi\psi})} + \left(\frac{\chi}{\psi}\right) \frac{K_{\lambda+2}(\sqrt{\chi\psi})}{K_{\lambda}(\sqrt{\chi\psi})}.
\end{aligned}$$

Figure 2 represents the p.d.f. of a Sichel random variable for three different parameters settings. A negative binomial ($\mathcal{NB}$) random variable $K \overset{d}{\sim} \mathcal{NB}(\omega, p)$ is a special case of a

Figure 2: Probability density function (p.d.f) of a Sichel random variable for three different parameter setting (λ, χ, ψ).

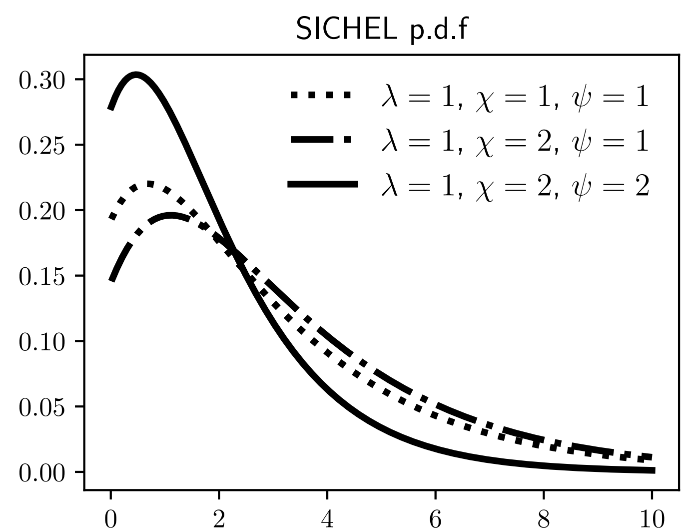

$\mathcal{S}\left(\lambda, \chi, \psi\right)$ random variable as χ tends to zero. In particular, a $\mathcal{NB}$ has probability mass function given by:

$$p(k|\omega, p) = \frac{\Gamma(\omega + k)}{\Gamma(\omega)\Gamma(k+1)} p^k (1-p)^{\omega}.$$

A.3 Non-central Gamma distribution

We say that a positive random variable X follows a non-central gamma distribution with parameters $\nu > 0$, $\beta > 0$ and $c > 0$, denoted with $X \overset{d}{\sim} \bar{\mathcal{G}}(\nu, \beta, c)$, if its conditional distribution given $Z \overset{d}{\sim} \mathcal{P}(\beta)$ is a gamma distribution $\mathcal{G}(\nu + Z, c)$. A non-central gamma distribution has probability distribution function:

$$p(x|\nu, \beta, c) = \exp\left(-\frac{x}{c}\right) \sum_{k=0}^{\infty} \left[\frac{x^{\nu+k-1}}{c^{\nu+k}\Gamma(\nu+k)} \frac{\exp\left(-\beta^{k+1}\right)}{k!}\right], \quad x \geq 0.$$

The two first moments of the non-central gamma distribution are:

$$\mathbb{E}[X] = c\nu + c\beta$$
$$\mathbb{V}(X) = c^2\nu + 2c^2\beta.$$

B The SV-ARG model

In this section, we derive the conditional likelihood $p(r_t, \mathrm{RV}_t | \widetilde{\mathcal{F}}^Z_{t-1})$, the Markov transition $p(z_t | \widetilde{\mathcal{F}}_{t-1})$, and the initial distribution of z_1 for the SV-ARG model, as in Proposition 2 of the main text. Then, we prove Proposition 3 and finally compute the marginal filtered $p(h_t | \mathcal{F}^Z_t)$ and smoothed $p(h_t | \mathcal{F}_T)$ distributions as in Proposition 4.

Proof of Proposition 2. First, we solve the following integrals:

$$p(r_t, \mathrm{RV}_t | \widetilde{\mathcal{F}}^Z_{t-1}) = \int_0^\infty p(r_t, \mathrm{RV}_t | h_t) p(h_t | z_t)\, dh_t \tag{B.1}$$

$$p(z_t | \widetilde{\mathcal{F}}_{t-1}) = \int_0^\infty p(z_t | h_{t-1}) p(h_{t-1} | r_{t-1}, \mathrm{RV}_{t-1})\, dh_{t-1} \tag{B.2}$$

$$p(z_1) = \int_0^\infty p(z_1 | h_0) p(h_0) dh_0, \tag{B.3}$$

and then we compute the *conditional likelihood*, the *Markov transition* and the *initial distribution* of z_1, respectively.

Given the following quantities

$$\mu_{1t} = r_t - \mu, \quad \mu_{2t} = \frac{\mathrm{RV}_t}{\exp(\kappa_2)}, \quad \varphi_t = \varphi \exp(-\kappa_2),$$

$$\eta(z_t) = \frac{\exp(\gamma \mu_{1t})}{\sqrt{2\pi}} \frac{\mathrm{RV}_t^{\varphi_t - 1}}{\Gamma(\varphi_t)(\exp(\kappa_2))^{\varphi_t}} \frac{c^{-\delta - z_t}}{\Gamma(\delta + z_t)},$$

$$\lambda(z_t) = \delta + z_t - \varphi_t - 1/2, \quad \chi^{(t)} = \mu_{1t}^2 + 2\mu_{2t}, \quad \psi = \gamma^2 + \frac{2}{c},$$

the *conditional likelihood* is

$$
\begin{aligned}
p(r_t, \mathrm{RV}_t | \widetilde{\mathcal{F}}^Z_{t-1}) &= \int_0^\infty p(r_t, \mathrm{RV}_t, h_t | z_t)\, dh_t \\
&= \int_0^\infty p(r_t|h_t) p(\mathrm{RV}_t|h_t) p(h_t|z_t)\, dh_t \\
&= \int_0^\infty (2\pi h_t)^{-1/2} \exp\left(-\frac{1}{2}\left((r_t-\mu)^2 \frac{1}{h_t} + \gamma^2 h_t\right)\right) \exp\left(\gamma\left(r_t - \mu\right)\right) \\
&\quad \cdot \frac{\mathrm{RV}_t^{\varphi_t - 1}}{\Gamma(\varphi_t)\left(\exp\left(\kappa_2\right) h_t\right)^{\varphi_t}} \exp\left(-\frac{\mathrm{RV}_t}{\exp(\kappa_2)} \frac{1}{h_t}\right) \\
&\quad \cdot \frac{c^{-\delta - z_t}}{\Gamma(\delta + z_t)} h_t^{\delta + z_t - 1} \exp\left(-\frac{h_t}{c}\right)\, dh_t \\
&\doteq \int_0^\infty (2\pi)^{-1/2}\, h_t^{-1/2} \exp\left(-\frac{1}{2}\left(\mu_{1t}^2 \frac{1}{h_t} + \gamma^2 h_t\right)\right) \exp\left(\gamma \mu_{1t}\right) \\
&\quad \cdot \frac{\mathrm{RV}_t^{\varphi_t - 1}}{\Gamma(\varphi_t)\left(\exp\left(\kappa_2\right)\right)^{\varphi_t}} h_t^{-\varphi_t} \exp\left(-\mu_{2t} \frac{1}{h_t}\right) \\
&\quad \cdot \frac{c^{-\delta - z_t}}{\Gamma(\delta + z_t)} h_t^{\delta + z_t - 1} \exp\left(-\frac{h_t}{c}\right)\, dh_t \\
&= \frac{\exp\left(\gamma \mu_{1t}\right)}{\sqrt{2\pi}} \frac{\mathrm{RV}_t^{\varphi_t - 1}}{\Gamma(\varphi_t)\left(\exp\left(\kappa_2\right)\right)^{\varphi_t}} \frac{c^{-\delta - z_t}}{\Gamma(\delta + z_t)} \\
&\quad \cdot \int_0^\infty h_t^{(\delta + z_t - \varphi_t - 1/2) - 1} \exp\left(-\frac{1}{2}\left(\left(\mu_{1t}^2 + 2\mu_{2t}\right) \frac{1}{h_t} + \left(\gamma^2 + \frac{2}{c}\right) h_t\right)\right)\, dh_t \\
&\doteq \eta\left(z_t\right) \int_0^\infty h_t^{\lambda(z_t) - 1} \exp\left(-\frac{1}{2}\left(\left(\mu_{1t}^2 + 2\mu_{2t}\right) \frac{1}{h_t} + \psi h_t\right)\right)\, dh_t \\
&= 2\eta\left(z_t\right) K_{\lambda(z_t)}\left(\sqrt{\psi \chi^{(t)}}\right) \left(\sqrt{\frac{\chi^{(t)}}{\psi}}\right)^{\lambda(z_t)}.
\end{aligned}
$$

The last equality follows from the definition of the kernel of the Generalized Inverse Gaussian distribution.

Markov transition

$$
\begin{aligned}
p(z_t|\widetilde{\mathcal{F}}_{t-1}) &= \int_0^\infty p(z_t, h_{t-1}|z_{t-1}, r_{t-1}, \mathrm{RV}_{t-1})\, dh_{t-1} = \\
&= \int_0^\infty p(z_t|h_{t-1}) p(h_{t-1}|z_{t-1}, r_{t-1}, \mathrm{RV}_{t-1})\, dh_{t-1} \\
&= \int_0^\infty p(z_t|h_{t-1}) \frac{p(h_{t-1}, z_{t-1}, r_{t-1}, \mathrm{RV}_{t-1})}{p(z_{t-1}, r_{t-1}, \mathrm{RV}_{t-1})}\, dh_{t-1} \\
&\propto \int_0^\infty p(z_t|h_{t-1}) p(h_{t-1}, z_{t-1}, r_{t-1}, \mathrm{RV}_{t-1})\, dh_{t-1} \\
&\propto \int_0^\infty p(z_t|h_{t-1}) p(r_{t-1}|h_{t-1}) p(\mathrm{RV}_{t-1}|h_{t-1}) p(h_{t-1}|z_{t-1})\, dh_{t-1} \\
&\propto \int_0^\infty \frac{1}{z_t!} \left(\beta^{(d)} h_{t-1}\right)^{z_t} \exp\left(-\beta^{(d)}\, h_{t-1}\right) p(r_{t-1}|h_{t-1}) \\
&\quad \cdot p(\mathrm{RV}_{t-1}|h_{t-1}) p(h_{t-1}|z_{t-1})\, dh_{t-1}.
\end{aligned}
\tag{B.4}
$$

Similarly to the computation of the *conditional likelihood* above, we have

$$
\begin{aligned}
& p(r_{t-1}|h_{t-1}) p(\mathrm{RV}_{t-1}|h_{t-1}) p(h_{t-1}|z_{t-1}) \\
&= h_{t-1}^{(\delta + z_{t-1} - \varphi_t - 1/2) - 1} \exp\Bigg(-\frac{1}{2}\Bigg(\Bigg((r_{t-1} - \mu)^2 \\
&\qquad + 2\frac{\mathrm{RV}_{t-1}}{\exp(\kappa_2)}\Bigg) \frac{1}{h_{t-1}} + \left(\gamma^2 + \frac{2}{c}\right) h_{t-1}\Bigg)\Bigg) \\
&= h_{t-1}^{\lambda(z_{t-1}) - 1} \exp\left(-\frac{1}{2}\left(\left(\mu_{1t}^2 + 2\mu_{2t}\right) \frac{1}{h_{t-1}} + \psi h_{t-1}\right)\right) \\
&\doteq h_{t-1}^{\lambda(z_{t-1}) - 1} \exp\left(-\frac{1}{2}\left(\chi^{(t-1)} \frac{1}{h_{t-1}} + \psi h_{t-1}\right)\right).
\end{aligned}
$$

Eq. (B.4) becomes

$$
\begin{aligned}
&p(z_t|z_{t-1}, r_{t-1}, \mathrm{RV}_{t-1}) \propto \\
&\propto \int_0^\infty \frac{1}{z_t!}\left(\beta^{(d)}h_{t-1}\right)^{z_t}\exp\left(-\beta^{(d)}h_{t-1}\right)h_{t-1}^{\lambda(z_{t-1})-1} \\
&\qquad \cdot \exp\left(-\frac{1}{2}\left(\chi^{(t-1)}\frac{1}{h_{t-1}}+\psi h_{t-1}\right)\right)dh_{t-1} \\
&= \frac{1}{z_t!}\left(\beta^{(d)}\right)^{z_t}\int_0^\infty h_{t-1}^{(\lambda(z_{t-1})+z_t)-1}\exp\left(-\frac{1}{2}\left(\chi^{(t-1)}\frac{1}{h_{t-1}}\right.\right. \\
&\qquad \left.\left.+\left(\psi+2\beta^{(d)}\right)h_{t-1}\right)\right)dh_{t-1} \\
&= \frac{1}{z_t!}\left(\beta^{(d)}\right)^{z_t}2K_{\lambda(z_{t-1})+z_t}\left(\sqrt{\chi^{(t-1)}\left(\psi+2\beta^{(d)}\right)}\right)\left(\sqrt{\frac{\chi^{(t-1)}}{\left(\psi+2\beta^{(d)}\right)}}\right)^{\lambda(z_{t-1})+z_t} \\
&\propto \frac{1}{z_t!}\left(\sqrt{\left(\beta^{(d)}\right)^2\frac{\chi^{(t-1)}}{\left(\psi+2\beta^{(d)}\right)}}\right)^{z_t}\left(\sqrt{\frac{\chi^{(t-1)}}{\left(\psi+2\beta^{(d)}\right)}}\right)^{\lambda(z_{t-1})}K_{\lambda(z_{t-1})+z_t}\left(\sqrt{\chi^{(t-1)}\left(\psi+2\beta^{(d)}\right)}\right).
\end{aligned}
$$

If we define

$$
\begin{aligned}
\bar{\chi}^{(t-1)} &\doteq \chi^{(t-1)}\beta^{(d)}, \\
\bar{\psi} &\doteq \psi\frac{1}{\beta^{(d)}},
\end{aligned}
$$

then the *Markov transition* can be written as

$$
\begin{aligned}
&p(z_t|\widetilde{\mathcal{F}}_{t-1}) \propto \\
&\propto \frac{1}{z_t!}\left(\sqrt{\frac{\bar{\chi}^{(t-1)}}{\bar{\psi}+2}}\right)^{z_t}\left(\sqrt{\frac{\bar{\psi}}{\left(\bar{\psi}+2\right)}}\right)^{\lambda(z_{t-1})}K_{\lambda(z_{t-1})+z_t}\left(\sqrt{\bar{\chi}^{(t-1)}\left(\bar{\psi}+2\right)}\right) \\
&\propto \mathcal{S}\left(\lambda(z_{t-1}), \bar{\chi}^{(t-1)}, \bar{\psi}\right) \\
&\propto \mathcal{S}\left(\delta+z_{t-1}-\varphi_t-1/2, \chi^{(t-1)}\beta^{(d)}, \psi\frac{1}{\beta^{(d)}}\right).
\end{aligned}
$$

where $\mathcal{S}\left(\lambda(z_{t-1}), \bar{\chi}^{(t-1)}, \bar{\psi}\right)$ is the Sichel distribution with parameters $\lambda(z_{t-1})$, $\bar{\chi}^{(t-1)}$ and $\bar{\psi}$.

Initial distribution

$$
\begin{aligned}
p(z_1) &= \int_0^\infty p(z_1, h_{t-1}) dh_{t-1} \\
&= \int_0^\infty p(z_1 | h_{t-1}) p(h_{t-1}) dh_{t-1} \\
&= \int_0^\infty \frac{1}{z_1!} \left(\beta^{(d)} h_{t-1}\right)^{z_1} \exp\left(-\beta^{(d)} h_{t-1}\right) \frac{1}{\Gamma(\delta)} h_{t-1}^{\delta-1} \left(\frac{1 - c\beta^{(d)}}{c}\right)^{\delta} \\
&\quad \cdot \exp\left(-h_{t-1}\left(\frac{1 - c\beta^{(d)}}{c}\right)\right) dh_{t-1} \\
&= \frac{1}{z_1!} \left(\beta^{(d)}\right)^{z_1} \left(\frac{1 - c\beta^{(d)}}{c}\right)^{\delta} \frac{1}{\Gamma(\delta)} \int_0^\infty h_{t-1}^{\delta+z_1-1} \exp\left(-\frac{h_{t-1}}{c}\right) dh_{t-1} \\
&= \frac{1}{z_1!} \left(\beta^{(d)}\right)^{z_1} \left(\frac{1 - c\beta^{(d)}}{c}\right)^{\delta} \frac{\Gamma(\delta + z_1)}{\Gamma(\delta)} c^{\delta+z_1} \\
&= \frac{1}{z_1!} \left(c\,\beta^{(d)}\right)^{z_1} (1 - c\,\beta^{(d)})^{\delta} \frac{\Gamma(\delta + z_1)}{\Gamma(\delta)\Gamma(z_1 + 1)} \\
&\propto \mathcal{NB}\left(\delta, c\,\beta^{(d)}\right),
\end{aligned}
$$

where $\mathcal{NB}\left(\delta, c\,\beta^{(d)}\right)$ is the Negative Binomial distribution with parameters δ and $c\,\beta^{(d)}$. □

Proof of Proposition 3. The predictive probabilities $p(z_t = k|\mathcal{F}_{t-1})$ are obtained by summing over l the joint probabilities

$$
p(z_t = k, z_{t-1} = l|\mathbf{r}_{1:t-1}, \mathrm{RV}_{1:t-1}) = p(z_{t-1} = l|\mathcal{F}_{t-1}) p\left(z_t = k|z_{t-1} = l, r_{t-1}, \mathrm{RV}_{t-1}\right)
$$

as in Hamilton (1994), pp. 692-693. By Bayes' theorem the filtered $p(z_t = k|\mathcal{F}_t)$ probabilities are proportional to $p(z_t = k|\mathcal{F}_{t-1}) p\left(r_t, \mathrm{RV}_t|z_t = k\right)$ (see Hamilton, 1994, p. 693). The validity of the recursion for the smoothed probabilities can be formally established following the arguments in Hamilton (1994), pp. 699-700. □

Proof of Proposition 4. Marginal filtered distribution

$$
\begin{aligned}
& p(h_t|\mathcal{F}_t^Z) \propto \\
& \propto p(r_t|h_t)p(\mathrm{RV}_t|h_t)p(h_t|z_t) \propto \\
& \propto h_t^{-1/2} \exp\left(-\frac{1}{2}\left((r_t-\mu)^2\frac{1}{h_t}+\gamma^2 h_t\right)\right) h_t^{-\varphi_t} \\
& \qquad \cdot \exp\left(-\frac{\mathrm{RV}_t}{\exp(\kappa)}\frac{1}{h_t}\right) h_t^{\delta+z_t-1} \exp\left(-\frac{h_t}{c}\right) \\
& = h_t^{(\delta+z_t-\varphi_t-1/2)-1} \exp\left(-\frac{1}{2}\left(\left((r_t-\mu)^2+2\frac{\mathrm{RV}_t}{\exp\left(\kappa_2\right)}\right)\frac{1}{h_t}\right.\right. \\
& \qquad \left.\left. +\left(\gamma^2+\frac{2}{c}\right)h_t\right)\right) dh_t \\
& = h_t^{\lambda(z_t)-1} \exp\left(-\frac{1}{2}\left(\left(\mu_{1t}^2+2\mu_{2t}\right)\frac{1}{h_t}+\psi h_t\right)\right) \\
& = h_t^{\lambda(z_t)-1} \exp\left(-\frac{1}{2}\left(\chi^{(t)}\frac{1}{h_t}+\psi h_t\right)\right) \\
& \propto \mathcal{G}ig(\lambda(z_t),\chi^{(t)},\psi).
\end{aligned}
$$

Marginal smoothed distribution

$$
\begin{aligned}
& p(h_t|\mathcal{F}_T) \propto \\
& \propto p(h_t|\mathbf{r}_{1:t},\mathbf{y}_{1:t},\mathbf{z}_{1:t})p(z_{t+1}|h_t) \propto \\
& \propto h_t^{\lambda(z_t)-1} \exp\left(-\frac{1}{2}\left(\chi^{(t)}\frac{1}{h_t}+\psi h_t\right)\right) h_t^{z_{t+1}} \exp\left(-\beta^{(d)}h_t\right) \\
& = h_t^{\lambda(z_t)+z_{t+1}-1} \exp\left(-\frac{1}{2}\left(\chi^{(t)}\frac{1}{h_t}+\left(\psi+2\beta^{(d)}\right)h_t\right)\right) \\
& \propto \mathcal{G}ig\left(\lambda(z_t)+z_{t+1},\chi^{(t)},\psi+2\beta^{(d)}\right).
\end{aligned}
$$

□

C Sampling of the parameters

The symbols $\odot$ and $\oslash$ correspond to the element-by-element multiplication and division, respectively. We indicate with $\mathbf{r} \doteq r_{p+1:T}$, $\mathbf{RV} \doteq \mathrm{RV}_{p+1:T}$, $\mathbf{h} \doteq h_{p+1:T}$, $\mathbf{z} \doteq z_{p+1:T}$ the observations and the latent variables collections and with $\boldsymbol{\theta}_{(*)}$ the vector of parameters deprived from the parameter $(*)$. We use the parametrization $\left(\left[\beta^{(d)}, \beta^{(w)}, \beta^{(m)}\right], c\right)$ for the centrality parameter of the non-central gamma distribution. The mixing of the MCMC chain crucially depends on the parametrization of the latent process (see Bernardo et al., 2003; Frühwirth-Schnatter, 2004; Roberts et al., 2004, for more details). Extensive experimentation shows that the latter parametrization allows for a good mixing of the MCMC chain.

C.1 SV-ARG

When estimating the SV-ARG model, we have to sample from the full conditional distribution of $\boldsymbol{\xi}$, φ, κ_2, δ, c and $\beta^{(d)}$. We refer to the next subsection for details on the sampling of the parameters $\boldsymbol{\xi}$, φ, κ_2, δ, c and c because their full conditional distributions are the same used for the SV-LHARG. The full conditional distribution of $\beta^{(d)}$ is:

$$\begin{aligned}
\pi\left(\beta^{(d)} | \mathbf{r}, \mathbf{RV}, \mathbf{h}, \mathbf{z}, \boldsymbol{\theta}_{\left(\beta^{d}\right)}\right) \propto \pi\left(\beta^{(d)} | \mathbf{h}, \mathbf{z}\right) &\propto \prod_{t=p+1}^{T} \left(\beta^{(d)}\right)^{z_t} \exp\left(-\beta^{(d)} h_{t-1}\right) \\
&\propto \left(\beta^{(d)}\right)^{\sum_{t=p+1}^{T} z_t} \exp\left(-\beta^{(d)} \sum_{t=p+1}^{T} h_{t-1}\right) \\
&\propto \mathcal{G}\left(k_{\beta^{(d)}}, \theta_{\beta^{(d)}}\right),
\end{aligned}$$

where $\mathcal{G}(k, \theta)$ indicates a gamma distribution with shape $k > 0$ and scale $\theta > 0$; $k_{\beta^{(d)}} = \sum_{t=p+1}^{T} z_t - 1$ and $\theta_{\beta^{(d)}} = \left(\sum_{t=p+1}^{T} h_{t-1}\right)^{-1}$.

C.2 SV-LHARG

The full conditional distribution of the two-dimensional vector $\boldsymbol{\xi}$ is

$$\begin{aligned}
\pi(\boldsymbol{\xi}|\mathbf{r},\mathbf{RV},\mathbf{h},\mathbf{z},\boldsymbol{\theta}_{(\boldsymbol{\xi})}) &\propto \pi(\boldsymbol{\xi}|\mathbf{r},\mathbf{h}) \\
&\propto \prod_{t=p+1}^{T} \exp\left(-\frac{1}{2}\frac{(\mathbf{r}-\boldsymbol{\xi}'\boldsymbol{w}_t)^2}{h_t}\right) \\
&\propto \exp\left(-\frac{1}{2}(\boldsymbol{r}-W\boldsymbol{\xi})'\Upsilon_{\mathbf{r}}^{-1}(\boldsymbol{r}-W\boldsymbol{\xi})\right) \\
&\propto \exp\left(-\frac{1}{2}\left(\boldsymbol{\xi}'W'\Upsilon_{\mathbf{r}}^{-1}W\boldsymbol{\xi}-2\boldsymbol{\xi}'W'\Upsilon_{\boldsymbol{r}}^{-1}\mathbf{r}\right)\right) \\
&\propto \mathcal{N}_2(\mu_{\boldsymbol{\xi}},\Upsilon_{\boldsymbol{\xi}}),
\end{aligned}$$

where $\boldsymbol{w}_t = (1, h_t)'$, and we indicate with $\boldsymbol{W}$ the $(T-p)\times 2$-dimensional matrix $\boldsymbol{W} = (\boldsymbol{w}'_{p+1};\ldots;\boldsymbol{w}'_T)$ and with $\Upsilon_{\boldsymbol{r}}$ the $(T-p)\times(T-p)$-dimensional diagonal matrix $\Upsilon_{\boldsymbol{r}} = \mathrm{diag}(\boldsymbol{r})$. For the parameter $\boldsymbol{\xi}$ the full conditional distribution can be sample exactly.

The full conditional distribution of φ is

$$\begin{aligned}
&\pi(\varphi|\mathbf{r},\mathbf{RV},\mathbf{h},\mathbf{z},\boldsymbol{\theta}_{(\varphi)}) \propto \pi\left(\varphi|\mathbf{RV},\mathbf{h},\kappa_2\right) \\
&\propto \prod_{t=p+1}^{T} \frac{1}{\Gamma\left(\varphi\exp\left(-\kappa_2\right)\right)}\frac{1}{\left(h_t\exp\left(\kappa_2\right)\right)^{\varphi\exp(-\kappa_2)}}\mathrm{RV}_t^{\varphi\exp(-\kappa_2)} \\
&\propto \exp\left(-\sum_{t=p+1}^{T}\log(\Gamma\left(\varphi\exp\left(-\kappa_2\right)\right)) - \sum_{t=p+1}^{T}\varphi\exp\left(-\kappa_2\right)\left(h_t\kappa_2-\log(\mathrm{RV}_t)\right)\right).
\end{aligned}$$

To simulate from this distribution we employ an MH step. We consider a gamma random walk proposal and, at the j-th iteration of the algorithm, given the previous value $\varphi^{(j-1)}$ of the chain, we simulate

$$\varphi^{(*)} \overset{d}{\sim} \mathcal{G}\left(\left(\varphi^{(j-1)}\right)^2/\xi_\varphi, \xi_\varphi/\varphi^{(j-1)}\right),$$

where ξ_φ represents the scale of the random walk. The proposal value generated from this density is then accepted or rejected according to the acceptance ratio of the MH algorithm.

The full conditional distribution of κ_2 is

$$\begin{aligned}
&\pi(\kappa_2|\mathbf{r},\mathbf{RV},\mathbf{h},\mathbf{z},\boldsymbol{\theta}_{(\kappa_2)}) \propto \pi\left(\varphi|\mathbf{RV},\mathbf{h},\varphi\right) \\
&\propto \prod_{t=p+1}^{T} \frac{1}{\Gamma\left(\varphi\exp\left(-\kappa_2\right)\right)}\frac{1}{\left(h_t\exp\left(\kappa_2\right)\right)^{\varphi\exp(-\kappa_2)}}\mathrm{RV}_t^{\varphi\exp(-\kappa_2)}\exp\left(-\frac{\mathrm{RV}}{h_t\exp\left(\kappa_2\right)}\right).
\end{aligned}$$

To simulate from this distribution we employ an MH step. Specifically, we consider a Normal random walk proposal and, at the j-th iteration of the algorithm, given the previous value $\kappa_2^{(j-1)}$ of the chain, we simulate

$$\kappa_2^{(*)} \overset{d}{\sim} \mathcal{N}_{n_2}\left(\kappa_2^{(j-1)}, (\xi_{\kappa_2})^2\right),$$

where ξ_{κ_2} represents the variance of the random walk. The proposal value generated from this density is then accepted or rejected according to the acceptance ratio of the MH algorithm.

The full conditional distribution of δ is

$$\pi(\delta|\mathbf{r}, \mathbf{RV}, \mathbf{h}, \mathbf{z}, \boldsymbol{\theta}_{(\delta)}) \propto \pi(\delta|\mathbf{h}, \mathbf{z}, c) \propto \prod_{t=p+1}^{T} \frac{1}{\Gamma(\delta + z_t)} \left(\frac{1}{c}\right)^{\delta} h_t^{\delta}$$

$$\propto \exp\left(-\sum_{t=p+1}^{T} \log(\Gamma(\delta + z_t)) - \delta(T-p)\log(c) + \delta \sum_{t=p+1}^{T} \log(h_t)\right).$$

Similarly to what was done for the parameter φ, in the MH step, we consider a gamma random walk proposal with scale ξ_δ. The proposal value generated from this density is the accepted or rejected according to the acceptance ratio of the MH algorithm.

The full conditional distribution of c is

$$\pi\left(c|\mathbf{r}, \mathbf{RV}, \mathbf{h}, \mathbf{z}, \boldsymbol{\theta}_{(c)}\right) \propto \pi\left(c|\mathbf{h}, \mathbf{z}, \delta\right) \propto \prod_{t=p+1}^{T} \left(\frac{1}{c}\right)^{\delta + z_t} \exp\left(-\frac{h_t}{c}\right)$$

$$\propto \left(\frac{1}{c}\right)^{(T-p)\delta + \sum_{t=p+1}^{T} z_t} \exp\left(-\frac{1}{c}\sum_{t=p+1}^{T} h_t\right)$$

$$\propto \mathcal{IG}\left(\bar{k}_c, \bar{\theta}_c\right),$$

where $\mathcal{IG}(\bar{k}, \bar{\theta})$ indicates an Inverse Gamma random variable with shape $\bar{k} > 0$ and scale $\bar{\theta} > 0$; $\bar{k}_c = (T-p)\delta + \sum_{t=p+1}^{T} z_t - 1$ and $\bar{\theta}_c = \sum_{t=p+1}^{T} h_t$.

In order to sample from $\boldsymbol{\beta}'$, $\boldsymbol{\alpha}'$ and λ, we introduce now the following (3×22)-dimensional matrix

$$\mathrm{E} = \begin{pmatrix} 1 & \mathbf{0}_4' & \mathbf{0}_{17}' \\ 0 & \frac{1}{4}\boldsymbol{\iota}_4' & \mathbf{0}_{17}' \\ 0 & \mathbf{0}_4' & \frac{1}{17}\boldsymbol{\iota}_{17}' \end{pmatrix},$$

where $\boldsymbol{\iota}_n$ and $\mathbf{0}_n$ indicate the n-dimensional unit and null vector. Besides, we indicate with $\boldsymbol{h_{t-1}}$ and $\boldsymbol{l_{t-1}}$ the 22-dimensional vectors $\boldsymbol{h_{t-1}} = (h_{t-1}, \ldots, h_{t-22})'$ and $\boldsymbol{l_{t-1}} = (l_{t-1}, \ldots, l_{t-22})'$, respectively.

The full conditional distribution of $\boldsymbol{\beta} = \left(\beta^{(d)}, \beta^{(w)}, \beta^{(m)}\right)'$ is

$$\pi\left(\boldsymbol{\beta}|\mathbf{r}, \mathbf{RV}, \mathbf{h}, \mathbf{z}, \boldsymbol{\theta}_{(\boldsymbol{\beta})}\right) \propto \pi\left(\boldsymbol{\beta}|\mathbf{r}, \mathbf{RV}, \mathbf{h}, \mathbf{z}, \lambda\right) \propto$$
$$\propto \prod_{t=p+1}^{T} \left((\mathrm{E}\boldsymbol{h_{t-1}})' \boldsymbol{\beta} + (\mathrm{E}\boldsymbol{l}_{t-1})' \boldsymbol{\alpha}\right)^{z_t} \exp\left(-\left(\mathrm{E}\boldsymbol{h}_{t-1}\right)' \boldsymbol{\beta}\right).$$

To simulate from this distribution we employ a Metropolis-Hastings step. We consider a Normal random walk proposal and, at the j-th iteration of the algorithm, given the previous value $\boldsymbol{\beta}^{(j-1)}$ of the chain, we simulate

$$\boldsymbol{\beta} \stackrel{d}{\sim} \mathcal{N}_3\left(\boldsymbol{\beta}^{(j-1)}, \Upsilon_{\boldsymbol{\beta}}\right),$$

where $\Upsilon_{\boldsymbol{\beta}}$ is a (3×3)-dimensional diagonal matrix with diagonal given by $\left(\xi_{\beta^{(d)}}, \xi_{\beta^{(w)}}, \xi_{\beta^{(m)}}\right)$. The latter represent the scale of the random walk.

The full conditional distribution of $\boldsymbol{\alpha} = \left(\alpha^{(d)}, \alpha^{(w)}, \alpha^{(m)}\right)$ is

$$\pi\left(\boldsymbol{\alpha}|\mathbf{r}, \mathbf{RV}, \mathbf{h}, \mathbf{z}, \boldsymbol{\theta}_{(\boldsymbol{\alpha})}\right) \propto \pi\left(\boldsymbol{\alpha}|\mathbf{r}, \mathbf{RV}, \mathbf{h}, \mathbf{z}, \boldsymbol{\beta}, \lambda\right) \propto$$
$$\propto \prod_{t=p+1}^{T} \left((\mathrm{E}\boldsymbol{h_{t-1}})' \boldsymbol{\beta} + (\mathrm{E}\boldsymbol{l}_{t-1})' \boldsymbol{\alpha}\right)^{z_t} \exp\left(-\left(\mathrm{E}\boldsymbol{l}_{t-1}\right)' \boldsymbol{\alpha}\right).$$

Similarly to what was done for the parameter $\boldsymbol{\beta}$, in the Metropolis-Hastings step, we consider a Normal random walk proposal with scales $(\xi_{\alpha^{(d)}}, \xi_{\alpha^{(w)}}, \xi_{\alpha^{(m)}})$.

Finally, the full conditional distribution of λ is

$$\pi\left(\lambda|\mathbf{r}, \mathbf{RV}, \mathbf{h}, \mathbf{z}, \boldsymbol{\theta}_{(\lambda)}\right) \propto \pi\left(\lambda|\mathbf{r}, \mathbf{RV}, \mathbf{h}, \mathbf{z}, \boldsymbol{\beta}, \boldsymbol{\alpha}\right)$$
$$\propto \prod_{t=p+1}^{T} \left((\mathrm{E}\boldsymbol{h_{t-1}})' \boldsymbol{\beta} + (\mathrm{E}\boldsymbol{l}_{t-1})' \boldsymbol{\alpha}\right)^{z_t} \exp\left(-\left(\mathrm{E}\boldsymbol{l}_{t-1}\right)' \boldsymbol{\alpha}\right),$$

where, we remind that $l_{t-i} = \left(\epsilon_{t-i} - \lambda\sqrt{h_{t-i}}\right)^2$, $i \in \{1, \ldots, 22\}$. To simulate from this distribution we employ a MH algorithm with a proposal distribution that makes use of the information on the structure of the leverage component. In particular, we would like to capture the asymmetric influence of shock: a large positive idiosyncratic component has a smaller impact on the CV than a large negative one. We consider a gamma random walk proposal and, at the j-th iteration of the algorithm, given the previous value $\lambda^{(j-1)}$ of the chain, we simulate

$$\lambda^{(*)} \overset{d}{\sim} \mathcal{G}\left(\lambda^{(j-1),2}/\xi_\lambda, \xi_\lambda/\lambda^{(j-1)}\right),$$

where ξ_λ represents the scale of the random walk. The proposal value generated from this density is then accepted or rejected according to the acceptance ratio of the MH algorithm.

D Simulation study

D.1 Simulation study: First part

In this section, we report a simulation setting which resembles the main features of the financial data. We focus our attention on the SV-LHARG model and generate 50 independent random samples with size $T = 1,000$. On each dataset, we iterate the proposed MCMC algorithm $M = 50,000$ times. Through the experiments we impose, as done in the financial application, the Feller condition ($\delta > 1$), the stationary constraint, as well as the preservation of the average value of the RV process (i.e. δ is not estimated). Concerning the parameters, to assess the efficiency of the MCMC algorithm we use the following measures: i) the acceptance rate (ACC) of the MH steps, ii) the inefficiency factor (INEFF) of the estimation of the posterior mean, iii) the Geweke's spectral density diagnostic (Geweke et al., 1991), iv) the Kolmogorov-Smirnov (KS) test (see Casella and Robert, 2004, Ch. 12), and v) the potential scale reduction factor (PSRF) of Gelman and Rubin (1992). We briefly describe some of these measures.

The inefficiency factor (INEFF) is defined as

$$\text{INEFF} = 1 + 2\sum_{k=1}^{\infty} \rho\left(k\right),$$

where $\rho\left(k\right)$ is the autocorrelation at lag k for the parameter of interest. We note that in Geweke et al. (1991) the quantity numerical efficiency is used, which corresponds to the inverse of the inefficiency factor. Regarding the Geweke's spectral density diagnostic, we refer to Geweke et al. (1991) for a rigorous description of the test. Nonetheless, we point out that we choose, as suggested from the author, $n_A = N/10$ and $n_B = N/2$ where N is the length of the chain. The KS test works as follows. For each component θ of the parameter vector $\boldsymbol{\theta}$ one splits the associated MCMC sample $\theta^{(j)}$, $j \in \{1, \cdots, N\}$ into two sub-samples $\theta_1^{(g)}$ and $\theta_2^{(g)}$ with $g \in \{1, \ldots, M\}$ and evaluates

$$\text{KS} = \frac{1}{M}\sup_{\eta}\left|\sum_{g=1}^{M}\mathbb{I}_{(0,\eta)}\left(\theta_1^{(gG)}\right) - \sum_{g=1}^{M}\mathbb{I}_{(0,\eta)}\left(\theta_2^{(gG)}\right)\right|$$

where G is the batch size, which is necessary in order to obtain quasi-indepindent samples. The independence of the samples is one of the assumptions to have a known limit distribution for the KS statistics. Finally, for the potential scale reduction factor we refer to the original work of Gelman and Rubin (1992).

We study the efficiency of the FFBS procedure through the Normalized Root Mean Square Error (NRMSE) averaged over the iterations of the Gibbs sampler. Specifically, indicating with M the effective number of the MCMC draws and with T the length of the sample, the NRMSE is defined as

$$\text{NRMSE} \doteq \frac{1}{M}\sum_{i=1}^{M} \frac{\sqrt{\frac{1}{T}\sum_{t=1}^{T}\left(\hat{h}_t^{(i)} - h_t\right)^2}}{\max\left(\hat{h}_{1:T}^{(i)}\right) - \min\left(\hat{h}_{1:T}^{(i)}\right)}$$

In the previous equation, we denote with $\hat{h}_t^{(i)}$ the estimate of the latent variable h_t on the $i-th$ iteration of the Gibbs sampler and with $\max\left(\hat{h}_{1:T}^{(i)}\right)$ (resp. $\min\left(\hat{h}_{1:T}^{(i)}\right)$) the maximum (resp. the minimum) value of $\hat{h}_t$ on the $i-th$ iteration of the Gibbs sampler. Finally, some practical considerations for the implementation of the inference algorithm are needed. Specifically, the initialization of the Hamilton filter algorithm and the choice of the number of states for the approximating Markov Chain of the process z_t. To initialize the Hamilton filter algorithm, we set $\widehat{\boldsymbol{\xi}}_{0|0} = \boldsymbol{\rho}$, where $\boldsymbol{\rho} = N^{-1}\boldsymbol{\iota}$ ($\boldsymbol{\iota}$ being the unit vector of dimension N). The number of states, instead, results to be equal to 300. We comment the results in what follow.

The following Table 7 reports the results of our simulation exercise. Precisely, we report the true value of the parameters, their estimates with the corresponding standard deviation as well as the above cited efficiency indicators. We refer to Table's caption for further technical details. We discuss now the results. Regarding the efficiency, the magnitude of the INEFF is always below thirty after applying a thinning procedure with a factor of 30. Actually, this is due to the analytical filtering and smoothing recursive formula that we have derived for the latent variables (cfr. Propositions 2, 3 and 4 in the main text). The ACCs are in line with the ideal values suggested in Roberts et al. (1997) thanks to the careful tuning of the proposal density in the MH steps to the target densities. The average p-values of the KS statistic suggest the acceptance of the null hypothesis that the sub-samples associated with the Markov chain have the same distribution, guaranteeing convergence. The latter is confirmed also from the value of the PSRF. Finally, Figure 3 reports an example of the estimation of the latent process h_t.

Figure 3: Black Line: Average true value. *Gray line*: Average smoothed value. Black dashed lines: Gray line plus or minus one standard deviation.

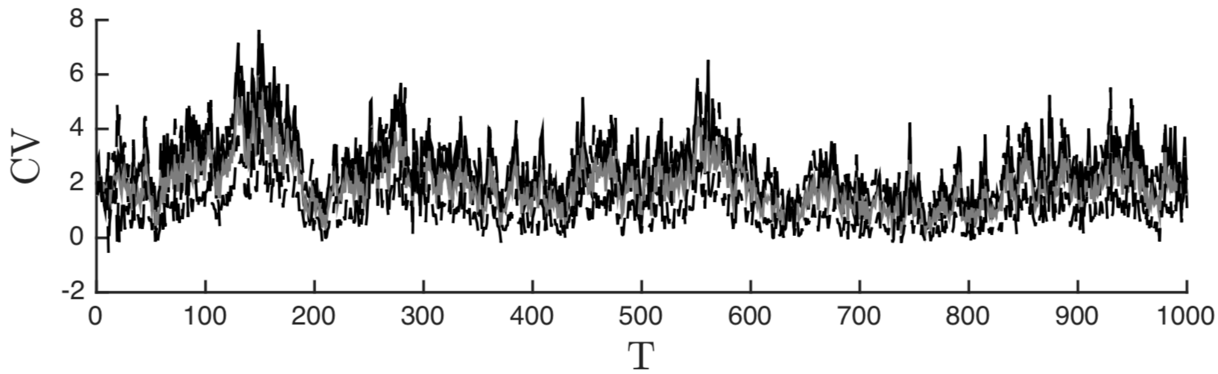

D.2 Simulation study: Second part

We generate data from the SV-ARG, SV-LARG, SV-HARG, and SV-LHARG models. For each model, we simulate 50 data-series of 1000 observations. For each data-series, we run the Gibbs sampler for 100,000 iterations, discard the first 10,000 draws to avoid dependence from initial conditions, and finally apply a thinning procedure to reduce the dependence between consecutive draws.

We devote particular attention to the SV-ARG because it is used as auxiliary model for making inference in the other models developed in this paper. After setting $c = 1$, we follow Chib et al. (2002) and Casarin et al. (2009) and test the efficiency of the algorithm in three different scenarios: *low-persistence* ($\beta^{(d)} = 0.3$), *medium-persistence* ($\beta^{(d)} = 0.6$) and finally *high-persistence* ($\beta^{(d)} = 0.9$). Values for the other parameters are reported in Table 1. Let us now comment the results. Table 1 contains the grand average of the parameter posterior means for the SV-ARG model along with their standard deviation. Table 2 reports efficiency indicators for the parameters. We refer to the on-line Appendix 1 and reference therein for further details on these indicators. Let us comment the results. Table 1 indicates that the accuracy of the MCMC scheme is remarkable for all the scenarios (*low persistence*, *medium persistence*, *high persistence*). As regards the efficiency, Table 2 suggests that the magnitudes of INEFF are below ten (we apply a thinning of 20 for the *low* and *medium persistence* scenario and of 50 for the *high persistence* one). The average ACCs are in line with the ideal values suggested in Roberts et al. (1997) thanks to the careful tuning of the proposal density in the MH steps. The average p-values of the KS statistics take values close to 0.5 in all cases. This suggests the acceptance of the null hypothesis that the sub-samples associated with the Markov chain have the same distribution. Finally, the PSRF is close to one, confirming the convergence of the algorithm.

Tables 4, 5 and 6 confirm that the accuracy of the parameters estimate is remarkable also for the SV-LARG SV-HARG and SV-LHARG models. The inefficiency factor of the parameters – after applying a thinning procedure with a factor of 50 – are slightly higher respect to those of the SV-ARG model, although fully satisfactory. This loss of efficiency is due to the use of a MH step for the latent variables $z_{1:T}$ and $h_{1:T}$. Nevertheless, only the INEFF for $\beta^{(m)}$ and $\alpha^{(m)}$ parameters in the SV-LHARG model are above 20. Also the other indicators confirm the effectiveness of the algorithm.

Table 1: SV-ARG parameters estimation results for three different volatility scenarios of the SV-ARG model. The results are averages over a set of independent MCMC experiments on 50 independent data set of 1,000 observations. On each data-set we run the proposed MCMC algorithm for 100,000 iterations and then discard the first 10,000. A thinning procedure is applied. The thinning rate is equal to 20 for *low-* and *medium-persistence* scenarios and 50 for the *high-persistence* scenario.

	Low-persistence		*Medium-persistence*		*High-persistence*	
$\boldsymbol{\theta}$	True	Estimates	True	Estimates	True	Estimates
μ	0.0	0.0018	0.0	-0.0052	0.0	-0.0072
		(0.0119)	(0.0178)		(0.0359)	
γ	1.0	1.0544	1.0	1.0523	1.0	1.0678
		(0.0738)		(0.0720)		(0.0784)
κ_2	-1.0	-0.9552	-1.0	-0.9652	-1.0	-0.9548
		(0.1200)		(0.1119)		
φ	0.8	0.8421	0.8	0.8326	0.8	0.8467
		(0.0738)		(0.0576)		(0.0647)
δ	0.8	0.8033	0.8	0.7982	0.8	0.8185
		(0.0371)		(0.0395)		(0.0578)
$\beta^{(d)}$	0.3	0.3010	0.6	0.6375	0.9	0.9695
		(0.0595)		(0.0744)		
c	1.0	0.9663	1.0	0.9707	1.0	0.9400
		(0.0940)		(0.0907)		
NRMSE		0.0906				

Table 2: Efficiency indicators for the SV-ARG parameters estimation results in three different volatility scenarios. The results are averages over a set of 50 independent MCMC experiments on 50 independent datasets of 1000 observations. On each dataset we ran the proposed MCMC algorithm for 100,000 iterations and then discard the first 10,000. A thinning procedure is applied. The thinning is equal to 20 for *low-* and *medium-persistence* scenarios and 50 for the *high-persistence* scenario. As efficiency indicators we report: the posterior mean inefficiency factor (INEFF), the acceptance rate (ACC) of the MH step, the Geweke's spectral density diagnostic, the Kolmogorov-Smirnov (KS) test and the potential scale reduction factor (PSRF).

	INEFF	ACC	Geweke's Test	KS	PSRF
Low persistence in volatility					
μ	1.1504		$(0.1009, 0.1967)$	0.5188	1.0000
γ	6.0176		$(-0.2554, 0.1240)$	0.2847	1.0010
κ_2	6.8813	0.1998	$(-0.0550, 0.0957)$	0.1980	1.0014
φ	7.8732	0.1972	$(-0.0884, 0.0984)$	0.1949	1.0010
δ	1.6774	0.2513	$(-0.0546, 0.2169)$	0.4502	1.0002
$\beta^{(d)}$	1.6087		$(0.0587, 0.1635)$	0.4250	1.0008
c	4.9442		$(0.0279, 0.1576)$	0.2770	1.0002
Medium persistence in volatility					
μ	1.1900		$(0.1266, 0.2335)$	0.4744	1.0001
γ	6.9712		$(0.0802, 0.1276)$	0.2243	1.0012
κ_2	6.6839	0.2160	$(0.0859, 0.1303)$	0.2043	1.0012
φ	7.9847	0.3230	$(0.0876, 0.1274)$	0.1810	1.0015
δ	1.3918	0.2320	$(-0.0490, 0.2275)$	0.5643	1.0000
$\beta^{(d)}$	5.0452		$(-0.1169, 0.1159)$	0.2678	1.0007
c	6.1434		$(-0.0208, 0.1052)$	0.2118	1.0010
High persistence volatility					
μ	1.2583		$(-0.0264, 0.2030)$	0.4505	1.0000
γ	7.1944		$(-0.7903, 0.1005)$	0.1946	1.0036
κ_2	6.1236		$(-0.5381, 0.1251)$	0.1577	1.0030
φ	7.1555	0.1964	$(-0.7037, 0.1184)$	0.1748	1.0035
δ	1.1547	0.1723	$(-0.1541, 0.2420)$	0.4979	1.0000
$\beta^{(d)}$	6.6867	0.2184	$(-0.8935, 0.1003)$	0.1793	1.0035
c	6.8945		$(0.8424, 0.1035)$	0.1859	1.0034

Table 3: Parameters estimation results for the SV-LARG, SV-HARG, SV-LHARGmodel. The results are averages over a set of 50 independent MCMC experiments on 50 independent data set of 1000 observations. On each data-set we run the proposed MCMC algorithm for 100000 iterations and then discard the first 10000. A thinning procedure is applied. The thinning is equal to 50

	SV-LARG		SV-HARG		SV-LHARG	
$\boldsymbol{\theta}$	True	Estimates	True	Estimates	True	Estimates
μ	0.0	-0.0240	0.0	0.3038	0.0	-0.5057
		(0.0491)	(0.1352)			(0.3100)
γ	1.0	1.038	1.0	0.8251	1.0	1.0034
		(0.03738)		(0.0582)		(0.0149)
κ_2	-1.0	-0.9358	-1.0	-1.2126	-1.0	-0.9620
		(0.06742)		(0.0925)		(0.0876)
φ	0.8	0.8650	0.8	0.8326	0.8	0.8773
		(0.0311)		(0.0576)		(0.0316)
δ	1.5	1.3254	1.5	1.5383	1.5	1.6004
		(0.0716)		(0.1574)		(0.2684)
$\beta^{(d)}$	0.3	0.3108	0.3	0.3169	0.3	0.2918
		(0.0618)		(0.0399)		
$\beta^{(w)}$			0.20	0.2245	0.2	0.2295
				(0.03951)		
$\beta^{(m)}$			0.6	0.0601	0.1	0.0839
				(0.0364)		(0.0352)
$\alpha^{(d)}$	0.15	0.1119			0.15	0.1688
		(0.0378)				(0.0146)
$\alpha^{(w)}$					0.10	(0.0883)
						(0.0249)
$\alpha^{(m)}$					0.05	0.0449
					(0.0358)	
λ	1.0	1.1608			1.0	1.000
		(0.473)				(0.0185)
c	1.0	1.0197	1.0	1.0763	1.0	0.9842
		(0.0450)		(0.0907)		(0.0155)
NRMSE		0.0758		0.1253		0.0782

Table 4: Efficiency indicators of the SV-LARG parameters estimation results. The results are averages over a set of 50 independent MCMC experiments on 50 independent datasets of 1000 observations. On each dataset we ran the proposed MCMC algorithm for 100000 iterations and then discard the first 10000. A thinning procedure is applied. The thinning is equal to 50 for all the models. As efficiency indicators we report: the inefficiency factor (INEFF) of the estimation of the posterior mean, the acceptance rate (ACC) of the MH step, the Geweke's spectral density diagnostic, the Kolmogorov-Smirnov (KS) test and the potential scale reduction factor (PSRF).

SV-LARG	INEFF	ACC	Geweke's Test	KS	PSRF
μ	5.71		$(1.55, 0.06)$	0.21	1.0047
γ	13.73		$(-1.22, 0.11)$	0.32	1.082
κ_2	8.58	0.16	$(1.10, 0.15)$	0.20	1.0314
φ	16.85	0.21	$(-1.30, 0.12)$	0.42	1.1089
δ	7.84	0.22	$(-1.16, 0.15)$	0.31	1.0864
$\beta^{(d)}$	8.44	0.19	$(1.11, 0.13)$	0.28	1.0006
$\alpha^{(d)}$	11.90	0.30	$(-0.65, 0.26)$	0.34	1.0003
c	13.72		$(1.33, 0.09)$	0.15	1.0510
λ	10.12	0.27	$(-1.50, 0.08)$	0.10	1.1757

Table 5: Efficiency indicators of the SV-HARG parameters estimation results. Please refer to the previous Figure's note for more technical details.

SV-HARG	INEFF	ACC	Geweke's Test	KS	PSRF
μ	5.77		$(0.35, 0.36)$	0.24	1.0140
γ	16.34		$(0.72, 0.23)$	0.35	1.0512
κ_2	12.89	0.26	$(-0.01, 0.50)$	0.63	0.9891
φ	17.05	0.28	$(0.34, 0.37)$	0.10	1.0390
δ	13.10	0.21	$(-1.04, 0.15)$	0.32	1.0030
$\beta^{(d)}$	12.51	0.24	$(0.31, 0.37)$	0.27	0.9896
$\beta^{(w)}$	11.90	0.24	$(1.48, 0.07)$	0.24	1.1619
$\beta^{(m)}$	18.19	0.24	$(-1.17, 0.12)$	0.23	1.0014
c	17.44		$(-0.88, 0.19)$	0.22	1.0973

Table 6: Efficiency indicators of the parameters estimation results for SV-LHARG model. Please refer to the previous Figure's note for more technical details.

SV-HARG	INEFF	ACC	Geweke's Test	KS	PSRF
μ	1.12		$(-0.65, 0.26)$	0.34	0.9929
γ	1.11		$(0.42, 0.34)$	0.34	0.9918
κ_2	1.11	0.23	$(-0.82, 0.21)$	0.30	1.0003
φ	1.23	0.26	$(-1.10, 0.14)$	0.88	0.9898
δ	1.29	0.27	$(-1.04, 0.15)$	0.61	1.0059
$\beta^{(d)}$	2.67	0.17	$(0.99, 0.16)$	0.22	0.9922
$\beta^{(w)}$	7.22	0.17	$(0.99, 0.16)$	0.10	0.9892
$\beta^{(m)}$	22.62	0.17	$(0.95, 0.17)$	0.20	0.9921
$\alpha^{(d)}$	1.79	0.32	$(1.49, 0.06)$	0.56	0.9934
$\alpha^{(w)}$	10.87	0.32	$(-0.65, 0.26)$	0.27	0.9959
$\alpha^{(m)}$	22.57	0.32	$(0.26, 0.40)$	0.15	0.9929
λ	1.03	0.29	$(0.94, 0.17)$	0.88	0.9928
c	1.17		$(0.50, 0.31)$	0.51	1.0033

Table 7: Parameters estimates and efficiency indicators for SV-LHARG . The results are averages over a set of 50 independent MCMC experiments on 50 independent dataset of 1,000 observations. On each dataset we ran the proposed MCMC algorithm for 50,000 iterations and then discard the first 5,000. A thinning procedure with a factor of 30 is applied. As efficiency indicators we report: the inefficiency factor (INEFF) of the estimation of the posterior mean, the acceptance rate (ACC) of the MH step, the Geweke's spectral density diagnostic, the Kolmogorov-Smirnov (KS) test and the potential scale reduction factor (PSRF). We set μ to $2.5/252\%$.

$\boldsymbol{\theta}$	True	Estimated	INEFF	ACC	Gweke's Test	KS	PSRF
γ	-0.0222	0.0370 (0.0438)	2.0305		$(-0.5633, 0.2171)$	0.3823	1.0098
φ	0.6207	0.6220 (0.005)	7.9394	0.6569	$(0.82, 0.21)$	0.6475	0.9950
δ	1.1429	1.4089					
κ_2	-2.7249	-2.7475 (0.0668)	6.1880	0.5303	$(-1.0562, 0.1073)$	0.2282	1.0351
c	0.0475	0.0491 (0.0014)	17.4468	0.5872	$(1.1001, 0.0610)$	0.1562	1.3904
$\beta^{(d)}$	2.9375	2.7051 (1.1166)	7.8314	0.4528	$(1.0994, 0.0637)$	0.2074	1.0916
$\beta^{(w)}$	2.3116	1.4806 (0.6877)	9.1835	0.4528	$(1.8866, 0.1122)$	0.1924	1.1124
$\beta^{(m)}$	1.8510	0.6188 (0.3955)	17.1422	0.4528	$(2.7459, 0.0669)$	0.1285	1.0716
$\alpha^{(d)}$	0.5570	0.9137 (0.1547)	21.4151	0.2224	$(-5.6038, 0.0524)$	0.2430	1.0888
$\alpha^{(w)}$	0.4601	0.8242 (0.1653)	20.2257	0.2224	$(-5.5044, 0.0535)$	0.2204	1.0562
$\alpha^{(m)}$	4.6643e-04	0.0309 (0.0415)	25.8293	0.2224	$(-5.5041, 0.0555)$	0.1371	1.0421
λ	3.5050	2.8402 (0.3237)	23.4727	0.0762	$(5.9606, 0.0546)$	0.1285	1.1128
NRMSE	0.0891						

E Properties of the SV-LHARG

This section reports the results linked to the affine property of the SV-LHARG. These results largely follow Majewski et al. (2015). For this reason, we refer to the latter paper for the complete proofs. Here, we give the MGF of the SV-LHARG(p) under the physical probability $\mathbb{P}$, the no-arbitrage conditions, and mapping of the parameters from $\mathbb{P}$ to $\mathbb{Q}$.

E.1 MGF under the physical probability $\mathbb{P}$

The MGF of the SV-LHARG(p) under the physical measure $\mathbb{P}$ can be readily obtained from Proposition 3 in Majewski et al. (2015) provided that Assumption 1 in the same paper holds true. This result is granted from the following Proposition 1.

Proposition 1. *Under $\mathbb{P}$, the conditional one-step-ahead* MGF *of the* SV-LHARG(p) *is given by*

$$\begin{aligned}\mathbb{E}^{\mathbb{P}}&\left[e^{\bar{z}r_{t+1}+\bar{b}h_{t+1}+\bar{c}l_{t+1}+\bar{d}\mathrm{RV}_{t+1}}|\widetilde{\mathcal{F}}_t\right]\\&=\exp\left(\mathcal{A}\left(\bar{z},\chi,\bar{c}\right)+\sum_{i=1}^{p}\mathcal{B}_i\left(\bar{z},\chi,\bar{c}\right)h_{t+1-i}+\sum_{i=1}^{p}\mathcal{D}_i\left(\bar{z},\chi,\bar{c}\right)l_{t+1-i}\right),\end{aligned}\tag{E.1}$$

where the functions $\mathcal{A}:\mathbb{R}\times\mathbb{R}\times\mathbb{R}\to\mathbb{R}$, $\mathcal{B}_i:\mathbb{R}\times\mathbb{R}\times\mathbb{R}\to\mathbb{R}$, and $\mathcal{C}_i:\mathbb{R}\times\mathbb{R}\times\mathbb{R}\to\mathbb{R}$, $i=1,\ldots,p$, are defined as:

$$\begin{aligned}\mathcal{A}(\bar{z},\chi,\bar{c})&=\bar{z}\mu-\frac{1}{2}\log\left(1-2\bar{c}\right)-\delta\mathcal{W}(x(\bar{z},\chi,\bar{c}),c),\\\mathcal{B}_i(\bar{z},\chi,\bar{c})&=\mathcal{V}(x(\bar{z},\chi,\bar{c}),c)\beta_i,\\\mathcal{D}_i(\bar{z},\chi,\bar{c})&=\mathcal{V}(x(\bar{z},\chi,\bar{c}),c)\varphi_i,\end{aligned}$$

with

$$\begin{aligned}&\mathcal{V}(x,c)=\frac{cx}{1-cx},\\&\mathcal{W}(x,c)=\log\left(1-cx\right),\\&x(\bar{z},\chi,\bar{c})=\bar{z}\gamma+\chi+\frac{\frac{1}{2}\bar{z}^2+\lambda^2\bar{c}-2\bar{c}\bar{z}\lambda}{1-2\bar{c}},\\&\chi=\bar{b}-\exp(\kappa_2)\log(1-\varphi\exp(-\kappa_2)\bar{d}).\end{aligned}$$

Proof. Firstly, one needs to show that

$$
\begin{aligned}
&\mathbb{E}^{\mathbb{P}}\left[e^{\bar{z}r_{t+1}+\bar{b}h_{t+1}+\bar{c}l_{t+1}+\bar{d}\mathrm{RV}_{t+1}}|\widetilde{\mathcal{F}}_t\right]\\
&=\mathbb{E}^{\mathbb{P}}\left[e^{\bar{z}r_{t+1}+\bar{b}h_{t+1}+\bar{c}l_{t+1}}\mathbb{E}^{\mathbb{P}}\left[e^{\bar{d}\mathrm{RV}_{t+1}}|r_{t+1},h_{t+1}\right]|\widetilde{\mathcal{F}}_t\right]\\
&=\mathbb{E}^{\mathbb{P}}\left[e^{\bar{z}r_{t+1}+(\bar{b}-e^{\kappa_2}\log(1-\varphi e^{-\kappa_2}\bar{d}))h_{t+1}+\bar{c}l_{t+1}}|\widetilde{\mathcal{F}}_t\right].
\end{aligned}
\tag{E.2}
$$

Then, the explicit form of the scalar functions $\mathcal{A}$, $\mathcal{B}_i$ and $\mathcal{C}_i$ follows from Appendix C in Majewski et al. (2015). □

E.2 No arbitrage conditions and mapping of the parameters

Proposition 2. *The* SV-LHARG(p) *satisfies the no-arbitrage condition if and only if*

$$\nu_2=\gamma+\frac{1}{2}. \tag{E.3}$$

Proof of Proposition 2. See Majewski et al. (2015), Appendix C. □

The one-to-one mapping of the parameters under $\mathbb{P}$ to those under the $\mathbb{Q}$ measure is given in the following Proposition 3, which ensures that the risk-neutral log-return dynamics is still governed by a SV-LHARG(p) process.

Proposition 3. *Under risk-neutral measure* $\mathbb{Q}$ *the conditional variance follows a* SV-LHARG(p) *process with parameters*

$$
\begin{aligned}
&\beta^{(d,*)}=\frac{1}{1-cy^*}\beta^{(d)}, &&\beta^{(w,*)}=\frac{1}{1-cy^*}\beta^{(w)}, &&\beta^{(m,*)}=\frac{1}{1-cy^*}\beta^{(m)},\\
&\alpha^{(d,*)}=\frac{1}{1-cy^*}\alpha^{(d)}, &&\alpha^{(w,*)}=\frac{1}{1-cy^*}\alpha^{(w)}, &&\alpha^{(m,*)}=\frac{1}{1-cy^*}\alpha^{(m)},\\
&c^*=\frac{1}{1-cy^*}c, &&\nu^*=\nu, &&\lambda^*=\lambda+\gamma+\frac{1}{2},
\end{aligned}
$$

where $y^*=-\frac{\gamma^2}{2}-\nu_1+\frac{1}{8}$.

Proof of Proposition 3. See Majewski et al. (2015), Appendix D. □

E.3 Properties of the SV-LHARG

E.3.1 Proof on stationarity conditions of the SV-LHARG(p)

Proof of Proposition 1 of the main text. Let us define the function $x : \mathbb{R} \times \mathbb{R} \times \mathbb{R} \to \mathbb{R}$ as

$$x(\bar{z}, \bar{b}, \bar{c}) = \bar{z}\lambda + \bar{b} + \frac{\frac{1}{2}\bar{z}^2 + \lambda^2\bar{c} - 2\bar{c}\bar{z}\lambda}{1 - 2\bar{c}},$$

and $x_1 \doteq x(0, u_1, v_1)$. Reasoning as in Appendix F of Gouriéroux and Jasiak (2006), we have to find the conditions which ensure that the solution of the $2p$-dimensional recursive system:

$$\begin{aligned} u_{1,t} &= \frac{cx_{1,t-1}}{1 - cx_{1,t-1}}\beta_1 + u_{2,t-1} \ldots u_{p-1,t} = \frac{cx_{1,t-1}}{1 - cx_{1,t-1}}\beta_{p-1} + u_{p,t-1}\,, u_{p,t} = \frac{cx_{1,t-1}}{1 - cx_{1,t-1}}\beta_p \\ v_{1,t} &= \frac{cx_{1,t-1}}{1 - cx_{1,t-1}}\alpha_1 + v_{2,t-1} \ldots v_{p-1,t} = \frac{cx_{1,t-1}}{1 - cx_{1,t-1}}\alpha_{p-1} + v_{p,t-1}\,, v_{p,t} = \frac{cx_{1,t-1}}{1 - cx_{1,t-1}}\alpha_p \end{aligned}$$

tends to $(0, \ldots, 0)'$ when t tends to infinity, for any non-negative initial values $(u_{1,0}, \ldots, u_{p,0})'$ and $(v_{1,0}, \ldots, v_{p,0})'$. System above is equivalent to the following one

$$\begin{aligned} u_{1,t} &= \frac{\beta_1}{\beta_p}u_{p,t} + u_{2,t-1} \ldots u_{p-1,t} = \frac{\beta_{p-1}}{\beta_p}u_{p,t} + u_{p,t-1},\ u_{p,t} = \frac{\beta_p}{1 - cx_{1,t-1}} - \beta_p \\ v_{1,t} &= \frac{\alpha_1}{\alpha_p}v_{p,t} + v_{2,t-1} \ldots v_{p-1,t} = \frac{\alpha_{p-1}}{\alpha_p}v_{p,t} + v_{p,t-1},\ v_{p,t} = \frac{\alpha_p}{1 - cx_{1,t-1}} - \alpha_p \end{aligned}$$

From the latter, it follows that $u_{i,t}$ and $v_{j,t}$ take non negative values for all $i, j \in \{1, \ldots, p\}$ and that $u_{p,t}$ and $v_{p,t}$ are always larger than $-\beta_p$ and $-\alpha_p$, respectively. Moreover, the sequence $(u_{p,t})$ satisfies the non-linear difference equation:

$$u_{p,t} = \frac{\beta_p}{1 - \frac{c}{\beta_p}\left(\sum_{i=1}^p u_{p,t-i}\beta_i + \lambda^2\beta_p\frac{\sum_{j=1}^p v_{p,t-j}\alpha_j}{1-2\sum_{j=1}^p v_{p,t-j}\alpha_j}\right)} - \beta_p. \tag{E.4}$$

In light of the relation $v_{p,t}\beta_p = u_{p,t}\alpha_p$, all $t \geq 0$, we rewrite previous Eq. (E.4) as follows:

$$u_{p,t} = \frac{\beta_p}{1 - \frac{c}{\beta_p}\left(\sum_{i=1}^p u_{p,t-i}\beta_i + \lambda^2\frac{\sum_{j=1}^p u_{p,t-j}\alpha_j}{1-\frac{2}{\beta_p}\sum_{j=1}^p u_{p,t-j}\alpha_j}\right)} - \beta_p.$$

Thus, a possible limiting value l for the rescaled sequence $(u_{p,t}\beta_p^{-1})$ satisfies:

$$l = \frac{1}{1 - lc\left(\sum_{i=1}^p \beta_i + \lambda^2\frac{\sum_{j=1}^p a_j}{1-2l\sum_{j=1}^p \alpha_j}\right)} - 1 \doteq \frac{1}{1 - lc\left(\|\boldsymbol{\beta}\| + \lambda^2\frac{\|\boldsymbol{\alpha}\|}{1-2l\|\boldsymbol{\alpha}\|}\right)} - 1.$$

Therefore, the admissible values are $l = 0$ and $l = \frac{1}{c(\|\boldsymbol{\beta}\|+\lambda^2\|\boldsymbol{\alpha})} - 1$. If $c(\|\boldsymbol{\beta}\| + \gamma^2\|\boldsymbol{\alpha}\|) < 1$ the rescaled sequence $(u_{p,t}\beta_p^{-1})$ takes values in the compact set $[-1, 0]$ and the unique solution is $l = 0$. Given the relation $v_{p,t} = u_{p,t}\alpha_p/\beta_p$, the same conclusion holds for $v_{p,t}$. $\square$

F Additional details on financial applications

F.1 Computational details

In this section, we explain how starting values for the parameters of SV-ARG , SV-LARG , SV-HARG and SV-LHARG have been initialized in the Bayesian inference procedure.
SV-ARG is characterized by the 7-dimensional parameter vector $\boldsymbol{\theta} = \left(\mu, \gamma, \varphi, \kappa_2, \delta, c, \beta^{(d)}\right)$. The risk-free rate is fixed as $\mu = (2.5/252)\,\%$. The parameter γ is set to zero. To fix the initial value of φ, we roughly estimate it by using a rolling-window analysis over the estimation period. Precisely, we use the quantity $\hat{\varphi}$, introduced in Hansen and Lunde (2005)

$$\hat{\varphi} = \frac{\sum_{t=1}^{m} (r_t - \bar{r})^2}{\sum_{t=1}^{m} \mathrm{RV}_t},$$

where r_t is the daily close-to-close return and $\bar{r}$ is its average over an m-day sample period. We set the rolling window size equal to $m = 20$ and then we average the $T - m + 1$ estimates to fix the initial guess. Specifically, we set $\hat{\varphi} = 0.66$. Starting values for the parameters $\beta^{(d)}$ and c are computed by matching the unconditional mean and variance of squared returns to the invariant distribution of the SV-ARG process (see also Creal, 2017). δ is fixed by targeting the sample mean of the realized variance. Finally, κ_2 is set by matching the unconditional variance of the observed RV to the invariant distribution of the RV process. Initial trajectory for $h_{1:T}$ is set as $h_{1:T} = \hat{\varphi}\mathrm{RV}_{1:T}$. Finally, by using initial guesses for $\boldsymbol{\theta}$ and $h_{1:T}$, we simulate $z_{1:T}$ according to the SV-ARG dynamics. The maximum number of states for the approximating Markov Chain of the process z_t results equal to 300. As done in Creal (2017), the Feller condition $\delta > 1$, as well as the stationary constraint, $0 < c\beta^{(d)} < 1$, are imposed throughout the estimation.
SV-LARG model is characterized by the parameter vector $\boldsymbol{\theta} = \left(\mu, \gamma, \varphi, \kappa_2, \delta, c, \beta^{(d)}, \alpha^{(d)}, \lambda\right)$. To fix $\left\{\mu, \gamma, \varphi, \kappa_2, c, \beta^{(d)}\right\}$ we proceed as before. To set $\alpha^{(d)}$ and λ, one observes that the variance of log-return idiosyncratic component is equal to one. The conditional expectation of the leverage component has to be of order one, too. So, as initial values, it is meaningful to guess $\alpha^{(d)} = T^{-1}\sum_{t=1}^{T} h_t$ and $\lambda = 1/\sqrt{\alpha^{(d)}}$. Then, after setting $h_{1:T} = \hat{\varphi}\mathrm{RV}_{1:T}$, $z_{1:T}$ is simulated according to the SV-LHARG dynamics. We fix $N = 300$, in order to have a

consistent and fair comparison among models. In this case too, both the Feller condition and the stationarity constraint are imposed throughout the estimation.

SV-HARG is characterized by the parameter vector $\boldsymbol{\theta} = \left(\mu, \gamma, \varphi, \kappa_2, \delta, c, \beta^{(d)}, \beta^{(w)}, \beta^{(m)}\right)$. We set $\{\mu, \gamma, \varphi, \kappa_2, c\}$ as for the SV-ARG, and the auto-regressive coefficients equal to $\left(0.5\hat{\beta}^{(d)}, 0.3\hat{\beta}^{(d)}, 0.2\hat{\beta}^{(d)}\right)$ where $\hat{\beta}^{(d)}$ is the parameter value estimated from SV-ARG. Initial guesses for $h_{1:T}$ and $z_{1:T}$ are set as before, and $N = 300$.

Finally, similar reasoning applies to the SV-LHARG, in which we set the auto-regressive coefficients equal to $\left(\alpha^{(d)}, \alpha^{(w)}, \alpha^{(m)}\right) = \left(0.5\hat{\alpha}^{(d)}, 0.3\hat{\alpha}^{(d)}, 0.2\hat{\alpha}^{(d)}\right)$, being $\hat{\alpha}^{(d)}$ the SV-LARG estimates. Moreover, we remind that SV-LHARG has been estimated over three different time intervals: January 1, 1997 – December 31, 2006; January 1, 1998 – December 31, 2007; January 1, 1999 – December 31, 2008. So, for instance, once the model has been estimated over the period January 1, 1997 – December 31, 2006, starting values for the parameters over the subsequent period have been set equal to the optimal parameters value of resulting from the estimation over the window January 1, 1997 – December 31, 2006. Similar reasoning applies for the remaining time periods.

F.2 Calibration of the variance risk-premium ν_1

This section explains the calibration procedure of the variance risk-premium ν_1 on the option data. We adopt a method based on the unconditional minimization of the distance between the market and the model implied volatility surface. For this reason, we divide our dataset in different intervals of moneyness and maturity – as described in the main text – obtaining a 5×4 moneyness-maturity grid and, thus, a 20-points discrete representation of the implied volatility surface. For each subset, we compute the unconditional average of the market implied volatilities. Then, we calculate the corresponding model implied volatility and obtain the optimal values of ν_1 as the one that minimizes the following objective function

$$f_{\text{obj}}(\nu_1) = \sqrt{\sum_{i=1}^{5} \sum_{j=1}^{4} \left(\text{IV}_{ij}^{\text{MOD}} - \text{IV}_{ij}^{\text{MKT}}\right)^2},$$

which represents the quadratic distance between the model implied volatility surface and the market one, whose elements are $\text{IV}_{ij}^{\text{MOD}}$ and $\text{IV}_{ij}^{\text{MKT}}$, respectively.

F.3 Additional results on Option pricing

F.3.1 Option pricing: Performance assessment for the SV class

In this section, we compare the performance of the different models belonging to the SV-LHARG class. The option time series span the interval from January 1, 1997 to December 31, 2006. Parameters are estimated over the same time period and are reported in Table 8. Table 11, Panels A, B, C report the relative RMSE_{IV} – with statistical significance – of the SV-LHARG with respect to the SV-ARG, SV-LARG, and SV-HARG respectively, sorted by moneyness and maturity . In particular, the Table highlights the importance of including the leverage component *together with* the multi-component structure of the volatility. The improvement of the SV-LHARG model over both SV-LARG and SV-ARG for DOTM and OTM options varies from 13% to 45%. Instead, it is less strict if we compare SV-LHARG with SV-HARG in the OTM region. This is due, as expected, to the adequate level of volatility persistence reached by the SV-HARG model. A similar condition holds for options in the ATM region. Our analysis suggests that heterogeneity, leverage, and persistence are all necessary ingredients for an accurate option pricing across different maturities and moneyness. For this reason the SV-LHARG consistently shows the best option pricing performance among the models belonging to the SV class.

F.3.2 Option pricing: Additional empirical evidences

This section presents (additional) empirical results for option pricing with the SV-LHARG, RV-LHARG, CGARCH, and RVM models (Christoffersen et al., 2015, 2016). The RVM model can be considered as an improved version of the Generalized Affine Realized Volatility (henceforth GARV) model introduced by Christoffersen et al. (2014). The RVM belongs to the more general approach to return and volatility dynamics modeling, dubbed BPJVM. The latter allows for the inclusion of a jump component and when jumps are switched off it boils down to the RVM. The following equations characterize the RVMmodel

$$\begin{aligned} r_{t+1} &= \mu + \gamma_z h_{z,t} + \sqrt{h_{z,t}}\varepsilon_{1,t+1}, \quad \text{with}\, \varepsilon_{1,t+1} \overset{d}{\sim} \mathcal{N}(0,1) \\ h_{z,t+1} &= \omega_z + \beta_z\, h_{z,t} + \alpha_z \mathrm{RV}_{t+1} \\ \mathrm{RV}_{t+1} &= h_{z,t} + \sigma \left[\left(\varepsilon_{2,t+1} - \gamma_1 \sqrt{h_{z,t}} \right)^2 - \left(1 + \gamma_1^2\, h_{z,t}\right) \right] \quad \text{with}\, \varepsilon_{2,t+1} \overset{d}{\sim} \mathcal{N}(0,1), \end{aligned}$$

where r_t indicates daily log-returns and $\gamma_z = \left(\lambda_z - \frac{1}{2}\right)$. Concerning the second and the third equation, the coefficient β_z captures the influence of the past latent conditional variance on its future level, while α_z describes the impact of the observable realized volatility.

Before proceeding, we point out that within the RVM the positive definiteness of the realized volatility is not guaranteed. Formally, for a particular realization of $\varepsilon_{2,t+1}$, it could happen that $\sigma \left[\left(\varepsilon_{2,t+1} - \gamma_1 \sqrt{h_{z,t}} \right)^2 - (1 + \gamma_1^2\, h_{z,t}) \right] < -h_{z,t}$. Let us assess in a quantitative way the probability of obtaining negative values. By using a given value of $h_{z,0}$, we evaluate the probability to obtain an entirely positive trajectory of length $T = 250$ (days) for the realized volatility by drawing a large number of Monte Carlo paths. We conduct this analysis by using values of the parameters estimated over the three (in-sample) periods considered in the main text, i.e. January 1, 1997 – December 31, 2006, January 1, 1998 – December 31, 2007, and January 1, 1999 – December 31, 2008. Tables 8, 9 and 10, last-column, report the estimated values. They statistically agree with those in Table 1 in Christoffersen et al. (2016). We find that the probability $\mathbb{P}\left(\mathrm{RV}_t > 0,\, t \in \{1, \ldots, 250\}\, | h_{z,0}\right)$ is equal to 18.05% for the first set of parameters, 17.93% for the second, and 14.52% for the third, when $h_{z,0}$ is set equal to the unconditional mean of RV. Thus, the probability of obtaining negative realized volatility value on a simulated trajectory is extremely high. Nonetheless, this drawback could be compensated by the ability of the model in capturing the implied volatility dynamics. To test this, we include the RVM among the competitor models of the SV-LHARG. In particular, as for the CGARCH, we assume the following SDF

$$M_{t,t+1} = \frac{e^{-\nu_1\, h_{z,t+2} - \nu_2\, r_{t+1}}}{\mathbb{E}^{\mathbb{P}} \left[e^{-\nu_1\, h_{z,t+2} - \nu_2\, r_{t+1}} | \widetilde{\mathcal{F}}_t \right]},$$

where ν_1 is the variance risk premium and ν_2 the usual equity risk premium. The former is calibrated to the market, whereas the latter is fixed through a non-arbitrage argument. Table 11, 12 and 13 reports the in-sample performance on S&P500 OTM options over the period January 1, 1997 – December 31, 2006, January 1, 1998 – December 31, 2007, and January 1, 1999 – December 31, 2008, respectively. Tables 14 and 15 detail the out-of-sample analysis. First, let us comments the (sign) of the variance risk premium. It is worth recalling that a positive or negative risk premium reduces or amplifies, respectively, the unconditional mean of the return conditional variance. Looking at the calibrated variance risk premium – see Tables 8, 9, and 10 – the premium ν_1 for the SV-LHARG model is negative for all periods. The conditional variance filtered from historical returns and realized volatilities needs to be inflated to reproduce the level implied by the option quotes. The negative value is consistent with the economic interpretation of the variance premium as a positive premium reuired by an economic agent as a compensation for baring the uncertainty of volatility. The same holds true for both RV-LHARG , CGARCH and RVM models until December 31, 2007. When the last year January 1, 2008 – December 31, 2008 is included in the estimation/calibration sample, the risk premium coefficient becomes positive for RV-LHARG and CGARCH . For the SV-LHARG and RVM model the coefficient remains negative, but reduces substantially with respect to the value calibrated in the previous periods. These latter results are consistent with a sizeable increase of the level of historical volatility observed in last year of the sample. The impact on the estimated model parameters is given by a positive shift of the unconditional volatility. As a balancing, the variance risk premium decreases to reconcile market- and model-implied volatilities over the entire calibration period. Second, let us focus on the relative percentage implied volatility root mean squared error (RMSE_{IV}) of the SV-LHARG model (benchmark) with respect to the RVM. Each relative RMSE_{IV} is accompanied by the statistical significance computed from a t-test with HAC errors. In-sample, the relative performances over the three periods are quite similar. The improvement of the SV-LHARG model for ATM options and near ATM put and call options is remarkable for all the maturities and varies from 20% to 40%. The SV-LHARG also perform better for DOTM options on call side, where the improvement is almost 40% . Globally, the SV-LHARG outperforms the RVM by 15% in the range of moneyness $0.9 < m < 1.1$ and by 10% in the range of moneyness $0.8 < m < 1.2$. Moreover, as far as the out-of-sample analysis is concerned, Tables 14 and 15 confirm that the SV-LHARG model outperforms the RVM model too. In particular, for the period January 1, 2008 - December 31, 2008, the improvement is almost 60% both in the moneyness region between 0.9 and 1.1 and when including DOTM options.

We now provide additional insight into the performance of the SV-LHARG by analysing the differences across models along different dimensions.

First, we plot the weekly average of the ATM implied volatility bias at the shortest maturity, defined as the average observed market implied volatility less average model implied volatility. Parameter values are taken from Table 9 for the period January 1, 1998 – December 31, 2007. Over the period January 1, 1998 – December 31, 2003, the SV-LHARG performances are in line with those of the RV-LHARG and better than those of both the CGARCH and RVM. We note that while the first three models show significant under-pricing (positive bias) in this period, the bias of the RVM model alternates in sign. On the other hand, during the low volatility period from January 1, 2004 to December 31, 2006, the situation is quite the opposite: SV-LHARG, RV-LHARG, and CGARCH models present a negative bias (over-pricing), whereas the RVM model shows a positive bias (under-pricing). Finally, over the last year – just before the global financial crisis – all the models show significant under-pricing. Nonetheless, the SV-LHARG shows a smaller positive bias, suggesting that it is able to better react to the fast changing dynamics of market volatility.

Figure 4: Weekly ATM Implied volatility bias for options at the shortest available maturity on a given Wednesday. Sample period: January 1, 1998 – December 31, 2007. From left to right, from top to bottom: SV-LHARG model, RV-LHARG model, CGARCH model, and RVM model. Parameters value are taken from Table 9.

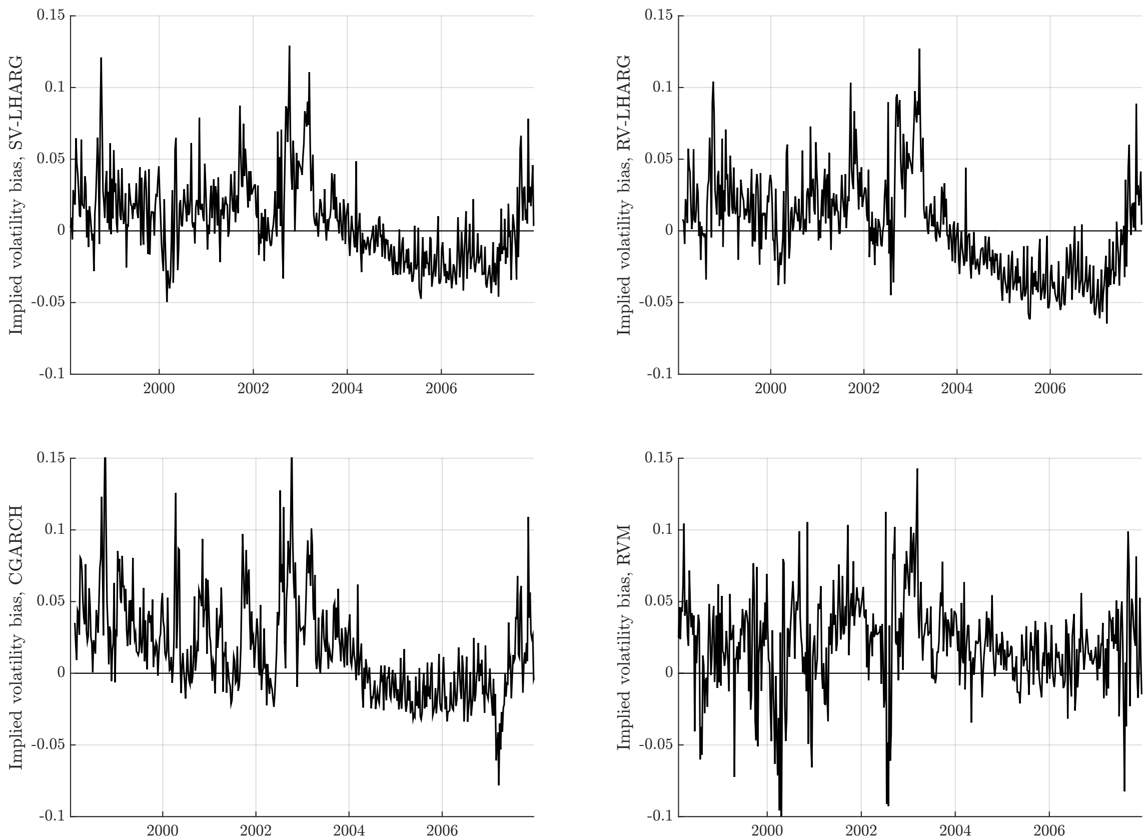

Second, we report two implied volatility smiles reproduced by the four classes of models. We consider time-to-maturities ranging from 10 to 50 days and from 50 to 90 days. In both cases, the smile is quite pronounced. The left panel in Figure 5 shows the smiles from the market together with those corresponding to SV-LHARG , RV-LHARG , CGARCH and RVM computed in-sample and averaged over the period January 1, 1999 – December 31, 2008 for time-to-maturities from 50 to 90 days. The right panel of the same figure reports the smiles obtained averaging the data out-of-sample for time-to-maturities ranging from 10 to 50 days. Both plots confirm the ability of the SV-LHARG to track the ATM level of implied volatility. Finally, we consider the time-series of absolute Root Mean Square

Figure 5: IV smiles from the market (triangles), from the CGARCH(circles), from the SV-LHARG (diamonds), from the RV-LHARG (squares), and from the RVM (stars). Left panel: in-sample period, January 1, 1999 to December 31, 2008. Right panel: out-of-sample smiles from January 1, 2008 to December 31, 2008.

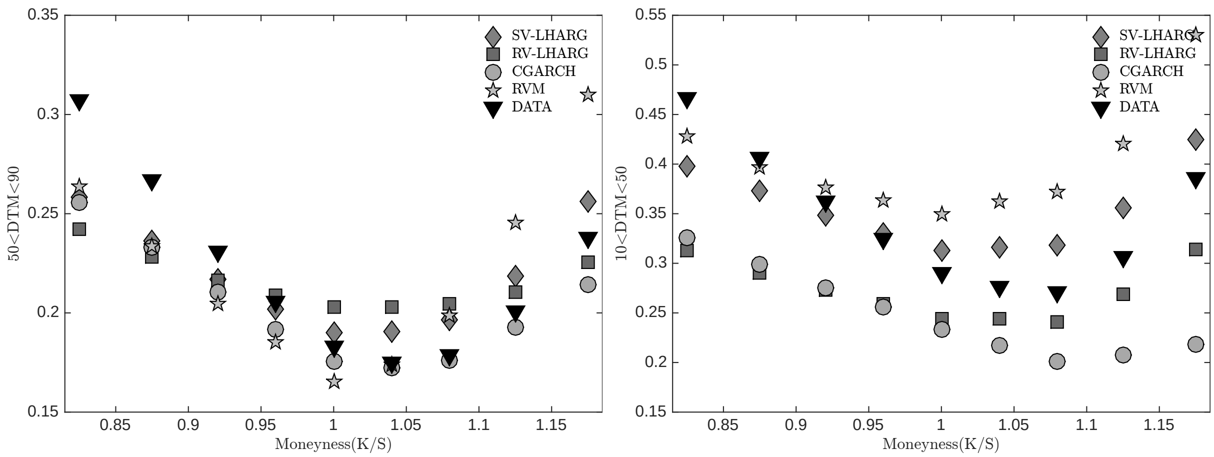

Error conditioning on the moneyness–time-to-maturity bucket. On each Wednesday, we compute the $\text{RMSE}_{\text{IV},t}$ for all models. Figures 6, 7, 8 and 9 report the time-series for the period January 1, 1998 – December 31, 2008. For the sake of readability, only the first Wednesday of each month is reported. A vertical black line divides the in-sample from the out-of-sample period. Shapes and colors of the markers associated to the different models are those used in Figure 5. The y-axis label provides the details about the bucket. The two most striking features, supporting the conclusions presented in the main text, are: i) the CGARCH model worsens its performances out-of-sample, especially for short time-to-maturities; ii) the RVM deteriorates out-of-sample when it comes to price long-horizon options.

Figure 6: Absolute $\text{RMSE}_{\text{IV},t}$ time-series for the period January 1, 1998 – December 31, 2008 for different moneyness–time-to-maturity buckets. Details can be recovered from the vertical axis label. The period January 1, 1998 – December 31, 2007 corresponds to the in-sample analysis, while January 1, 2008 – December 31, 2008 corresponds to the out-of-sample one. Parameter values are taken from Table 9.

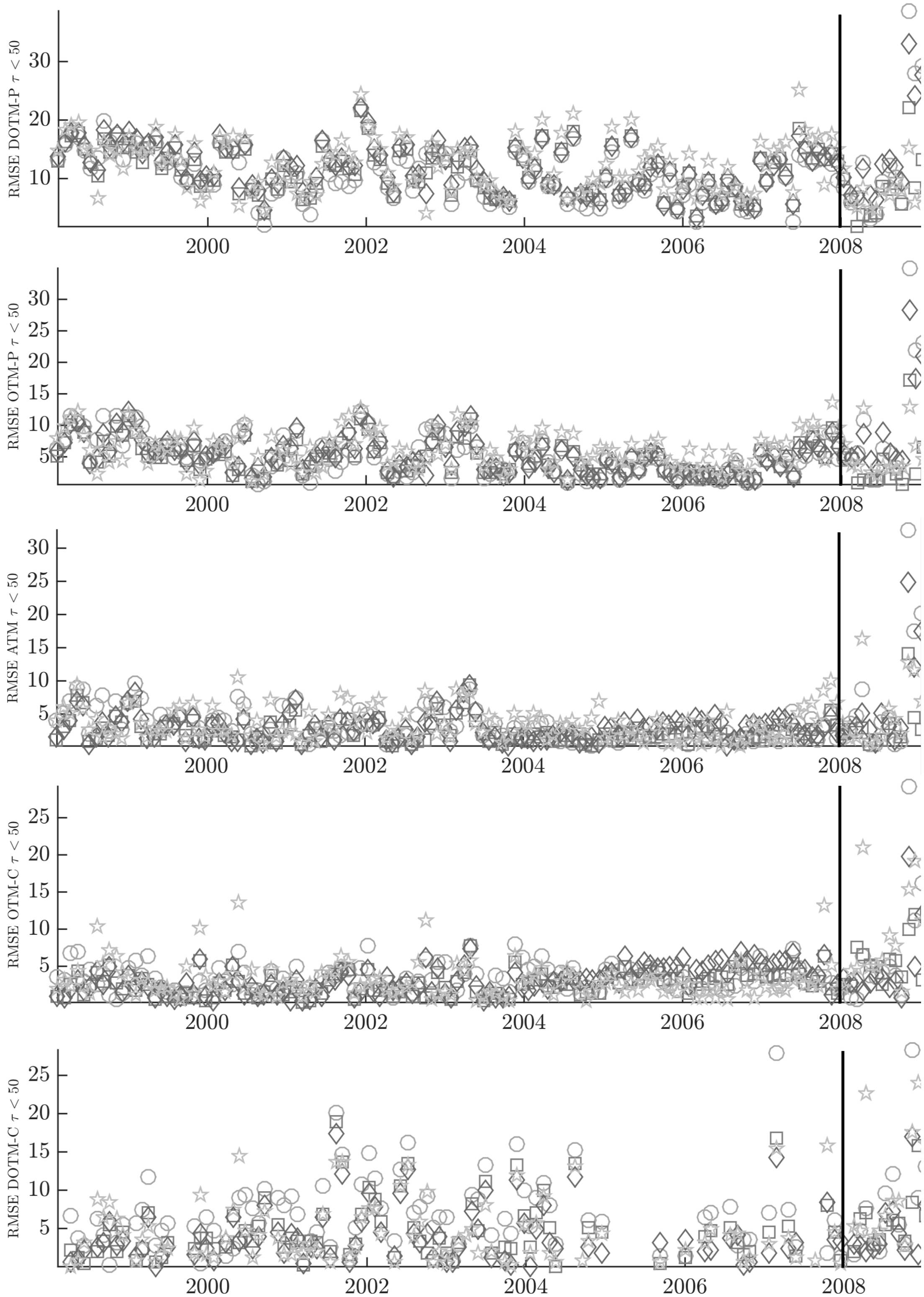

Figure 7: Absolute $\text{RMSE}_{\text{IV},t}$ time-series for the period January 1, 1998 – December 31, 2008 for different moneyness–time-to-maturity buckets. Details can be recovered from the vertical axis label. The period January 1, 1998 – December 31, 2007 corresponds to the in-sample analysis, while January 1, 2008 – December 31, 2008 corresponds to the out-of-sample one. Parameter values are taken from Table 9.

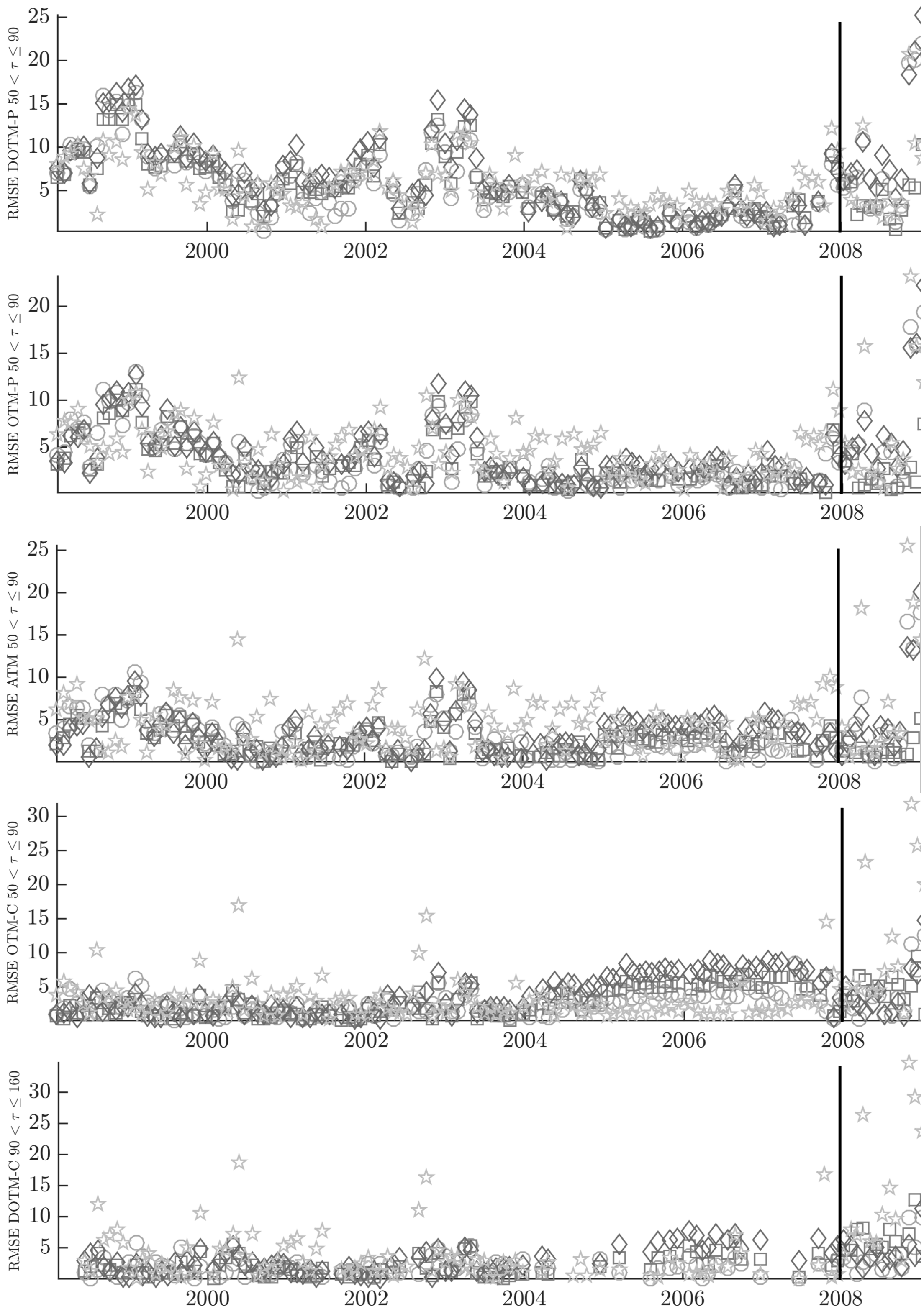

Figure 8: Absolute $\text{RMSE}_{\text{IV},t}$ time-series for the period January 1, 1998 – December 31, 2008 for different moneyness–time-to-maturity buckets. Details can be recovered from the vertical axis label. The period January 1, 1998 – December 31, 2007 corresponds to the in-sample analysis, while January 1, 2008 – December 31, 2008 corresponds to the out-of-sample one. Parameter values are taken from Table 9.

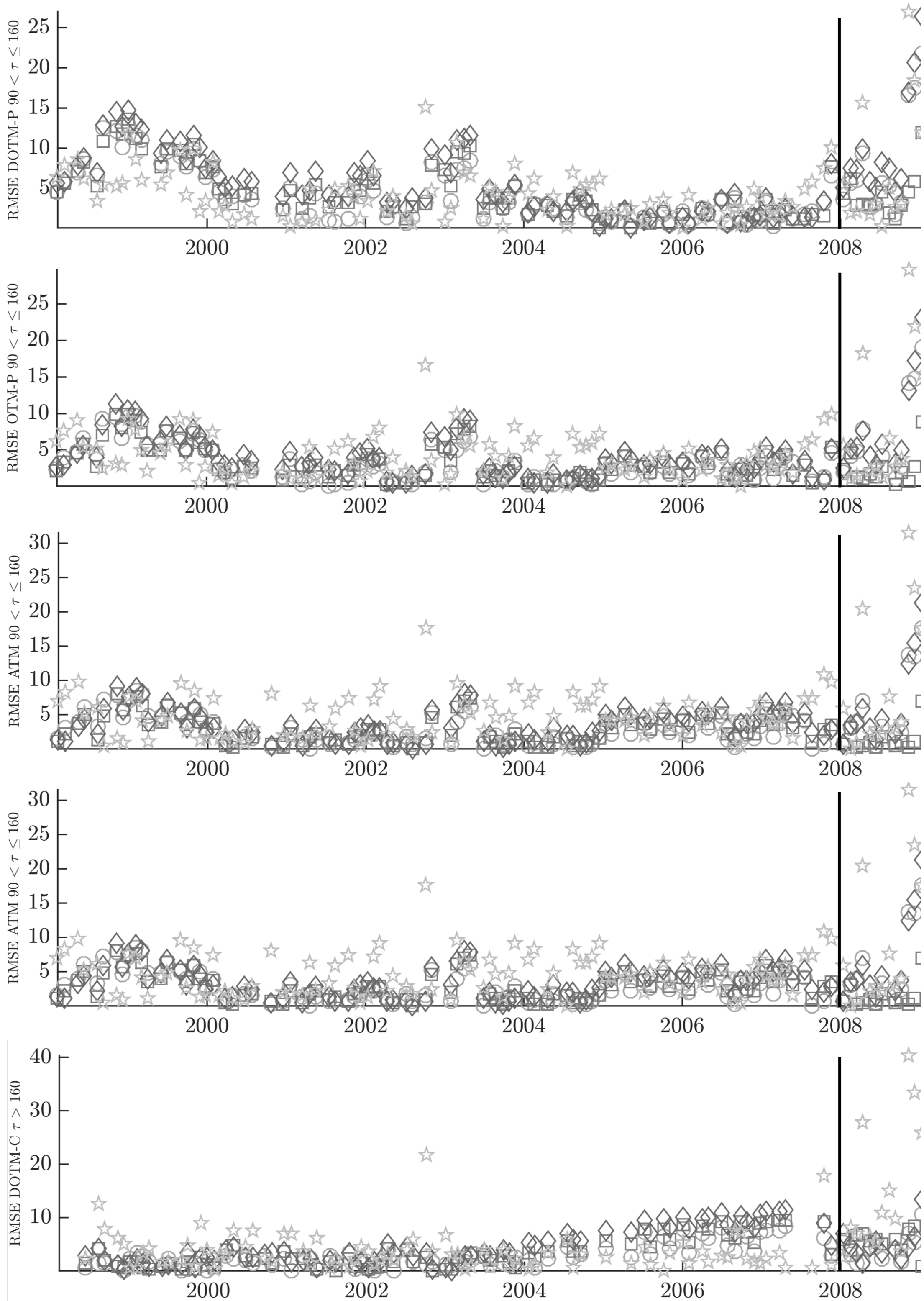

Figure 9: Absolute $\mathrm{RMSE}_{\mathrm{IV},t}$ time-series for the period January 1, 1998 – December 31, 2008 for different moneyness–time-to-maturity buckets. Details can be recovered from the vertical axis label. The period January 1, 1998 – December 31, 2007 corresponds to the in-sample analysis, while January 1, 2008 – December 31, 2008 corresponds to the out-of-sample one. Parameter values are taken from Table 9.

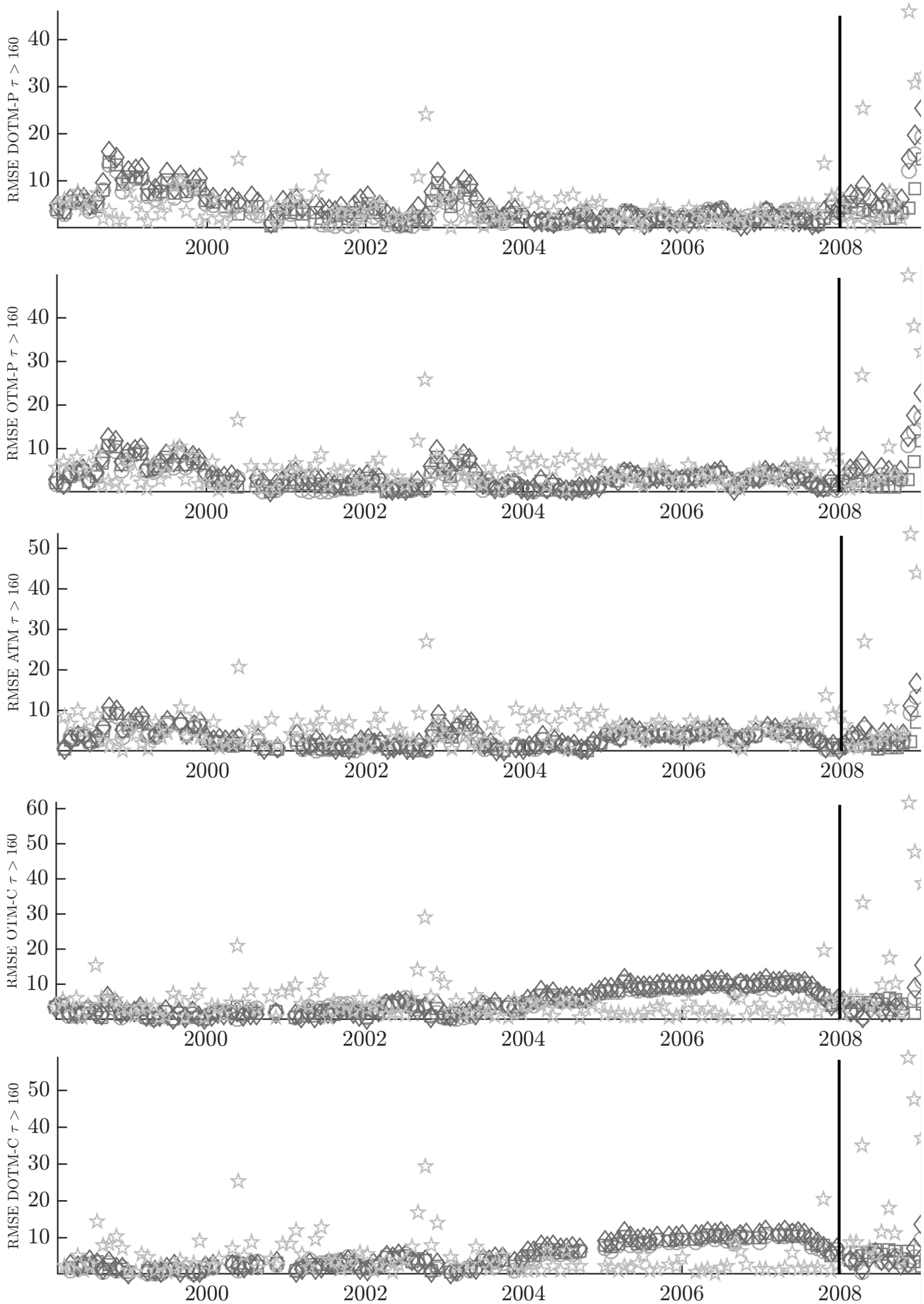

Table 8: From left to right, from bot to bottom: Maximum likelihood estimates with robust standard errors for the RV-LHARG, MCMC estimates with standard errors for the SV-LHARG, SV-ARG, SV-LARG , and SV-HARG. Maximum likelihood estimates with standard errors for the CGARCH. Quasi maximum likelihood estimates with standard errors for the RVM. The estimation period ranges from the period January 1, 1997 – December 31, 2006. The risk premium ν_1 has been calibrated on option prices. The last entry of each column is the conditional volatility persistence.

	RV-LHARG	SV-LHARG	SV-ARG	SV-LARG	SV-HARG
Parameters					
γ	0.9	-0.03	-0.13	-0.08	-0.13
	(1.7)	(0.03)	(0.03)	(0.03)	(0.03)
φ	–	0.60	0.62	0.62	62
		(0.01)	(0.01)	(0.01)	(0.01)
κ_2	–	-2.72	-2.61	-2.36	-2.65
		(0.05)	(0.04)	(0.03)	(0.03)
c	1.29e-05	4.75e-06	2.23e-06	3.19e-06	2.30e-06
	(1e-07)	(8e-08)	(5e-08)	(5e-08)	(8e-09)
δ	1.22	1.15	3.02	2.66	1.15
β_d	1.8e+04	2.9e+04	4.29e+05	2.79e+05	3.61e+05
	(1e+03)	(5e+03)	(8e+03)	(5e+03)	(4e+03)
β_w	1.5e+04	2.3e+04	—	—	3.8e+04
	(1e+03)	(3e+03)			(4e+03)
β_m	1.0e+04	1.8e+04	—	—	2.7e+04
	(4e+03)	(4e+03)			(3e+03)
α_d	0.263	0.56	—	1	—
	(1e-03)	(0.05)		(0.1)	
α_w	0.195	0.45	—	—	—
	(4e-03)	(0.08)			
α_m	0.03	4e-04	—	—	—
	(0.03)	(1e-04)			
λ	214	350		92	
	(4)	(10)		(8)	
ν_1	-1424	-2439	-2537	-2938	-2327
Persistence	0.84	0.93	0.95	0.92	0.98

	CGARCH		RVM
Parameters		Parameters	
γ	1.0	λ_z	-0.67
	(0.8)		(1.43)
b_s	0.73	b_z	0.64
	(0.05)		(0.5e-03)
a_s	3e-06	a_z	0.36
	(1e-06)		(1.6e-03)
c_s	4e+02	σ	7.55e-07
	(2e+02)		(2.26e-08)
c_l	1.4e+02	γ_1	4.6e+03
	(2e+01)		(125)
ω	1.30e-06	ω_z	1.37e-04
φ	2.4e-06	ρ	0.27
	(4e-07)		(5.6e-03)
ρ	0.991		
	(2e-03)		
ν_1	-12242	ν_1	-2.22
Persistence	0.997		0.999

Table 9: From left to right, from top to bottom: Maximum likelihood estimates with robust standard errors for the RV-LHARG, MCMC estimates with standard errors for the SV-LHARG . Maximum likelihood estimates with standard errors for the CGARCH. Quasi maximum likelihood estimates with standard errors for the RVM. The estimation period ranges from the period January 1, 1998 – December 31, 2007. The risk premium ν_1 has been calibrated on option prices. The last entry of each column is the conditional volatility persistence.

	RV-LHARG	SV-LHARG		CGARCH		RVM
Parameters			Parameters		Parameters	
γ	0.1	-0.02	γ	0.9	λ_z	0.93
	(1.8)	(0.03)		(0.7)		(1.71)
φ	–	0.60	b_s	0.75	b_z	0.66
		(0.02)		(0.04)		(9.6e-03)
κ_2	–	-2.79	a_s	2e-06	a_z	0.34
		(0.06)		(1e-06)		(8.9e-03)
c	1.24e-05	4.7e-06	c_s	6e+02	σ	5.44e-07
	(1e-07)	(1e-07)		(3e+02)		(3.41e-09)
δ	1.30	1.22	c_l	1.6e+02	γ_1	5.6e+03
				(3e+01)		(74)
β_d	1.34e+04	3.2e+04	ω	1.37e-06	ω_z	1.34e-04
	(1e+02)	(5e+03)				
β_w	6.1e+03	8e+03	φ	2.2e-06	ρ	0.28
	(3e+02)	(3e+03)		(4e-07)		(4.1e-03)
β_m	3.9e+03	2.2e+04	ρ	0.990		
	(4e+02)	(5e+03)		(2e-03)		
α_d	0.169	0.44				
	(8e-03)	(0.05)				
α_w	0.168	0.32				
	(1e-03)	(0.07)				
α_m	0.069	2.4e-04				
	(2e-03)	(9e-04)				
λ	333	411				
	(3)	(30)				
ν_1	-1584	-2308		-17339		-2.24
Persistence	0.84	0.93		0.998		0.999

Table 10: From left to right, from top to bottom: Maximum likelihood estimates with robust standard errors for the RV-LHARG. MCMC estimates with standard errors for the SV-LHARG . Maximum likelihood estimates with standard errors for the CGARCH. Quasi maximum likelihood estimates with standard errors for the RVM. The estimation period ranges from the period January 1, 1999 – December 31, 2008. The risk premium ν_1 has been calibrated on option prices. The last entry of each column is the conditional volatility persistence.

	RV-LHARG	SV-LHARG		CGARCH		RVM
Parameters			Parameters		Parameters	
γ	-1.7	-0.04	γ	0.0	λ_z	-0.67
	(1.4)	(0.02)		(0.7)		(1.43)
φ	–	0.52	b_s	0.72	b_z	0.63
		(0.02)		(0.04)		(5.4e-04)
κ_2	–	-3.04	a_s	1.9e-06	a_z	0.36
		(0.05)		(8e-07)		(1.5e-03)
c	1.68e-05	5.40e-06	c_s	6e+02	σ	7.55e-07
	(2e-07)	(1e-07)		(2e+02)		(2.2e-08)
δ	1.27	1.24	c_l	1.6e+02	γ_1	4.65e+03
				(2e+01)		(125)
β_d	9.9e+03	3.0e+04	ω	1.35e-06	ω_z	1.87e-04
	(1e+02)	(1e+04)				
β_w	3.0e+03	1.7e+04	φ	3.2e-06	ρ	0.27
	(1e+02)	(5e+03)		(3e-07)		(5.6e-03)
β_m	0.0102	9.4e+03	ρ	0.991		
	(2e-04)	(3e+03)		(3e-07)		
α_d	0.1455	0.37				
	(8e-04)	(0.04)				
α_w	0.158	0.25				
	(1e-03)	(0.04)				
α_m	0.055	8e-04				
	(4e-03)	(3e-04)				
λ	323	430				
	(3)	(10)				
ν_1	31	-757		7710		-0.35
Persistence	0.85	0.94		0.997		0.99

Table 11: Option pricing performance on S&P500 OTM options from January 1, 1997 to December 31, 2006. Parameter values are from Table 8. From top to bottom: The relative RMSE_{IV} with statistical significance (*: p-value < 0.05, **: p-value < 0.01, ***: p-value < 0.001) of the SV-LHARG with respect to the SV-ARG, SV-LARG, SV-HARG, RV-LHARG, CGARCH, and RVM models.

Moneyness	Maturity			
	$\tau \leq 50$	$50 < \tau \leq 90$	$90 < \tau \leq 160$	$160 < \tau$
Panel A	SV-LHARG/SV-ARG Implied Volatility RMSE			
$0.8 \leq m \leq 0.9$	0.83***	0.76***	0.74***	0.75***
$0.9 < m \leq 0.98$	0.82***	0.80***	0.81***	0.88***
$0.98 < m \leq 1.02$	0.88***	0.75***	0.79***	0.89***
$1.02 < m \leq 1.1$	0.86***	0.60***	0.65***	0.83***
$1.1 < m \leq 1.2$	1.47***	0.79***	0.57***	0.76***
Panel B	SV-LHARG/SV-LARG Implied Volatility RMSE			
$0.8 \leq m \leq 0.9$	0.92***	0.81***	0.76***	0.72***
$0.9 < m \leq 0.98$	0.89***	0.75***	0.75***	0.79***
$0.98 < m \leq 1.02$	0.79***	0.62***	0.69***	0.81**
$1.02 < m \leq 1.1$	0.72***	0.54***	0.60***	0.88***
$1.1 < m \leq 1.2$	1.22***	0.75***	0.57***	0.84***
Panel C	SV-LHARG/SV-HARG Implied Volatility RMSE			
$0.8 \leq m \leq 0.9$	0.77***	0.69***	0.70***	0.82***
$0.9 < m \leq 0.98$	0.73***	0.73***	0.82**	1.06**
$0.98 < m \leq 1.02$	0.93***	1.02	1.03**	1.07**
$1.02 < m \leq 1.1$	1.03	1.06***	0.99	1.03***
$1.1 < m \leq 1.2$	1.32***	0.65***	0.55***	0.81***
Panel D	SV-LHARG/RV-LHARG Implied Volatility RMSE			
$0.8 \leq m \leq 0.9$	0.96***	0.88***	0.86***	0.84***
$0.9 < m \leq 0.98$	0.97***	0.89***	0.88***	0.89***
$0.98 < m \leq 1.02$	0.90***	0.81***	0.85***	0.89***
$1.02 < m \leq 1.1$	0.88***	0.69***	0.72***	0.89***
$1.1 < m \leq 1.2$	1.22***	0.89***	0.69***	0.84***
Panel E	SV-LHARG/CGARCH Implied Volatility RMSE			
$0.8 \leq m \leq 0.9$	1.02***	0.99	0.99***	1.07***
$0.9 < m \leq 0.98$	0.95**	0.94	0.98***	1.07***
$0.98 < m \leq 1.02$	0.81***	0.93	0.99***	1.07***
$1.02 < m \leq 1.1$	0.81***	1.21***	1.19***	1.05
$1.1 < m \leq 1.2$	0.75***	0.88**	1.15***	1.07***
Panel F	SV-LHARG/RVM Implied Volatility RMSE			
$0.8 \leq m \leq 0.9$	1.03***	1.16**	1.20	0.84
$0.9 < m \leq 0.98$	0.90***	0.84***	0.84***	0.67***
$0.98 < m \leq 1.02$	0.82***	0.67***	0.67***	0.59***
$1.02 < m \leq 1.1$	0.60***	0.75*	0.73	0.96
$1.1 < m \leq 1.2$	0.58	0.42***	0.40	0.73

Panel G		
Model	Moneyness	
	$0.9 < m < 1.1$	$0.8 < m < 1.2$
SV-LHARG	4.58	5.67
SV-LHARG/SV-ARG	0.87*	0.86*
SV-LHARG/SV-LARG	0.80	0.84
SV-LHARG/SV-HARG	0.95	0.88
SV-LHARG/RV-LHARG	0.91***	0.93***
SV-LHARG/CGARCH	0.96***	0.97*
SV-LHARG/RVM	0.87***	0.90***

Table 12: Option pricing performance on S&P500 OTM options from January 1, 1998 to December 31, 2007. Parameters values are from Table 9. Panel A: Percentage $\mathrm{RMSE}_{\mathrm{IV}}$ of the SV-LHARG model sorted by moneyness and maturity. Panels B, C and E: Relative $\mathrm{RMSE}_{\mathrm{IV}}$ with statistical significance (*: p-value < 0.05, **: p-value < 0.01, ***: p-value < 0.001). Panel F: global option pricing performance. First row: The percentage $\mathrm{RMSE}_{\mathrm{IV}}$ of the SV-LHARG model (benchmark) for different moneyness range. Second and subsequent rows: Relative $\mathrm{RMSE}_{\mathrm{IV}}$ of the selected models.

Moneyness	Maturity			
	$\tau \leq 50$	$50 < \tau \leq 90$	$90 < \tau \leq 160$	$160 < \tau$
Panel A	SV-LHARG Implied Volatility RMSE			
$0.8 \leq m \leq 0.9$	13.01	7.45	6.32	4.80
$0.9 < m \leq 0.98$	5.74	3.88	4.15	3.97
$0.98 < m \leq 1.02$	3.08	2.92	3.39	3.80
$1.02 < m \leq 1.1$	3.33	3.66	3.94	6.29
$1.1 < m \leq 1.2$	7.41	2.97	2.79	5.67
Panel B	SV-LHARG/RV-LHARG Implied Volatility RMSE			
$0.8 \leq m \leq 0.9$	0.98***	0.91***	0.88***	0.84***
$0.9 < m \leq 0.98$	0.99***	0.89***	0.88***	0.88***
$0.98 < m \leq 1.02$	0.91***	0.80***	0.83**	0.89***
$1.02 < m \leq 1.1$	0.90***	0.74***	0.77***	0.89***
$1.1 < m \leq 1.2$	1.12***	0.95***	0.79***	0.92***
Panel C	SV-LHARG/CGARCH Implied Volatility RMSE			
$0.8 \leq m \leq 0.9$	1.06***	1.03***	1.03***	1.07***
$0.9 < m \leq 0.98$	0.99	0.94	0.99***	1.05***
$0.98 < m \leq 1.02$	0.80***	0.90	0.96**	0.99***
$1.02 < m \leq 1.1$	0.79***	1.17***	1.15***	1.03
$1.1 < m \leq 1.2$	0.70***	0.85**	1.12***	1.06***
Panel D	SV-LHARG/RVM Implied Volatility RMSE			
$0.8 \leq m \leq 0.9$	1.01***	1.16	1.22	0.88
$0.9 < m \leq 0.98$	0.91***	0.83***	0.85***	0.68***
$0.98 < m \leq 1.02$	0.80***	0.76***	0.66***	0.60***
$1.02 < m \leq 1.1$	0.62**	0.83	0.76	0.98
$1.1 < m \leq 1.2$	0.56	0.44***	0.41	0.74

Panel E		
Model	Moneyness	
	$0.9 < m < 1.1$	$0.8 < m < 1.2$
SV-LHARG	4.48	5.65
SV-LHARG/RV-LHARG	0.91***	0.93***
SV-LHARG/CGARCH	0.94***	0.97*
SV-LHARG/RVM	0.85***	0.89***

Table 13: Option pricing performance on S&P500 OTM options from January 1, 1999 to December 31, 2008.

Moneyness	Maturity $\tau \leq 50$	$50 < \tau \leq 90$	$90 < \tau \leq 160$	$160 < \tau$
Panel A	SV-LHARG Implied Volatility RMSE			
$0.8 \leq m \leq 0.9$	12.43	7.32	6.22	5.30
$0.9 < m \leq 0.98$	5.75	4.14	4.32	4.32
$0.98 < m \leq 1.02$	3.57	3.44	3.78	4.01
$1.02 < m \leq 1.1$	3.88	4.22	4.25	6.11
$1.1 < m \leq 1.2$	6.71	3.63	3.46	5.51
Panel B	SV-LHARG/RV-LHARG Implied Volatility RMSE			
$0.8 \leq m \leq 0.9$	0.99	0.87***	0.85***	0.87***
$0.9 < m \leq 0.98$	0.94***	0.78***	0.81***	0.87***
$0.98 < m \leq 1.02$	0.79***	0.69***	0.73***	0.85***
$1.02 < m \leq 1.1$	0.82***	0.71***	0.71***	0.85***
$1.1 < m \leq 1.2$	0.99***	0.79***	0.73***	0.83***
Panel C	SV-LHARG/CGARCH Implied Volatility RMSE			
$0.8 \leq m \leq 0.9$	0.95**	0.94***	0.98**	1.04***
$0.9 < m \leq 0.98$	0.85***	0.88	0.98**	1.07***
$0.98 < m \leq 1.02$	0.77**	0.92*	0.98***	1.09**
$1.02 < m \leq 1.1$	0.79*	1.15***	1.35***	1.38***
$1.1 < m \leq 1.2$	0.64***	0.81**	1.08***	1.47***
Panel D	SV-LHARG/RVM Implied Volatility RMSE			
$0.8 \leq m \leq 0.9$	1.11***	1.26	1.15	0.88***
$0.9 < m \leq 0.98$	1.03***	0.85***	0.80***	0.65***
$0.98 < m \leq 1.02$	0.91***	0.69***	0.63***	0.57***
$1.02 < m \leq 1.1$	0.70	0.75	0.68	0.88
$1.1 < m \leq 1.2$	0.55*	0.39***	0.41	0.76***
Panel E				
Model	Moneyness $0.9 < m < 1.1$		$0.8 < m < 1.2$	
SV-LHARG	4.71		5.78	
SV-LHARG/RV-LHARG	0.83***		0.87***	
SV-LHARG/CGARCH	0.94		0.92	
SV-LHARG/RVM	0.86***		0.89***	

Table 14: Option pricing performance on S&P500 OTM options for two out-of-sample periods. Panels A1, A2, A3, B1, B2, and B3: Relative $\mathrm{RMSE}_{\mathrm{IV}}$ with statistical significance (*: p-value < 0.05, **: p-value < 0.01, ***: p-value < 0.001).

Moneyness	Maturity $\tau \leq 50$	$50 < \tau \leq 90$	$90 < \tau \leq 160$	$160 < \tau$
Out of sample period: January 1, 2007 – December 31, 2008				
Panel A1	SV-LHARG/RV-LHARG Implied Volatility RMSE			
$0.8 \leq m \leq 0.9$	0.85***	0.69***	0.70***	0.72*
$0.9 < m \leq 0.98$	0.78***	0.68***	0.43**	0.93
$0.98 < m \leq 1.02$	1.00	0.93*	0.90	1.00
$1.02 < m \leq 1.1$	1.18**	1.06	0.94	1.04***
$1.1 < m \leq 1.2$	1.14***	1.39	1.08	1.02
Panel A2	SV-LHARG/CGARCH Implied Volatility RMSE			
$0.8 \leq m \leq 0.9$	0.99**	0.81***	0.88***	0.85*
$0.9 < m \leq 0.98$	0.83***	0.67***	0.82	0.97
$0.98 < m \leq 1.02$	0.86	0.79	1.02	1.07
$1.02 < m \leq 1.1$	1.46***	1.46***	1.20***	1.10***
$1.1 < m \leq 1.2$	0.86	2.97***	1.73***	1.14***
Panel A3	SV-LHARG/RVM Implied Volatility RMSE			
$0.8 \leq m \leq 0.9$	0.85***	0.81***	0.96**	0.63*
$0.9 < m \leq 0.98$	0.72***	0.71***	0.62***	0.63**
$0.98 < m \leq 1.02$	0.71**	0.71**	0.59***	0.65***
$1.02 < m \leq 1.1$	1.03***	1.34***	1.08***	1.53***
$1.1 < m \leq 1.2$	0.77	0.86	0.73	1.21***
Out of sample period: January 1, 2008 – December 31, 2008				
Panel B1	SV-LHARG/RV-LHARG Implied Volatility RMSE			
$0.8 \leq m \leq 0.9$	0.59***	0.45***	0.43***	0.49***
$0.9 < m \leq 0.98$	0.47***	0.34***	0.38***	0.44***
$0.98 < m \leq 1.02$	0.52***	0.38***	0.38***	0.41***
$1.02 < m \leq 1.1$	0.98	1.01	1.09	0.90
$1.1 < m \leq 1.2$	1.05	1.49**	1.46	1.05
Panel B2	SV-LHARG/CGARCH Implied Volatility RMSE			
$0.8 \leq m \leq 0.9$	0.55***	0.45***	0.49***	0.61***
$0.9 < m \leq 0.98$	0.39***	0.32***	0.43***	0.54***
$0.98 < m \leq 1.02$	0.39***	0.30***	0.38***	0.49***
$1.02 < m \leq 1.1$	0.64	0.78	0.99	1.03
$1.1 < m \leq 1.2$	0.57***	1.02**	1.35	1.21
Panel B3	SV-LHARG/RVM Implied Volatility RMSE			
$0.8 \leq m \leq 0.9$	1.28	0.60**	0.36***	0.26***
$0.9 < m \leq 0.98$	0.75**	0.28***	0.25***	0.17***
$0.98 < m \leq 1.02$	0.51***	0.19***	0.19***	0.13***
$1.02 < m \leq 1.1$	0.53***	0.78***	0.99***	1.03***
$1.1 < m \leq 1.2$	0.57***	0.33***	0.29***	0.17***

Table 15: Option pricing performance on S&P500 OTM options for the out-of-sample period January 1, 2009 – December 31, 2009. Panels C1, C2, and C3: Relative RMSE_{IV} with statistical significance (*: p-value < 0.05, **: p-value < 0.01, ***: p-value < 0.001). Panel D: Global option pricing performance over the three out-of-sample periods.

Moneyness	Maturity			
	$\tau \leq 50$	$50 < \tau \leq 90$	$90 < \tau \leq 160$	$160 < \tau$
Out of sample period: January 1, 2009 – December 31, 2009				
Panel C1	SV-LHARG/RV-LHARG Implied Volatility RMSE			
$0.8 \leq m \leq 0.9$	0.98	0.93	0.92	0.90
$0.9 < m \leq 0.98$	0.95**	0.91	0.94***	0.92***
$0.98 < m \leq 1.02$	0.95***	0.95***	0.96**	0.92***
$1.02 < m \leq 1.1$	1.04*	0.95***	0.95***	0.85***
$1.1 < m \leq 1.2$	1.07***	0.97**	0.91***	0.85***
Panel C2	SV-LHARG/CGARCH Implied Volatility RMSE			
$0.8 \leq m \leq 0.9$	1.05	1.06	1.05	0.99
$0.9 < m \leq 0.98$	1.04	1.05	1.04	0.97
$0.98 < m \leq 1.02$	0.99	1.03*	1.00	0.93
$1.02 < m \leq 1.1$	0.85*	0.92	0.91	0.85
$1.1 < m \leq 1.2$	0.80	0.77	0.80	0.75
Panel C3	SV-LHARG/RVM Implied Volatility RMSE			
$0.8 \leq m \leq 0.9$	1.18	1.13	1.09	0.97***
$0.9 < m \leq 0.98$	1.19***	0.94***	0.88**	0.86***
$0.98 < m \leq 1.02$	1.08***	0.83***	0.84***	0.93
$1.02 < m \leq 1.1$	0.76*	0.59	0.45	0.41***
$1.1 < m \leq 1.2$	0.96*	0.69***	0.50*	0.45

Panel D		
Model	Moneyness	
	$0.9 < m < 1.1$	$0.8 < m < 1.2$
Out of sample period: January 1, 2007 – December 31, 2007		
SV-LHARG/RV-LHARG	0.93	0.97***
SV-LHARG/CGARCH	1.01	1.03
SV-LHARG/RVM	0.94	0.89*
Out of sample period: January 1, 2008 – December 31, 2008		
SV-LHARG/RV-LHARG	0.62***	0.59***
SV-LHARG/CGARCH	0.52***	0.49***
SV-LHARG/RVM	0.34***	0.39***
Out of sample period: January 1, 2009 – December 31, 2009		
SV-LHARG/RV-LHARG	0.92***	0.94***
SV-LHARG/CGARCH	0.98*	0.98*
SV-LHARG/RVM	0.87***	0.96***

References

Bernardo, J., M. Bayarri, J. Berger, A. Dawid, D. Heckerman, A. Smith, and M. West (2003). Non-centered parameterisations for hierarchical models and data augmentation. In *Bayesian Statistics 7: Proceedings of the Seventh Valencia International Meeting*, pp. 307. Oxford University Press, USA.

Casarin, R., J.-M. Marin, et al. (2009). Online data processing: Comparison of Bayesian regularized particle filters. *Electronic Journal of Statistics 3*, 239–258.

Casella, G. and C. P. Robert (2004). *Monte Carlo Statistical Methods*. New York: Springer Verlag.

Chib, S., F. Nardari, and N. Shephard (2002). Markov chain Monte Carlo methods for stochastic volatility models. *Journal of Econometrics 108*(2), 281–316.

Christoffersen, P., B. Feunou, K. Jacobs, and N. Meddahi (2014). The economic value of realized volatility: Using high-frequency returns for option valuation. *Journal of Financial and Quantitative Analysis 49*(03), 663–697.

Christoffersen, P., B. Feunou, and Y. Jeon (2015). Option valuation with observable volatility and jump dynamics. *Journal of Banking & Finance 61*, S101–S120.

Christoffersen, P., B. Feunou, and Y. Jeon (May 13, 2016). Option valuation with observable volatility and jump dynamics. *Available at SSRN 2494379.*.

Creal, D. D. (2017). A class of non-Gaussian state space models with exact likelihood inference. *Journal of Business & Economic Statistics 35*(4), 585–597.

Frühwirth-Schnatter, S. (2004). Efficient Bayesian parameter estimation for state space models based on reparameterizations. *State Space and Unobserved Component Models: Theory and Applications*, 123–151.

Gelman, A. and D. B. Rubin (1992). Inference from iterative simulation using multiple sequences. *Statistical science*, 457–472.

Geweke, J. et al. (1991). *Evaluating the accuracy of sampling-based approaches to the calculation of posterior moments*, Volume 196. Federal Reserve Bank of Minneapolis, Research Department Minneapolis, MN, USA.

Gouriéroux, C. and J. Jasiak (2006). Autoregressive gamma processes. *Journal of Forecasting 25*(2), 129–152.

Hamilton, J. D. (1994). *Time series analysis*. Princeton University Press.

Hansen, P. R. and A. Lunde (2005). A forecast comparison of volatility models: Does anything beat a GARCH (1, 1)? *Journal of Applied Econometrics 20*(7), 873–889.

Majewski, A. A., G. Bormetti, and F. Corsi (2015). Smile from the past: A general option pricing framework with multiple volatility and leverage components. *Journal of Econometrics 187*(2), 521–531.

Roberts, G. O., A. Gelman, W. R. Gilks, et al. (1997). Weak convergence and optimal scaling of random walk Metropolis algorithms. *The Annals of Applied Probability 7*(1), 110–120.

Roberts, G. O., O. Papaspiliopoulos, and P. Dellaportas (2004). Bayesian inference for non-Gaussian Ornstein–Uhlenbeck stochastic volatility processes. *Journal of the Royal Statistical Society: Series B (Statistical Methodology) 66*(2), 369–393.